ABSTRACT

Title of Document: FIRE DYNAMICS AND WOODY COVER CHANGES IN THE SERENGETI-MARA ECOSYSTEM 2000 to 2005 – A REMOTE SENSING APPROACH

Jan Dempewolf, Doctor of Philosophy, 2007

Directed By: Professor Dr. Ruth S. DeFries
Department of Geography

The Serengeti-Mara savanna environment in East Africa is characterized by changing levels of woody cover and a dynamic fire regime. The relative proportion of woodland to grassland savanna affects animal habitat, biodiversity, and carbon storage, and is regulated by factors such as the fire regime (frequency, intensity, seasonality), and precipitation. The main objectives of this dissertation are to determine recent changes in woody cover at a regional scale and identify fire regimes and climate associated with these changes. Understanding these relationships is important for the assessment of future trajectories of woody cover under changing

climate. Required spatially coherent data layers can only be obtained at the regional scale through the analysis of remote sensing data.

Woody cover changes between 2000 and 2005 were derived from field data and a time series of MODIS satellite imagery at 500 m spatial resolution. Data layers on the controlling variables (fire frequency, seasonality, intensity and rainfall) were developed using a combination of remote sensing and model-based approaches. Burned areas were mapped using daily MODIS imagery at 250 m resolution. Outputs were used to make the requisite layers depicting fire frequency and seasonality. Fire intensity was derived using a model based on empirical relationships, mainly estimating fire fuel load as a function of rainfall and grazing.

The combined data layers were analyzed using regression and decision tree techniques. Results suggest woody cover in central and northern Serengeti National Park continued to increase after 2000. Woody cover decreases were strongest in the wider Maswa Game Reserve area (MSW) under low precipitation conditions and late season burning. Woody cover losses in burned areas were also higher in the low fire frequency region of the Maasai Mara National Reserve (MNR). Fire seasonality was the most important fire regime parameter controlling woody cover in burned woodland savanna areas while fire intensity was most relevant for grassland savanna areas. Continued late season burning in drought years might cause further decrease of woody cover in MSW. MNR is expected to continue to be dominated by grassland savanna at similar fire frequency and browsing levels.

FIRE DYNAMICS AND WOODY COVER CHANGES IN THE SERENGETI-MARA ECOSYSTEM 2000-2005 – A REMOTE SENSING APPROACH

by

Jan Dempewolf

Dissertation submitted to the Faculty of the Graduate School of the
University of Maryland, College Park, in partial fulfillment
of the requirements for the degree of
Doctor of Philosophy
2007

Advisory Committee:

Professor Ruth S. DeFries, Chair
Professor Catherine Dibble
Professor William F. Fagan
Professor Christopher O. Justice
Dr. Marc Steininger
Dr. Simon N. Trigg

Preface

Chapter 2 of this dissertation has been accepted for publication as a peer-reviewed journal article. This research as well as the remainder of the thesis, was carried out in its entirety by Jan Dempewolf.

To my parents,

Walter and Trautlind

Acknowledgements

I am particularly grateful to my advisor Ruth DeFries for her steadfast encouragement and support and openness for discussion. Her mentoring and guidance were invaluable. I thank Simon Trigg who has been very generous with his time and support during the preparation of this dissertation. I would also like to thank the other members of my committee, Christine Dibble, William Fagan, Christopher Justice, and Marc Steininger for supplying guidance and encouragement.

This study was carried out in collaboration with the International Livestock Research Institute (ILRI) in Nairobi, Kenya. For generous and indispensable support of my field work and inspiring discussions I am very grateful to Robin Reid and Suzanne Serneels who introduced me to the Maasai Mara ecosystem and provided guidance and critical advice. James Kaigil, Josef Temut and Andrew Muchiro provided essential support in the field. I have also greatly benefited from collaborations and discussions with Mohammed Said, Grant Hopcraft, Andrew Hansen, Denne Reed, Axel Kleidon, Konrad Wessels, Stephanie Eby, Douglas Morton and Charlene Dimiceli. Funding for this research was provided by NASA's Earth System Science Fellowship. Finally my deepest thanks go to my family particularly my wife for their loving support and patience throughout this endeavor.

Table of Contents

List of Tables

List of Figures

Chapter 1: Introduction

1.1. Background

Savannas constitute approximately 12% of the world's surface (Scholes and Hall 1996) and are the dominant vegetation of Africa, covering 60% of the continent south of the Sahara (Scholes and Walker 1993). Savannas are tropical vegetation types co-dominated by woody plants and grasses. A defining characteristic of savannas is a high frequency of grass-layer fires (Scholes 1997). Fire has long been recognized as an important factor for the development and maintenance of savanna structure, particularly in combination with climate and the grazing effects of great herds of herbivores (Trollope 1984; Bond 1997).

The Serengeti-Mara savanna environment in East Africa provides a representative example for the interaction between factors controlling the balance of woodland and grassland savanna. The Serengeti-Mara ecosystem was historically subject to dramatic changes of the landscape and the fire regime. Fire has been used in the region since decades as a management tool. The current main objectives associated with fire management in the Serengeti National Park (SNP) in Tanzania are the control of woody cover to create suitable conditions for tourism and poaching patrols, preserve vegetation communities and improve forage quality for animals (Trollope et al. 2005). The area of SNP and its northern extension, the Maasai Mara National Reserve (MNR) in Kenya are important tourist hot spots and generate millions of dollars of revenue every year (Lamprey and Reid 2004; Emerton and

Mfunda 1999). SNP is a world heritage site best known for its spectacular annual wildebeest migration, which regularly extends into MNR (UNEP 2003).

Woody cover in the Serengeti-Mara region has been changing significantly over the last 100 years. Those who traveled through the region in the early 1900s found open grassland with occasional *Acacia* trees throughout the Serengeti-Mara region (Dublin 1995). In the last decade of the 19th century a rinderpest epidemic reduced wildebeest and domestic cattle in the entire region by more than 95% (Sinclair 1979a). Human population decreased dramatically through famine and emigration and as a result anthropogenic burning declined and fires became infrequent. Elephant numbers were greatly reduced by ivory poaching (Dublin 1986). Probably due to the low fire frequency and low browsing pressure the region had by the mid 20th century developed into a dense woodland savanna infested by tsetse fly. Tsetse flies are vectors for the deadly sleeping sickness, preventing humans from returning to the area and potentially changing the landscape (Waller 1990). During this time the Serengeti and Mara were set aside as protected areas. In the mid 20th century the Maasai returned with their animals vaccinated against rinderpest. In the early 1960s rainfall was unusually high and increased grass biomass production throughout the region. Fires set by hunters, park authorities and the Maasai population burned with very high intensity due to the large accumulation of fire fuel, clearing large areas of bush and thickets. At the same time elephant numbers increased, most likely through immigration from surrounding areas. As a result by the mid 1960s the woodlands began to decline (Dublin 1986). In the mid 1980s woody cover in most of the region had reached a minimum. The migrating wildebeest

(*Connochaetes taurinus*), unimpeded by rinderpest, had increased dramatically and numbers have remained stable at approximately 1.3 million ever since (Mduma et al. 1999). Since the early 1990s woody cover has been steadily increasing again in central and northern Serengeti (Sinclair and Arcese 1995), but not so in the Masai Mara which continued to be dominated by grassland savanna (Dublin 1995).

Woody cover changes, the fire regime, and climate are important factors for ecosystem functioning of savannas. Changes of the balance between woodland and grassland savanna have ecological implications for vegetation and animal distribution and, within a larger framework, for carbon stocks and climate change (Pacala et al. 2001). An improved understanding of the interaction between the fire regime, precipitation and woody cover changes in the Serengeti-Mara ecosystem can potentially be applied to other savanna areas with similar ecological characteristics.

Woody canopy cover in the Serengeti-Mara region can change substantially over a period of one or two decades (Dublin 1991; Sinclair and Arcese 1995), but it is only recently that remote sensing data has become available with which to monitor these changes. Reliable, high resolution, daily remote sensing imagery from the MODerate Resolution Imaging Spectroradiometer (MODIS) sensor has been available at no cost since 2000. At the time of this study the MODIS record covered a time period of six years. The MODIS time series at 250 m resolution (red and near-infrared band) and 500 m resolution (mid and longer wave infrared bands) constitutes a fundamental resource for the type of analysis used in this study. The data allow a spatially coherent analysis of woody cover changes and the fire regime over the entire

region which has not been possible before at a similar level of detail and spatial extent.

To evaluate how woody cover is being altered requires an understanding of the role of fire and precipitation as factors driving this changes; specifically it requires characterization of the fire regime, defined here as fire frequency, seasonality, and intensity. Fire seasonality and frequency can be determined with high confidence and spatial accuracy through near-daily burned area mapping. Burned area maps at high temporal and spatial resolution are also essential for many fire related research questions in the ecosystem. The outcomes of this study are of potential use for other researchers and management.

1.2. Research Objectives

A regional scale analysis was made across the Serengeti-Mara ecosystem to determine relationships between two factors that affect woody cover density: fire regime and precipitation. The principal objectives of this research were: (1) characterize spatial patterns of woody cover change between 2000 and 2005; (2) analyze the role of fire regime parameters as potential drivers of these changes. Addressing the above objectives required the development of spatially comprehensive data layers extending over the entire region. Additional objectives to address these requirements were: (3) map burned areas at high spatial and temporal resolution; (4) detect changes of woody canopy cover at regional scales; (5) estimate fire intensity. To reach these objectives remote sensing and model-based methods were developed using recently available time series of high resolution satellite imagery and field data as inputs.

1.3. Outline of the Dissertation

The dissertation is structured in six chapters. The four main chapters are self-contained and structured in the format of journal articles. Chapter 2 has been accepted for publication in a peer-reviewed journal. Each chapter uses results of the previous ones and the chapters are ordered accordingly. The division into subregions is not the same for all chapters and therefore a description of the study area is provided in each. Literature specific to each chapter is reviewed in the corresponding introduction sections. Chapters 2 to 4 introduce novel remote-sensing based techniques and models developed for this research to derive respectively fire frequency and seasonality (Chapter 2), changes in woody cover (Chapter 3), and fire intensity (Chapter 4). The results provide an unprecedented, spatially coherent view of both the fire regime and woody cover changes between 2000 and 2005. Chapter 5 brings together these results in a combined analysis of the interaction between the fire regime and woody cover changes. Chapter 6 summarizes the dissertation and discusses implications of the results. The following paragraphs introduce each chapter in more detail.

Chapter 2 provides fire frequency and seasonality by generating a series of burned area maps using a newly developed automated algorithm. The algorithm processes daily MODIS imagery at a spatial resolution of 250 m; this necessitates the use of only two bands, red and near infrared (NIR). The exclusive and successful use of these two bands in an automated algorithm for near-daily burned area mapping at a regional scale sets the methodology apart from previous work.

Chapter 3 detects woody cover changes using a MODIS time series of 16-day composites at 500 m resolution and field measurements of vegetation structure. The methodology converts yearly data sets of red, NIR, and mid infrared (MIR) spectral bands and NDVI to annual metrics. The approach uses field data and a random forest statistical approach to estimate percent woody cover for each year, taking advantage of the different phenological characteristics of woody and herbaceous plants.

Particular attention was given to the potential contamination of the MODIS data with burned area spectral effects. This was addressed by eliminating all annual metrics significantly correlated with burned areas detected in the previous chapter. The combination of the annual results for all six years allows the detection of prolonged changes in woody cover as they are typical for savanna environments.

Chapter 4 estimates fire intensity at a spatial resolution of 250 m using a novel application of published empirical equations derived for southern African and Australian savannas. Fire intensity largely depends on fire fuel load or grass biomass. Input data layers to the spatially explicit model are results from the previous two chapters (fire dates and locations, percent woody canopy cover), amount and distribution of rainfall based on Meteosat and microwave satellite observations, and census counts of grazing animals which reduce grass biomass through grazing.

Chapter 5 analyzes the interaction between the fire regime, precipitation and woody cover changes using the results and datasets generated or used in the chapters 2-4. The chapter focuses on the wider area of the Maswa Game Reserve, which has experienced larger decreases in woody cover than other areas and on the Maasai Mara

National Reserve where woody cover shows significantly stronger reactions to fire events than in SNP.

Chapter 6 provides a comprehensive summary of the dissertation and the developed methodologies and results. It discusses implications for the future development of the Serengeti-Mara ecosystem. It further discusses potential applications and extensions of the developed algorithms and future research directions.

Chapter 2: Burned Area Mapping of the Serengeti-Mara Region Using MODIS Reflectance Data

2.1. Abstract

Fire is a key factor for vegetation structure and ecosystem functioning in the Serengeti-Mara region in East Africa. However, there is a lack of accurate and consistent information on fires. We developed an algorithm for mapping burned areas in the wider Serengeti-Mara region from remote sensing data. The algorithm is automated and once trained for one year, runs independently for all years. It uses daily measurements of red and near-infrared (NIR) reflectance acquired by the Moderate-Resolution Imaging Spectroradiometer (MODIS) sensor at a spatial resolution of 250 m. The MODIS time series was first converted to 10-day minimum NIR composites. Each composite was then classified into new and old burned areas, by thresholding Burned Area Index (BAI) and temporal difference of NIR reflectances. The algorithm adjusts detection thresholds dynamically using measures related to atmospheric and vegetation conditions. Having trained the algorithm once on 2003 data it was applied to MODIS data from April 21, 2000 to November 10, 2005. Accuracy was improved by size and location sensitive filters. Overall accuracy was 90.3% as determined from Advanced Spaceborne Thermal Emission and Reflection Radiometer (ASTER) satellite imagery from 2005, and 87.1% as determined using field data from 2005. The algorithm holds the potential to be applied to other savanna areas. This study provides a reliable product useful for future investigations of fire ecology and fire management.

2.2. Introduction

Fire is a major factor in determining savanna structure and impacts above-ground net primary productivity (Oesterheld et al. 1999). In savannas, fire is thought to control the balance between grasses and woody plants (Higgins et al. 2000). The combined effects of fires and elephants have altered levels of woody vegetation in the Maasai Mara National Reserve (MMNR) and Mara Group Ranges (MGRs) in Kenya and Serengeti National Park (SNP) in Tanzania (Dublin 1995). Norton-Griffiths (1979) suggested that fire in combination with grazing, browsing and climatic effects is the main controlling factor for vegetation structure in SNP.

Burned area maps are needed to provide a quantitative description of the seasonality and frequency of burning in different ecological zones of the SNP-MMNR region (Trollope et al. 2005). An automated algorithm that maps burned areas at a relatively high spatial resolution would provide researchers and park authorities a new tool with which to monitor and analyze fire dynamics and fire regimes.

We mapped burned areas in the Serengeti-Mara region using a novel automated algorithm, which runs, once trained for one year, independently for all years. The algorithm uses daily red and near infrared (NIR) spectral reflectances from the Moderate-Resolution Imaging Spectroradiometer (MODIS) sensor at the spatial resolution of 250 m. Other automated algorithms have been developed, but only at larger spatial scales between 0.5 km and 1 km and including spectral bands beyond the Red/NIR domain. They were designed for continental or global estimations of burned areas but were not optimized for highly accurate estimates at small spatial scales for local applications. Existing algorithms include Barbosa et al. (1999) using

Advanced Very High Resolution Radiometer (AVHRR) data, Roy et al. (2005) (MODIS), Tansey et al. (2004) (SPOT VEGETATION), and Simon et al. (2004) Along Track Scanning Radiometer (ATSR-2).

The MODIS sensor provides necessary characteristics for consistent burned area mapping. MODIS has an almost daily return interval, high spatial resolution of 250 m for the red and NIR bands, and high geolocation accuracy. Although MODIS data are well-adapted to detecting burned areas, designing an algorithm to detect them in an automatic manner faces many challenges, including inherent variations of surface reflectance caused by varying geometry of viewing and illumination, atmospheric conditions and imperfect cloud screening (Roy et al. 2005). The confounding effects of these problems can be reduced by compositing methods that retain the burned area signal (Stroppiana et al. 2002; Chuvieco et al. 2005). For example, Stroppiana et al. (2003a) classified 10-day SPOT-VGT minimum NIR composites of the Australian continent for burned and unburned pixels. Here, spectral indices were derived from the red, NIR and short-wave NIR bands and applied a series of fixed thresholds selected by a decision tree algorithm over one year, though did not automate over several years (Stroppiana et al. 2003b).

A number of indices defined in the red-near-infrared bi-spectral space have been tested previously for burned area detection, including the Normalized Difference Vegetation Index (NDVI), Second Modified Soil Adjusted Vegetation Index (MSAVI2), the Global Environmental Monitoring Index (GEMI) and the Burned Area Index (BAI). Compared to using spectral reflectances alone, spectral indices

have the advantage of reducing some anisotropic and atmospheric effects (Chuvieco et al. 2002).

In this study, 10-day minimum NIR composites were derived for both the red and NIR bands of a MODIS time series. The composites were used to map burned areas with high accuracy using dynamically adjusted BAI and temporal difference NIR thresholds as a function of average spectral characteristics for each composite. The threshold adjustment algorithm was trained for one year using a decision tree method. Problems resulting from varying viewing and illumination angles are reduced, but not eliminated, by compositing and the use of a spectral index (Trigg et al. 2005). However, although compositing and bi-directional effects may remain, they did not reduce the reported validation metrics to an unacceptably low level. Residual cloud shadows were reduced using temporal persistence criteria and time, location, and area sensitive filters. The developed methodology holds the potential to be applied to other savanna areas of similar ecological characteristics.

2.3. Methodology

2.3.1. Study Area

The core of the study area comprises SNP and MMNR. It is bounded by the coordinates (degrees): upper left: -0.8 latitude, 33.8 longitude, lower right -3.8 latitude, 36.1 longitude. Its climate is characterized by distinct rainy and dry seasons with the main rainy season during March-May and short rains in November-December. Dominant vegetation types are tree-, shrub- and grass savannas (Dublin

1995; Norton-Griffiths 1979). The study area supports large herds of migrating ungulates, dominated by wildebeest.

2.3.2. Dataset

This research created a burned area product from MODIS/Terra Surface Reflectance Daily L2G 250 m data (MODIS product MOD09GQK, version v004). The dataset provides atmospherically corrected red surface reflectance, centered at the spectral wavelength of 0.648 μm, and NIR surface reflectance, centered at 0.858 μm (Vermote and Vermeulen 1999). The dataset also includes quality assurance (QA) flags for each pixel. The MODIS time series covered April 21, 2000 to November 10, 2005.

Two further datasets were used to develop reference data for accuracy assessment of the MODIS burned area product. The first reference dataset comprised a pair of Advanced Spaceborne Thermal Emission and Reflection Radiometer (ASTER) satellite imagery from July 3 and 10, 2005, covering parts of southern SNP and the Maswa Game Reserve (MGR). The ASTER scenes were acquired in partnership with the Global Land Cover Facility (GLCF) at the University of Maryland. The second dataset comprised field data collected between June 13 and July 11, 2005 along 10 transects in central SNP (total length = 182.9 km).

2.3.3. MODIS Algorithm to Detect Burned Areas

The method used to map burned areas extends the work of (Stroppiana et al. 2002, Stroppiana et al. 2003a, Stroppiana et al. 2003b). We use higher resolution data at 250 m in the red-NIR spectral domain, apply a new procedure to remove

misclassified cloud shadows, improve accuracy by relaxing detection thresholds for pixels with high burning probability, and apply the algorithm in a new ecosystem. Crucially, we solve the problem of automation over several years by adjusting detection thresholds dynamically to detect burns automatically and accurately despite changing environmental conditions. Our method consists of five distinct phases: preprocessing, creating spectral indices, training, automating, and applying the algorithm. These stages are described below:

1) Preprocessing: This stage included first filtering the MODIS time series for low quality pixels, then applying minimum value compositing. The MODIS time series was filtered for low quality pixels using the QA flags. Pixels were replaced by a no-data value if their QA bits flagged them as any of the following: not produced or processed, missing input, cloudy, dead detector, solar zenith angle > 85 degrees, correction out of bounds, or L1B data faulty.

The filtered time series was converted into 10-day minimum NIR composites using a method designed after (Stroppiana et al. 2002). The method attempts to minimize the unwanted selection of shadow contaminated pixels It selects the four pixels with the lowest NIR reflectance. The pixel with the minimum NIR reflectance within the four selected pixels is set aside. For the remaining three pixels, both the mean and range are calculated. If the minimum NIR reflectance pixel, set aside earlier, is within the interval mean +/- range, it is selected as the composite value. If not, the pixel with the minimum NIR value of the remaining three pixels is selected for the composite. For the selected pixel the red and NIR values and the acquisition date is saved.

MODIS data was unavailable for some dates. Any 10-day composite missing three days of input data or more was disregarded, due to quality concerns. As a result, burned area was not mapped for the following time periods: August 1 to 20, 2000; June 11 to June 30, 2001; March 21 to 31, 2002; and December 11 to 31, 2003.

2) Creating spectral indices: We provided a selection of six promising indices for the decision tree algorithm to select as the basis of burned area detection. The subsequently applied decision tree algorithm then statistically selected those indices that discriminate most strongly between burned and unburned areas (Stroppiana et al. 2003a).

The six spectral indices used were calculated for each composite, BAI (Equation 1), delta NIR reflectance (dNIR), ratio of red to NIR reflectance (RNIR), GEMI (Equation 2), MSAVI2 (Equation 3) (Qi et al. 1994) and NDVI (Equation 4), as follows:

$$BAI = 1/\left((\rho c_{red} - \rho_{red})^2 + (\rho c_{NIR} - \rho_{NIR})^2\right) \quad (1)$$

$$GEMI = \eta(1-0.25\eta) - (\rho_{red} - 0.125)/(1-\rho_{red}) \quad (2)$$

where

$$\eta = \left(2(\rho_{NIR}^2 - \rho_{red}^2) + 1.5\rho_{NIR} + 0.5\rho_{red}\right)/(\rho_{NIR} + \rho_{red} + 0.5)$$

$$MSAVI2 = \frac{1}{2}\left(2\rho_{NIR} + 1 - \sqrt{(2\rho_{NIR}+1)^2 - 8(\rho_{NIR} - \rho_{Red})}\right) \quad (3)$$

$$NDVI = (\rho_{NIR} - \rho_{Red})/(\rho_{NIR} + \rho_{Red}) \quad (4)$$

where ρ_{red} and ρ_{NIR} are the red and NIR surface reflectances and ρc_{red} and ρc_{NIR} are red and NIR reference reflectances. The first of these indices, the BAI, is nonlinear and based on the spectral distance to a reference spectral point, around which recently

burned areas tend to concentrate. Empirically determined values for $\rho c_{red} = 0.1$ and $\rho c_{NIR} = 0.6$ were designed for BAI to emphasize the charcoal signal (Chuvieco et al. 2002). dNIR is calculated as the NIR reflectance of the current composite minus the NIR reflectance of the previous composite. The RNIR is calculated as ρ_{red} divided by ρ_{NIR}. GEMI is an improved vegetation index, claimed to be less sensitive to atmospheric effects and the soil background than NDVI (Pinty and Verstraete 1992).

The above indices were chosen because they all can be calculated from the MODIS 250 m red and NIR bands and have all been used previously to detect burned areas. The only one of these indices that was developed specifically to detect burned areas is the BAI (Chuvieco et al. 2002).

3) Training the algorithm: The above indices were supplied to a decision tree classifier, as well as the red and NIR reflectances and all corresponding difference values between reflectances and indices of the current composite and the previous composite. This was carried out for between 1500 and 12000 training pixels from each of 14 different dry-season composites from the year 2003. Training data for unburned, newly burned, and previously burned areas were derived by visual interpretation of image pairs; in this way, burned areas can be identified confidently as distinct areas of reduced reflectance that appear from one image date to the next. The algorithm was trained using the S-Plus 7.0 for Windows software package. Decision trees recursively split the training data into subsets, or nodes, which minimize the overall residual sum of squares (Breiman et al. 1984). The decision tree classifier consistently showed high classification accuracy of 94.4 to 99.8% after the

first 2 splits, selecting BAI for the root node separating burned areas from unburned areas and dNIR for the succeeding node separating new from old burns.

4) Automating the algorithm: The resulting BAI and dNIR thresholds varied between composites depending on atmospheric and vegetation conditions. This necessitated a novel adaptation of the basic algorithm to automate it in the context of the varying environmental conditions. Threshold selection for each composite was automated by deriving a generally applicable regression equation in dependence of an average index value of the composite. The adjusted threshold value was selected by correlating the threshold index values determined by the decision tree algorithm for the 14 training composites with the average and median of the index values of all pixels in the study area, as well as the mean and median of the first, second, third, and fourth quartiles of all pixels. This method was applied to both the BAI threshold for separating burned from unburned areas, and the dNIR threshold for separating old from new burns.

The highest correlation was found between the BAI thresholds (BAI_{thresh}) and the mean values of the fourth (uppermost) quartiles of RNIR images ($RNIR_{mn(q4)}$). The second order polynomial regression (5) showed a significantly higher coefficient of determination ($r^2 = 0.62$) than the corresponding linear or higher order regressions.

$$BAI_{thresh} = 0.2137 - 0.6731 RNIR_{mn(q4)} + 0.5477 RNIR^2_{mn(q4)} \quad (5)$$

To ensure that the chosen BAI thresholds would not result in large commission errors (i.e. false detection of burned areas), the resulting BAI threshold was compared with the BAI values of a small region in the southeastern Serengeti short grass plains which is known to not burn, due to high grazing pressure and low

fuel loads. No burns were detected in this area by visual interpretation of successive 10-day composites for all years 2000 through 2005. The bounding coordinates are latitude / longitude: -2.96 / 35.09; -2.84 / 35.36; -2.89 / 35.49; -3.05 / 35.38; -3.06 / 35.16. A minimum BAI value was calculated as the median plus three times the standard deviation of the BAI values within this area. If the BAI threshold established by the regression equation was lower than the minimum BAI, the threshold was set to this minimum value. This adjustment came into effect almost exclusively during the wet season months.

The highest correlation for the dNIR threshold ($dNIR_{thresh}$), separating new burns from old burns, was found with the median of the first (lower most) quartiles of the temporal difference GEMI values ($dGEMI_{md(q1)}$), calculated over the entire study area for each of the 14 training composites. The linear regression equation (6) had the highest determination coefficient with $r^2 = 0.67$. Equations (5) and (6) allow the automation of the algorithm over different seasons and years.

$$dNIR_{thresh} = -0.0273 + 0.2976 dGEMI_{md(q1)} \quad (6)$$

5) Applying the algorithm: Having trained and automated the algorithm using training data from 2003, it was applied to the full April 2000 to November 2005 time series and ran automatically. It was programmed and executed in IDL 6.1 for Windows. The algorithm classified each 10-day composite for unburned, old and new burns, using dynamically adjusted thresholds as described above. It then combined the classified composites into final, yearly products, showing the date and location of burned areas. New burns were only accepted as burned, if they were classified as old burns in the subsequent composite. A similar persistence criterion was used by

(Stroppiana et al. 2003b). In the final product, small burned area patches of less than 48 ha (9 pixels) were removed as being residual cloud shadows if isolated in time and space. They were maintained when contingent with areas burned up to 10 days before or 10 days after and thus part of a larger, spreading fire front. The accuracy was further improved by relaxing the BAI thresholds for pixels adjacent to groups of burned pixels, thus extending the size of burned areas. It was applied by identifying all unburned pixels with at least four neighboring pixels, which have burned in the present, previous or subsequent compositing period. These pixels were reprocessed using a 20% lower BAI threshold. The same threshold was used in a similar approach by (Kasischke and French 1995). The algorithm created a final product for each 12 month period from May 1 to April 30 of the subsequent year. Maps from all years were combined into a final map showing fire return interval.

Validation: An accuracy analysis was carried out based on both ASTER and field data. Spatially overlapping ASTER scenes, acquired in short time sequence, were only available for July 3 and 10, 2005, for the southern parts of SNP and MGR. ASTER data were selected for data availability and the high spatial resolution of 15 m, allowing visual interpretation of burned areas with high confidence. The ASTER scenes were co-registered and areas newly burned between the first and second date detected visually. Pixels in the MODIS burned area product at 250 m resolution were counted as correctly classified, if the ASTER data showed at least half of it as burned, and the MODIS burn date was between July 3 and July 20 (thus allowing the algorithm 10 days, or one compositing period, to detect the most recent burns)

Field data were collected between June 13 and July 11, 2005 in central SNP, along transects of total length 182.9 km. Along each transect geographic coordinates were recorded at 250 m intervals, using a Global Positioning System (GPS) receiver. The state of the vegetation, burned or unburned, was recorded. Areas were classified as burned if at least 50% of the vegetation was burned. Pixels were counted as correctly classified, if the field and MODIS data agreed within 20 days before and 10 days after the date of ground truthing.

2.4. Results and Discussion

The results of applying the burned area algorithm to the 2000-2005 time series of 250m MODIS data are expressed as a map of fire return interval in Figure 2-1. The spatial pattern and sharp edges of burned areas seen in the map accurately reflect how burns tend to terminate at boundaries caused by distinct land cover changes. E.g., burned areas are truncated as one moves from the woodlands to agricultural areas along the western border of the MGR and northwestern border of SNP.

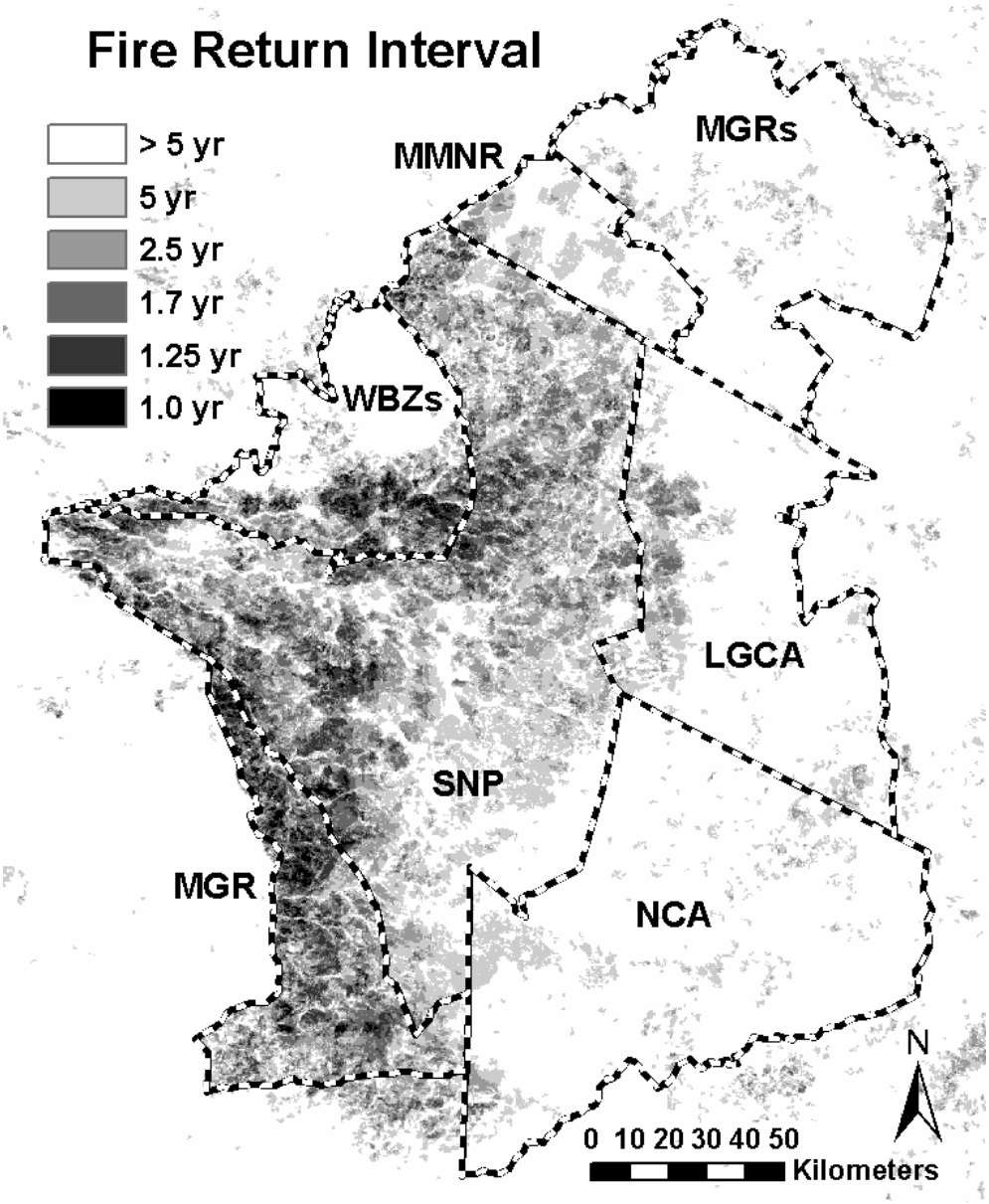

Figure 2-1 : Based on five year time series May 1, 2000 to April 30, 2005. Zones are the Serengeti National Park (SNP), Maswa Game Reserve (MGR), Ngorongoro Conservation Area (NCA), Loliondo Game Controlled Area (LGCA), the western buffer zones (WBZs) encompassing the Grumeti and Ikorongo Reserves and adjacent Tanzanian wards, the Maasai Mara National Reserve (MMNR), and Mara group ranches (MGRs).

Burned areas appearing during the existing time gaps in the MODIS time series might have been missed. The effect is limited by the briefness of the time gaps and the likeliness of subsequent detection. Our analysis of pre- and post burn BAI values showed that 30 days after the fire the BAI values of 96.6% of all burned pixels in 2003 remained above their pre-burn level. During the field campaign S. Eby observed, but not explicitly measured, black char visibly covering burned areas at least two weeks after the fire. The burned area algorithm itself provides further evidence for the lasting detectability of the burned areas. It only accepts areas as burned if they are detectable in two subsequent 10-day composites.

Producer's and user's accuracies determined from an ASTER satellite image pair and field data are given in Table 2-1. The Kappa coefficient is shown to test whether the classification results are significantly better than if the map had been generated by assigning classes randomly (Congalton 1991). Kappa for the accuracy assessment with ASTER data was $\kappa_{ASTER} = 0.81$, and for the accuracy assessment with field data Kappa was $\kappa_{Field} = 0.74$, in both cases representing strong agreement. Overall accuracies are high for both the ASTER (90.3%) and field (87.1%) assessments, with no individual accuracy less than 74.4%, thus the maps exceed accuracy requirements for thematic products as recommended by (Thomlinson et al. 1999). The validation datasets and the data used for training the algorithm originate from different years. This is a vindication of the accurate performance of the algorithm over several years.

Table 2-1: Error Matrix. B: burned pixels; UB: unburned pixels; PA: producer's accuracy; UA: user's accuracy; Italic ciphers: overall accuracy.

Class	B ASTER	UB ASTER	UA %	B Field	UB Field	UA %
B MODIS	870	15	98.2	166	1	99.4
UB MODIS	190	1045	81.6	57	224	79.7
PA %	82.1	98.6	*90.3*	74.4	99.6	*87.1*

The algorithm's ability to detect burns accurately can be explained in three ways. The first is that in the study area, burned areas are generally large enough to be well resolved at a resolution of 250 m. Second, the spectral index used to detect burned areas (the BAI) was designed to maximize its sensitivity to char, which presents >50% of a burned area. Third, char visibly persists for more than 10 days after burning, allowing the detection of burned pixels even using 10-day composites.

The algorithm was trained using data from one dry season. It is therefore optimized for burned area detection during the dry season months and less so for the wet season. However, the dry season shows by far the greatest amount of burning.

Lower accuracies for burned than for unburned areas indicate that the algorithm is underestimating burned areas. In particular, some small, isolated burned areas are excluded erroneously as misclassified cloud shadows. Other burns are missed in cases of persistent cloud cover or data gaps. Fractional burns are likely not detected by either the algorithm or the accuracy assessment methods. The algorithm was trained using visually interpreted MODIS imagery and the accuracy assessment was carried out using visually interpreted ASTER imagery, both of which require clearly visible and non-patchy burns. Data collected in the field for accuracy assessment only included areas at least 50% burned.

2.5. Conclusion

The described burned area algorithm holds the potential for further improvement and advancement to an operational status. We expect that the algorithm will be applicable to other savannas that also exhibit a dominant and temporally persistent char layer. Future research could test the feasibility of extending the methods geographical validity by incorporating training data from areas without a temporally persistent char layer (if so, we expect that the decision tree procedure would select a band or index other than the BAI). We anticipate the high resolution burned area data produced by this study to be of great value for fire management and future investigations of fire ecology in the Serengeti-Mara region.

Chapter 3: Woody Cover Changes in the Serengeti-Mara Savanna Environment from 2000 to 2005 - A Remote Sensing Approach

3.1. Abstract

Woody plants are important for savanna ecosystem functioning and habitat characteristics. Changes of woody canopy cover on regional scales can only be realistically determined with analysis of remotely sensed data. We determine woody cover changes in the Serengeti-Mara-Narok (SMNR) savanna environment in East Africa using for the first time a spatially comprehensive, consistent methodology over the entire SMNR region. Percent woody cover (PWC) ground truthing data were collected at 157 field plots throughout the Serengeti – Mara region in East Africa. The field data were used as training to derive PWC estimates from two Landsat ETM scenes using a random forest approach. The Landsat derived PWC served as training data for estimating yearly PWC from a time series of MODerate-Resolution Imaging Spectroradiometer (MODIS) 16-day composites at 500 m resolution. Annual metrics were calculated from the MODIS time series. Metrics significantly correlated with burned areas were disregarded to avoid false detection of woody cover change. Locations of training areas with minimal woody cover change through time were identified by selecting pixels with no statistically significant temporal trends in any of the metrics. The most important metrics were based on the near-infrared and mid-infrared bands (MIR), MODIS bands 2 and 7. MIR throughout the year showed high

separability of woodlands and grasslands except during the wet season. The results indicate overall increases in the Serengeti central and northern woodlands, decreases in the Maswa Game Reserve and less intense decreases in the Serengeti western corridor, Maasai Mara National Reserve and Mara pastoral areas. Results agree well with tree and shrub counts determined from 24 time series of ground-based photographs at 10 locations in Serengeti. This study provides a basis for the analysis of potential drivers of woody cover change, such as fire regime and browsing pressure.

3.2. Introduction

The balance between woody and herbaceous plants in savannas is dynamic. Woody cover in the Serengeti-Mara-Narok region (SMNR) in Kenya and Tanzania has a documented history of change over the last 120 years as a result of fire, herbivory, and climate variations (Dublin 1991). The objectives of this study are to determine recent (2000 to 2005) trends in woody cover over the entire SMNR region and to develop a methodology to do so.

Woody cover plays a critical role for ecosystem functioning (Scholes and Archer 1997). The woodland to grassland ratio defines savanna structure. Changes in woody cover affect the habitat characteristics of grazers, browsers, predators, and birds. Wildebeest (*Connochaetes taurinus*) are the dominant grazing animal in SMNR and depend on abundant grass food resources (Mduma et al. 1999). Wildebeest prefer open savanna habitat and avoid woodlands with greater predation risk (Darling 1960). They tend to enter thick brush only under conditions of high ground-level visibility, e.g. after fire (Talbot and Talbot 1963). Woody plant material is a major food source

for elephants, which consume large quantities in the Maasai Mara National Reserve (MMNR) (Dublin 1986). Acacia woodlands are the primary food resource for giraffes in Serengeti National Park (SNP) (Pellew 1983). Lions and other predators in SNP use shrubs as cover behind which they can stalk their prey (Schaller 1972). Vegetation structure in SNP is a causal factor for the distribution of individual bird species (Folse 1982). Changes of woody cover in savannas have a potential impact on carbon stocks (Asner et al. 2004). Woody cover levels in African savannas might change considerably in response to changing precipitation regimes as a consequence of climate change (Sankaran et al. 2005).

Our literature review has revealed no previous study producing a spatially comprehensive estimate of woody cover change over the entire SMNR region and none after 1991. Norton-Griffiths (1979) found decreasing woody cover in SNP between 1962 and 1972. He measured woody cover density representatively in confined areas around the photocenters of a series of 1:60,000 scale aerial photographs. Sinclair and Arcese (1995) determined tree and shrub coverage by use of ground-based photographs taken at fixed photopoint locations in the SNP woodlands. They found an upward trend from 1980 at least until 1991. Lamprey (1984) detected decreasing canopy coverage of trees and large shrubs between 1950 and 1983 in the Mara pastoral areas (MPA) by analyzing a time series of aerial photographs. Dublin et al. (1990) likewise found in a similar analysis decreasing woody cover for MMNR between 1950 and 1982.

Existing large scale continental and global percent tree cover products were generated from Advanced Very High Resolution Radiometer (AVHRR) data for 1992

at a spatial resolution of 1 km (DeFries et al. 1999; DeFries et al. 2000b), and from MODIS data for 2000 at 500 m resolution (Hansen 2003). DeFries et al. (2002) derived percent tree cover of tropical forests from an AVHRR time series at 8 km resolution for three 5-year intervals (1982–87, 1988–92, and 1992–99). Continental and global products are useful to provide large scale estimates and can help to determine locations of dramatic changes through time, e.g. forest clear cuts or rapid forest regrowth. These products are designed to work well at large regional and continental scales over a wide range of conditions and land cover types. They are less accurate at small regional or local scales and are not suited to assess prolonged changes in areas of low woody cover densities, such as savannas.

In light of the ecological importance of woody cover in savanna ecosystems and the lack of information on recent trends, we developed a method to determine woody cover changes for the entire SMNR savanna region in Kenya and Tanzania. The methodology uses satellite data from the Landsat Enhanced Thematic Mapper (ETM) and Moderate-Resolution Imaging Spectroradiometer (MODIS) sensor and field data. A MODIS time series from 2000 to 2005 was converted to annual metrics, which are related to the phenological behavior of vegetation. The use of multi-temporal remotely sensed data for vegetation classification based on derived phenological properties of vegetation has been described by a number of authors (Tucker et al. 1985; Townshend et al. 1987; Hansen et al. 2000; Hansen et al. 2002; DeFries et al. 2000a; Mayaux et al. 2004).

3.3. Study Area

The study area is defined by the range of the world's largest herds of migrating ungulates, the Serengeti and Maasai Mara wildebeest. The area extends across the Kenyan-Tanzanian border in East Africa. The geographic bounding coordinates are -0.8 to -3.8 degrees latitude and 33.8 to 36.1 degrees longitude. The core area is comprised of the Maasai Mara National Reserve (MMNR) and Serengeti National Park (SNP), excluding the short grass plains in the southeast (Figure 3-1). The study area includes the surrounding protected areas Maswa Game Reserve (MGR), Grumeti Game Reserve (GGR), Ikorongo Game Reserve (IGR), and the unprotected areas of the Kenyan MPA north of MMNR. Industrial agricultural areas have been excluded using ground truth data and visual interpretation of the Landsat ETM scenes described below. The study area totals 19,905 km^2.

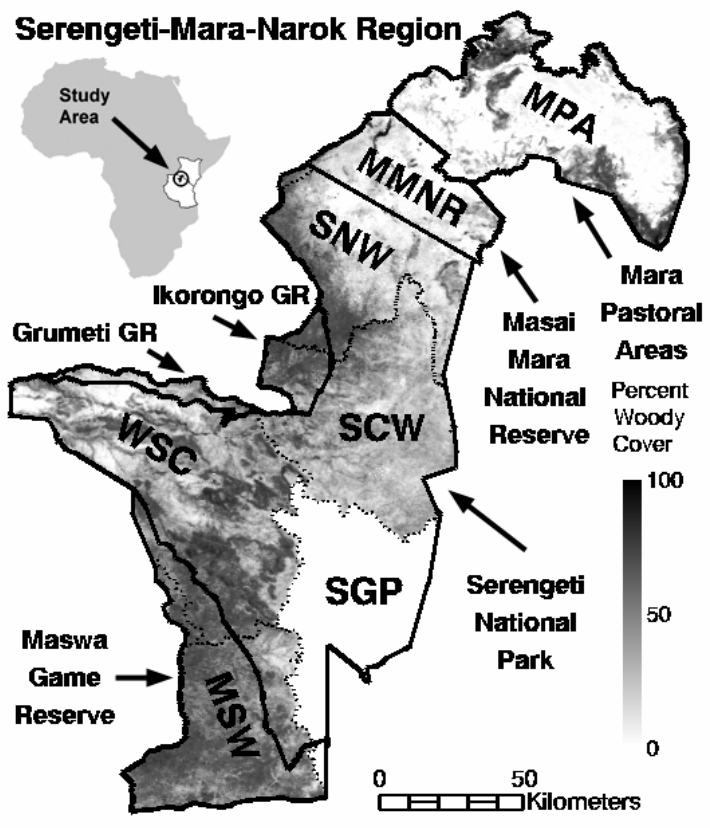

Figure 3-1: Serengeti-Mara-Narok region in East Africa. In Kenya: Mara pastoral areas (MPA); Maasai Mara National Reserve (MMNR). In Tanzania: Serengeti National Park (SNP); Maswa, Ikorongo, and Grumeti Game Reserves (GR). Ecological subregions of SNP, aggregated from Gerresheim (1974): Serengeti northern woodlands (SNW), includes northern Ikorongo GR; Serengeti central woodlands (SCW), includes southern Ikorongo GR; Western Serengeti and corridor (WSC), includes Grumeti GR; Serengeti short grass plains (SGP); Maswa (MSW). Percent woody cover shows MODIS derived PWC estimates averaged over all years 2000-2005.

For this study the combined areas of SNP, IGR, GGR, and MGR were subdivided into ecologically meaningful subregions. Gerresheim (1974) identified more than twenty land regions based on differences in topography, geology, soil, and vegetation. Pennycuick (1975) aggregated these land regions in her analysis of

seasonal wildebeest movements to a smaller number of more manageable units. For purposes of this study the Gerresheim regions were combined in the same way to represent the northern woodlands: SNW (Gerresheim regions 3, 4, 7, 8); central woodlands: SCW (10, 11); western Serengeti and corridor: WSC (9, 12, 13); and the woodlands of the Maswa Game Reserve including southwesternmost SNP: MSW (17, 19).

The climate is characterized by a distinct rainy and dry season. In most years the precipitation pattern is bimodal with the main rainy season from March to May and short rains in November and December. Precipitation increases from 500 mm per year in the southeastern plains of SNP to 1,200 mm in northwestern MPA (Sinclair 1995). Dominating vegetation types are tree-, shrub- and grass savannas. Open grasslands occur predominantly in southern SNP, MMNR and northern MPA and are often combined with dwarf shrubs. Continuous tall shrublands are most common in MSW, and otherwise appear in mixed land cover types, along drainage lines and on hilltops. Woodlands occupy large parts of northern and western SNP, MSW and parts of MPA and are often associated with hilly or dissected topography. Dense forests can be found along the Mara and Grumeti Rivers and in some hilly regions (Stelfox et al. 1986; Sinclair 1975; Serneels and Lambin 2001b; Reed et al. 2004).

The Serengeti short grass plains (SGP) were excluded from this study for both methodological and ecological reasons. The area was delineated as described in Gerresheim (1974) (region 14). It receives the lowest amount of precipitation within SMNR and has high grazing pressure. As a consequence its grass cover is exceptionally low during the dry season, exposing bare soil. Bare soil surfaces can

significantly affect the spectral reflectance of a landscape, which is a common problem for remote sensing of vegetation (Huete and Tucker 1991). None of the training areas in this study are located in the plains area and do not reflect their unique spectral characteristics. The second reason for excluding SGP is the principal lack of shrubs and trees due to its subsurface calcium carbonate hard pan. The hard pan is impermeable for roots and in combination with highly saline and alkaline soils prevents the establishment of significant, lasting woody cover (Sinclair 1979b).

3.4. Methods

Field measurements of percent woody cover (PWC) were collected in the study area. The field data were used to derive PWC from two Landsat ETM scenes from 2000, using a random forest approach. The Landsat derived PWC served as training data to derive woody cover changes from 2000 to 2005 using a MODIS time series (Figure 3-2). Each of these steps is described in detail below.

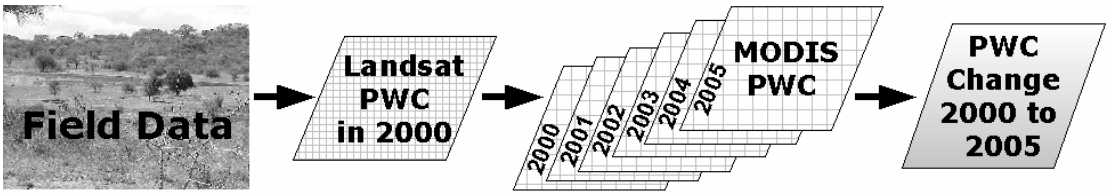

Figure 3-2: Flow chart outlining the main methodological steps used in this study.

3.4.1. Field Data

Field data was collected throughout the study area as described in Reed et al. (2004). For this study a total of 157 field plots were collected between 1998 and 2003. Percent tree and shrub canopy coverage was visually estimated in 30m x 30m plots, separately for trees and shrubs. Trees were defined as woody plants taller than

2m, and shrubs were defined as woody plants less than 2m tall. Shrubs also included dwarf shrubs, which in many areas were only 20 cm tall. Initial plots were placed in part at random and later stratified after using Landsat satellite imagery and field observations in order to capture the full range of vegetation structural types present in the study area. For this study tree and shrub coverage was combined into a single PWC measure. The conversion was based on the assumption that tree and shrub canopies overlap by half of their extent, e.g. a vegetation plot with 30% tree cover and 50% shrub cover would have 50% + 0.5 * 30% = 65% woody cover.

3.4.2. Landsat Data

PWC was derived from two Landsat ETM scenes and field measurements. The two scenes are part of the same swath and hence no radiometric normalization was necessary. The scenes were acquired on February 12, 2000, WRS path/row 169/61 and 169/62. The Landsat data covered 77% of the study area except the western part of WSC. The two scenes were mosaicked together and georeferenced using road locations collected in the field. Landsat bands 1-6 were converted from digital numbers (DN) to radiance and Normalized Difference Vegetation Index (NDVI) values were calculated. NDVI is a ratio calculated from red and near infrared (NIR) spectral reflectance as NDVI = (NIR-Red) / (NIR+Red). The index is a measure of vegetation properties related to photosynthesis and biomass production. It can be used to study phenological and biophysical characteristics of the vegetated land surface.

Training areas for estimating PWC from the Landsat scenes were derived from field measurements. Each field measurement was taken within a homogeneous

area of the same vegetation type covering at least the area of one 30x30 m Landsat pixel. The PWC field value was assigned to the corresponding Landsat pixel at that location. Additional training pixels were selected for each plot by region growing in the ERDAS Imagine (v. 8.7) software package. Spectral euclidean region growing thresholds were selected interactively. For every 10th training pixel the PWC value, the radiance values for all six Landsat bands and the NDVI value were exported, resulting in a total number of 4025 training records. PWC was estimated from the Landsat scenes using a random forest approach. The resulting PWC layer was aggregated to MODIS resolution by calculating the mean for each corresponding 500 m MODIS pixel.

3.4.3. Random forest analysis

Random forests are based on the concept of regression trees. Morgan and Sonquist (1963) introduced the statistical concept of classification trees as a way to efficiently analyze and reduce large numbers of independent qualitative data variables. The idea was further developed by Breiman et al. (1984) and in the form of classification and regression trees applied to quantitative data. The method, also known as recursive partitioning regression, is a binary tree structured classifier. It repeatedly splits the supplied data into two subsets, by using the independent predictor variable values to define the splitting rules. Predictor variable and critical value for the split rules are chosen so that the homogeneity of each subset is maximized based on the residual sum of squares of the dependent variable, in this case PWC. This process is repeated until all subsets are pure or there are not enough data left to split further. Accuracy of the classification result can further be improved

by generating not one but several trees, each based on a different random sample of the training data, a technique called "bagging" (Breiman 1996). Regression trees have been used successfully to predict vegetation characteristics from remotely sensed data, but only at coarser spatial resolutions of 500 m to 8 km (Hansen et al. 1996; Friedl and Brodley 1997; DeFries et al. 1998; Hansen et al. 2000; Lawrence and Wright 2001; Moisen and Frescino 2002; Hansen 2003; and others).

Breiman (2001) advanced the concept of regression trees by introducing random forests. Random forests use a higher level of randomness and grow a larger number of trees. This method can achieve higher prediction accuracies than either standard regression trees or bagging. Each tree in the random forest is grown using a different random subset of the training data records. At each node in the tree a random subset of the independent predictor variables is used to find the optimal split, rather than using all the predictor variables as is the case for regular regression trees. The trees are always grown to the maximum depth. The predicted value for classification is the average of the classification results of all trees. Ham et al. (2005) found that random forest techniques improve the classification accuracy of Hyperion spaceborne hyperspectral remote sensing data. The importance of each independent variable at a certain node can be determined by analyzing by how much the purity of a child node decreases when the training data for that variable is permuted while all others are left unchanged. The purity of the child nodes are determined by calculating the mean squared error (MSE).

In this study 4025 training records were imported into the R 2.2.1 statistical software and a total number of 1000 random forest trees were generated using the R

randomForest 4.5-16 package. Each random forest tree was applied to the Landsat mosaic. The resulting 1000 different PWC estimates were averaged to arrive at the final Landsat PWC product.

3.4.4. MODIS Data

Changes in PWC from 2000 to 2005 were derived by using the Landsat PWC data to drive the classification of a MODIS time series. The MODIS instrument aboard the Terra satellite platform began collecting data at the end of February 2000. For this study we used the MODIS/Terra Vegetation Indices 16-Day L3 Global product version 4 at 500 m resolution (MOD13A1). Woody cover was estimated for six 12-month periods starting on March 5, 2000 and ending on March 4, 2006. In the following text one year corresponds to a 12-month time period starting March 5. This time period was chosen to cover the maximum available MODIS record.

The MODIS time series was filtered for clouds. Pixels were replaced with a no-data value if the MOD13A1 quality assessment (QA) bits 0 and 1 indicated cloud contamination (bit combination 10) or no data due to bad quality (bit combination 11). For each year annual phenological metrics were calculated. The metrics served as independent variables to predict PWC. Initially, a total of 180 metrics were calculated for each pixel, based on basic descriptive statistical parameters for each band and on interrelations between the bands (Table 3-1). Hansen et al. (2002) used a similar selection of metrics.

Table 3-1: 180 metrics calculated for each pixel and 12-month period. Red: red reflectance (MODIS band 1, centered at 645 nm); NIR: near infrared (band 2, 858.5 nm); MIR: mid infrared (band 7, 2130 nm); NDVI: Normalized Difference Vegetation Index.

1) Minimum, maximum, mean, median Red, NIR, MIR, and NDVI (16 values)
2) Minimum, maximum, mean, median of the four darkest and four brightest values of Red, NIR, MIR, and NDVI (32 values)
3) The corresponding Red, NIR, MIR, and NDVI value at the annual minimum, maximum, and median Red, NIR, MIR, and NDVI (36 values)
4) The corresponding minimum, maximum, mean, median Red, NIR, MIR, and NDVI at the four brightest and four darkest values of Red, NIR, MIR, and NDVI (96 values)

Remote sensing analyses of savanna environments often suffer from the presence of burned areas. Burned areas manifest themselves in many metrics, resulting in spectral contamination and a potential source of error. We address this problem by excluding metrics significantly correlated with the presence of burned areas. Burned areas were mapped from 2000 to 2004 throughout the study region using MODIS daily observations at 250 m resolution (Chapter 2). The burned area product provided burned and unburned areas throughout each year. All 180 metrics layers of each year were sampled using 15 circular areas of 12.5 km radius. Each sample area had a distance of 25 km from neighboring circles. The separation distance of 25 km was chosen to minimize spatial autocorrelation between individual measurements. The separation distance was determined by calculating empirical variograms for all 180 metrics of the year 2003. The variograms were calculated

using the S-PLUS SpatialStats 1.5.7 module of the statistical software package S-PLUS 7.0 for Windows. The derived variograms showed a typical range of 25 km or less. For each circular sample area the overall mean values for burned and unburned pixels were calculated. This was done for all 15 circles for each year and for all metrics. This resulted in a maximum number of 75 spatially independent measurements of burned and unburned areas per metric. Circles containing less than 10% of either burned or unburned pixels were disregarded. For each metric the overall means of burned and unburned areas were calculated. The two means were tested for significant differences using Student's t-test. 56 of the 180 original metrics showed a statistically significant difference between burned and unburned areas at p=0.05. These metrics were disregarded and only the remaining 124 metrics were used for the woody cover analysis. Figure 3-3 shows burned areas in 2003 and examples of a strongly burned area related metric (minimum NIR of the four darkest NDVI) and not significantly burned area related metric (annual mean NDVI).

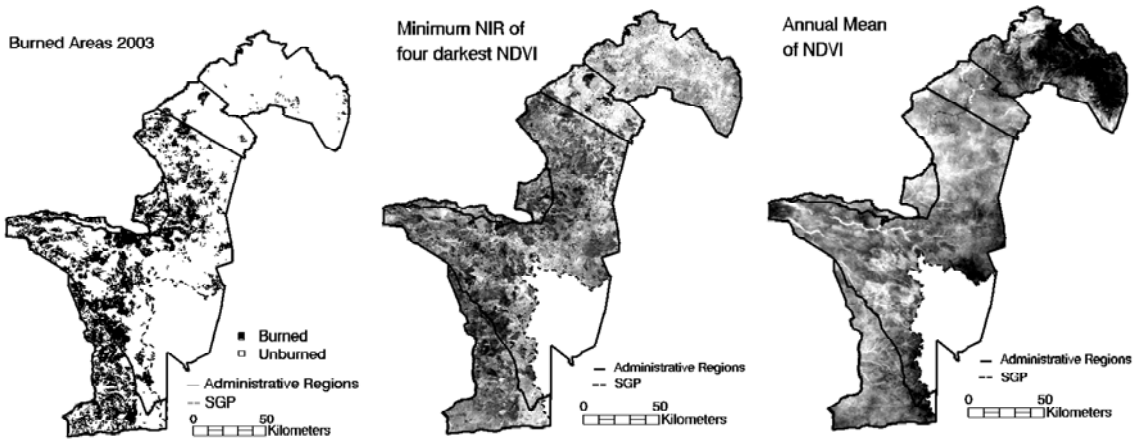

Figure 3-3: Left: burned areas in 2003; Middle: burned area related metric (minimum NIR of the four darkest NDVI); Right: not significantly burned area related metric (annual mean NDVI).

3.4.5. MODIS time series analysis

Annual PWC was calculated for the available MODIS time record from 2000 to 2005. Training data for all years were derived from the Landsat PWC estimates for 2000. The selection of Landsat training data is based on two assumptions. First it is assumed that parts of the study area do not show any or minimal changes in PWC. Secondly it is assumed that these areas are characterized by showing no statistically significant trend through time in any metric. For each of the 124 metrics a linear regression was fitted, separately for each pixel. The significance of the regression coefficient was determined using a t-test. A total of 1,968 pixels of the MODIS time series showed no significant trend from 2000 to 2005 in any of the metrics at $p=0.025$. From these pixels 5% were set aside for later validation. The validation pixels were chosen using stratified random sampling, ensuring a better distribution over the existing PWC range. The remaining pixels served as training areas with stable woody cover.

The Landsat derived PWC values were aggregated to MODIS resolution by calculating the mean PWC value for each MODIS pixel. At the location of each training pixel the Landsat PWC value and the corresponding 124 metric values were exported, separately for each year. From each set of exported values 1000 random forest trees were generated. The trees were applied to the metrics data sets and averaged, resulting in annual woody cover estimates. The processing was done in IDL Version 6.2 for Linux using code developed for this project. Processing time for one year of MODIS data was ~3.5 hours on a i686 PentiumII processor at 3.00GHz.

Changes of PWC between consecutive years varied substantially. These variations are most likely due to irregularities in the remote sensing data introduced by atmospheric disturbances and variations in sun- and view angles. Rather than assessing annual changes, we estimated woody cover changes over the entire six-year time period by predicting PWC for 2000 and 2005 using linear regression individually for each pixel. Relative change was calculated as the ratio of predicted PWC for 2005 over predicted PWC for 2000 (Figure 3-5).

3.4.6. Validation

The Landsat PWC product was validated against 36,220 unused training pixels set aside before the random forest analysis. For each percentage value present in the training data (whole numbers 0 to 100) the mean PWC value of the corresponding pixels was calculated. Pearson's correlation coefficient between the training data and the corresponding mean values of the PWC estimates was $r = 0.947$ (Figure 3-4).

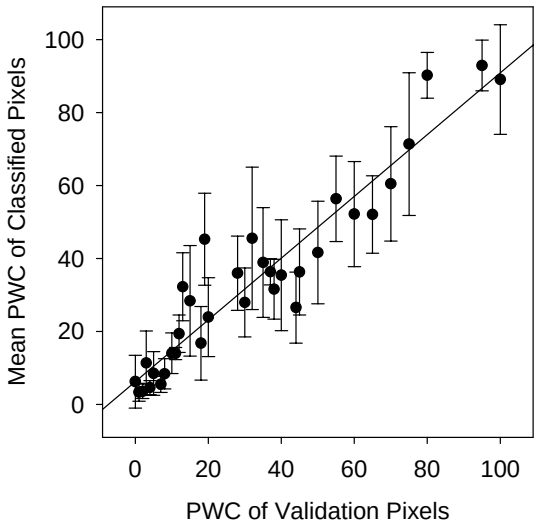

Figure 3-4: PWC of Landsat validation pixels versus mean PWC and standard deviation of corresponding pixels with PWC estimates.

The data allowed to determine error ranges of the MODIS woody cover change product in two ways. The first estimate is based on the predicted PWC values for the training areas with stable woody cover. Ideally the 2005 to 2000 PWC ratio for these stable areas would be 1.000. The observed mean over all training pixels was 1.007 and the standard error 0.100.

The second estimate is based on the standard errors for the predicted PWC values for 2000 and 2005, derived from the MODIS time series. The standard error was calculated as shown in Equation (1).

$$s_{\hat{w}} = \sqrt{s_{w\cdot t}^2 \left(\frac{1}{n} + \frac{\left(W_t - \overline{W}\right)^2}{\sum w^2} \right)} \qquad (1)$$

where

$s_{\hat{w}}$	Standard error	$s_{w\cdot t}^2$	Standard deviation
W	PWC	n	Number of years

$s_{\hat{w}}$	Standard error	$s^2_{w \cdot t}$	Standard deviation
t	Time in years	$\sum w^2$	Sum of squares of deviations for PWC

The minimum and maximum values within the standard error range were determined for the 2000 and 2005 predicted PWC values (Figure 3-5). The extreme values within the error range for the two years were used to calculate error limits. The error limits are the smallest and largest of the two ratios (Equations 2.1; 2.2; 2.3; 2.4; 2.5).

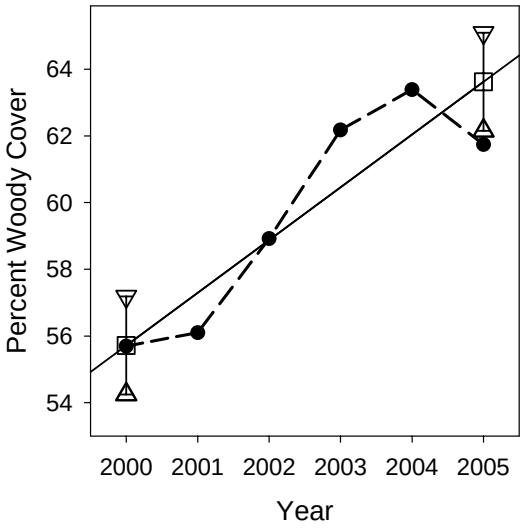

Figure 3-5: Yearly PWC estimates (filled circles) for one pixel in western SNW (latitude -1.690; longitude 34.751). The graph also shows the regression line, predicted values for 2000 and 2005 (squares) and associated error ranges (triangles).

$$r_{(05/00)} = \hat{w}_{(05)} / \hat{w}_{(00)} \quad (2.1)$$

$$\hat{w}_{(t)\min} = \hat{w}_{(t)} - s \quad (2.2)$$

$$\hat{w}_{(t)\max} = \hat{w}_{(t)} + s \quad (2.3)$$

$$r_{(05/00)\min} = \min(\hat{w}_{(05)\min} / \hat{w}_{(00)\min}, \hat{w}_{(05)\max} / \hat{w}_{(00)\max}) \quad (2.4)$$

$$r_{(05/00)\max} = \max(\hat{w}_{(05)\min} / \hat{w}_{(00)\min}, \hat{w}_{(05)\max} / \hat{w}_{(00)\max}) \quad (2.5)$$

where

$r_{(05/00)}$	Predicted PWC ratio 2005 to 2000	$\hat{w}_{(05)}, \hat{w}_{(00)}$	Predicted PWC for 2005, 2000
$\hat{w}_{(T)\min}$	Minimum predicted PWC at time t	$\hat{w}_{(t)\max}$	Maximum predicted PWC at time t
s	Standard deviation	$r_{\min}$	Minimum predicted PWC ratio
$r_{\max}$	Maximum predicted PWC ratio		

The yearly MODIS PWC estimates were validated using the 5% unused training pixels, set aside before the PWC estimation. For these validation pixels the Pearson's correlation coefficients r were calculated between the PWC aggregated from Landsat and a) the resulting MODIS PWC classification result for each year and b) the average MODIS PWC classification results over all years (Table 3-2).

The correlation coefficients for individual years were between r = 0.843 and r = 0.892. The correlation coefficient was highest with r = 0.921 for MODIS PWC averaged over all years (Figure 3-6). This increased correlation underlines the validity and benefit of our approach of analyzing data combined over all years, rather than PWC estimates for individual years.

Table 3-2: Correlation coefficient R between Landsat PWC and MODIS PWC estimates for the 94 MODIS validation pixels. R is shown for each individual year and for PWC results averaged over all years.

Year	**R**
2000	0.883
2001	0.843
2002	0.867
2003	0.863
2004	0.852
2005	0.892
All	0.921

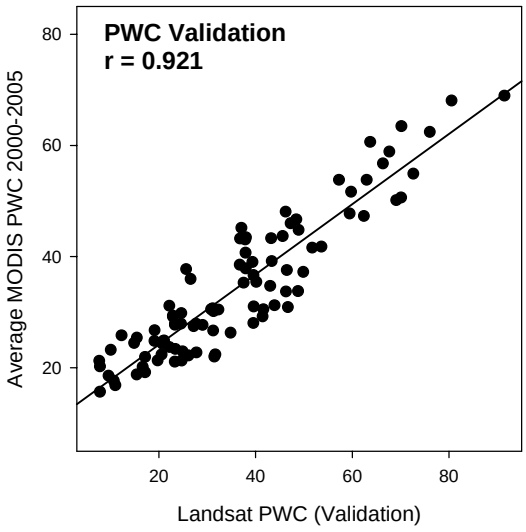

Figure 3-6: Correlation between Landsat PWC and MODIS PWC estimates averaged over all years 2000 to 2005 for the 94 MODIS validation pixels. Correlation coefficient r=0.921.

Further validation of the MODIS woody cover change product was conducted using field data. Sinclair and Arcese (1995) collected a time series of oblique photographs taken from elevated locations in the Serengeti woodlands. The photo

time series was continued at 10 locations in SNW and SCW until 2003 (Sinclair, A.R.E., unpublished; locations shown in Figure 9). His analysis identified overlapping spatial areas on photo pairs and counted large (adult) and small (juvenile) trees, but no low or dwarf shrubs. For this study the tree counts were converted to average yearly rates of change c (Equation 3).

$$c = \frac{N_0}{N_0 - ((N_0 - N_t)/t)} \qquad (3)$$

where t is the time in years, N_0 the number of trees at time 0, and N_t the number of trees at time t. At some locations multiple frames were taken in different compass directions. For these locations the annual rate of change was calculated separately for each frame and then averaged over all frames. The average annual rate of change of MODIS derived PWC was also calculated according to Equation (2) with N_t and N_0 replaced by the predicted PWC estimates for 2005 and 2000. A 3x3 low pass filter was applied to the MODIS rate of change product, a standard technique for validation of remote sensing products to minimize geolocation errors (Jensen 2005).

The photo point and MODIS PWC time series measure slightly different parameters and the magnitude of the change rates are not directly comparable. However, at 9 of 10 locations both the photo point and MODIS time series agree in increasing woody cover (Table 3-3). The one location of disagreement also has the least temporal overlap between the two time series.

Table 3-3: Woody cover change at 10 locations in SCW and SNW derived from ground based photographs and from the MODIS time series. Explanation of column headings: Year: latest year of photo collection before 2003; Frames: number of photos taken in different compass directions; Lat/Long: latitude and longitude of photo point locations; Photo: Average annual rate of change of tree counts in the photo point time series; MODIS: Average annual rate of change of PWC in the MODIS product.

Year	Frames	Lat / Long	Photo	MODIS
1999	2	-1.78 / 35.02	1.023	1.040
1999	1	-1.71 / 34.90	1.022	1.018
1992	4	-2.32 / 34.84	1.043	1.024
1991	6	-2.31 / 34.69	1.023	1.016
1991	3	-1.77 / 34.86	1.051	1.025
1991	3	-2.38 / 34.79	1.037	1.002
1991	2	-2.32 / 34.84	1.017	1.021
1991	1	-2.36 / 34.76	1.050	1.008
1991	1	-1.65 / 34.92	1.040	1.028
1988	1	-1.85 / 35.24	1.044	0.986

3.5. Results and Discussion

3.5.1. Metrics

The methodology used in this study performs a subpixel classification resulting in a percentage estimate of woody plants versus other land cover types, i.e. herbaceous vegetation and bare soil. Woody plant and grass vegetation types are distinguishable within a single pixel, based on their spectral reflectance. Other authors have attempted subpixel classification based on spectral mixture analysis, which assumes a linear mixing process of endmember spectral reflectances, each

endmember representing a pure land cover type (Roberts et al. 1993). Linear mixture models do not account for complex nonlinearities in the spectral mixing process resulting from vegetation structural characteristics and the orientation of photon scatterers (plant parts) in three-dimensional space. Random forest analysis on the other hand is non-parametric and not confined by the assumption of linearity. However, the spectral metrics selected by the random forest algorithm similarly exploit unique differences in reflectance characteristics between woody plant and grass vegetation types.

Figure 3-7 shows the importance of the metrics used in the random forest analysis for the year 2000 in form of their MSE values. Table 3-4 lists the 9 most important metrics, their MSE values, and the mean rank of each metric according to their MSE values averaged over all six years 2000-2005.

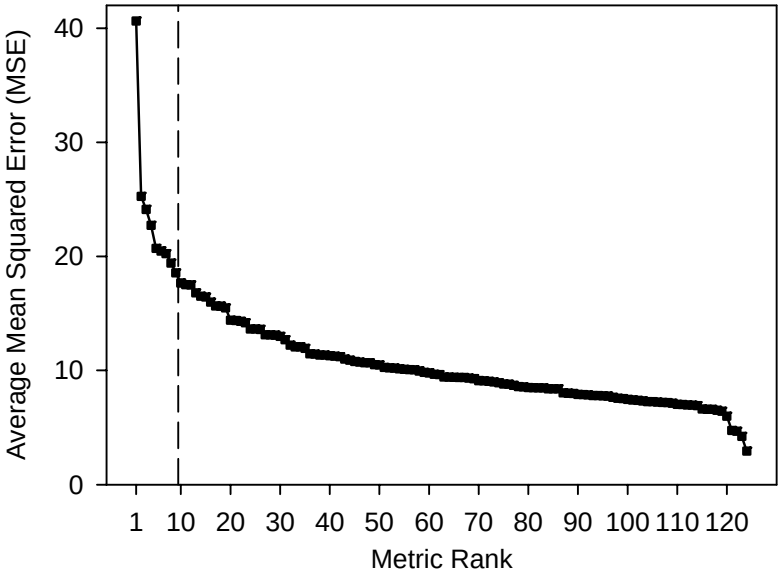

Figure 3-7: Average mean squared error (MSE) of all metrics for the year 2000 used in the random forest algorithm. The metrics have been ordered in decreasing

importance. The 9 most important metrics (left of dashed line) are discussed in the text.

Table 3-4: Metrics for 2000 ranked in order of their importance. MSE: mean squared error, indicating importance; Mean Rank: average rank of the listed metrics over all years 2000-2005.

Metric	**MSE**	**Mean Rank**
Annual median of NIR	40.63	1
Annual mean of MIR	25.26	2
Mean MIR at four darkest NDVI	24.11	3
Mean of four brightest MIR	22.73	8
NIR at median NDVI	20.70	59
Maximum MIR at four darkest NIR	20.47	5
Annual median of MIR	20.23	9
Maximum of four darkest NDVI	19.41	10
Median NIR at four brightest Red	18.55	11

The most important metric is the annual median of NIR for both 2000 and on average for all years. Figure 3-8 shows the temporal development of mean red, MIR, and MIR spectral reflectances and NDVI, for low (0-20) PWC and high (60-80) PWC areas within the study region for the 12-month time period starting on March 5, 2000. In the NIR band low and high density woody areas show the least overlap during the dry season, for which the annual median NIR metric is selecting.

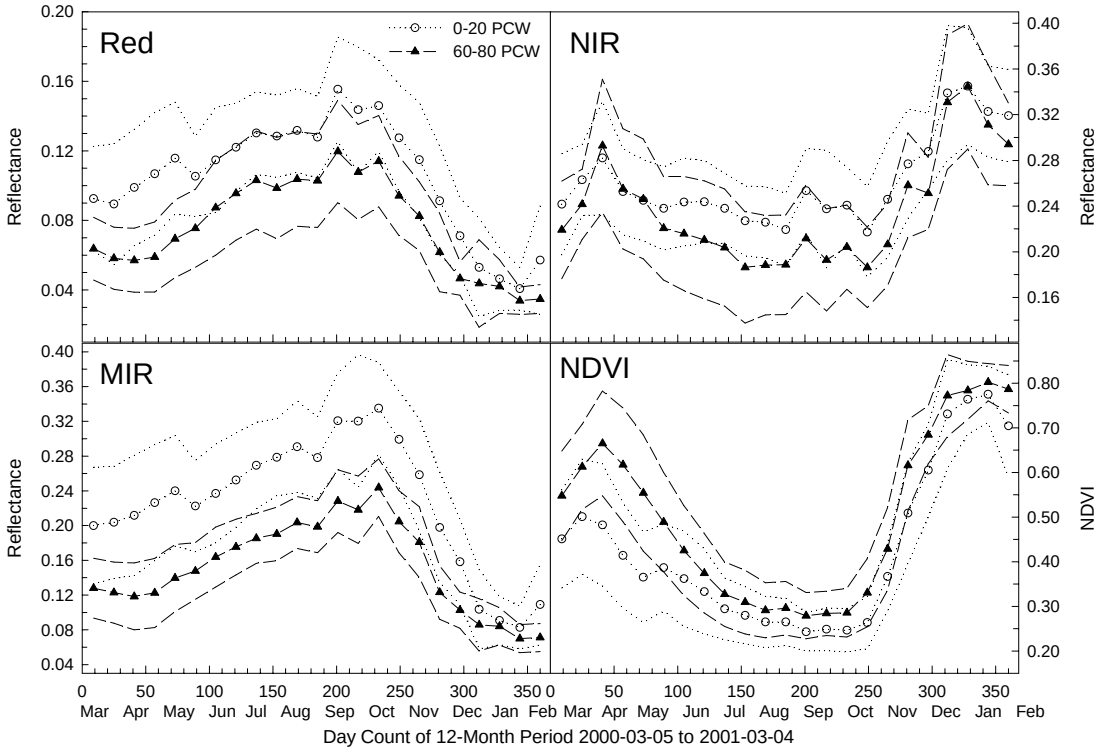

Figure 3-8: Mean +/- 1 standard deviation of spectral reflectances and NDVI for areas of high (0-20) and low (60-80) PWC. The 12-month time period starts on March 5, 2000. Pixels of high and low PWC were selected from the Landsat PWC product and reflectance values averaged over each PWC range.

Our analysis showed that throughout the year MIR showed the highest consistent separability of low and high density woody areas except during the height of the wet season (day count 310-350 of the 12-month period). Five of the nine most relevant metrics for both 2000 and on average over all years use MIR. The annual mean of MIR ranks second of all metrics. Mean MIR at four darkest NDVI, mean of four brightest MIR, maximum MIR at four darkest NIR, and annual median of MIR all select for the dry season months August through November. This can be explained by the distinct phenological characteristics of grass and herbaceous cover, which is

most apparent in the dry season. Woody plants have better access to moisture in deeper soil layers because of their extended root systems and thus remain green longer into the dry season than the grasses (Walter and Breckle 2002). Woody vegetation in the Serengeti ecosystem is dominated by *Acacia* and *Commiphora* species. Timing and degree of leaf loss vary during the dry season. Many Acacia species may not experience any leaf loss at all or retain their leaves long into the dry season (Herlocker 1976).

Asner et al. (1998) found that throughout the NIR, 700-1300 nm, green leaves of woody species in grasslands, shrublands, savannas, and tropical woodlands had higher reflectance values than grass species (t-test, $p<0.05$). No significant reflectance differences were observed over the shortwave infrared range (SWIR), 1500-2450 nm, although the narrower MODIS MIR spectral range, 2105-2155 nm, still showed the largest difference within the SWIR range. However, their study focused on the spectral separability of green leaves prevalent during the wet season, while the MODIS time series analysis presented here takes advantage of phenological differences apparent during the dry season.

3.5.2. Woody Cover Changes

Figure 3-9 illustrates the spatial distribution of relative changes in woody cover between 2005 and 2000. Increases in MPA concentrate in the wider area along the Narok – Sekenani road, which runs from Narok in north-central MPA south, then continues southwest parallel to the southern border of MPA. These observations are supported for the area along the road south of Narok by anecdotal evidence about expanding whistling thorn (*Acacia drepanolobium*) bush lands since the late 1990s.

This information was received from local residents during our field campaign in March 2003. Further increases occur in MMNR south of the border to MPA, in central SNW and north-central SCW, and in the hilly areas west of Seronera (eastern-central WSC). Decreases in MPA are most prominent in the larger area north of Talek just north of the central border between MPA and MMNR. This area is under high grazing and browsing pressure from cattle and goats, which could result in declining woody cover. Further decreases occur in confined areas of easternmost MMNR, western GGR (northwestern border of WSC), and throughout MSW, all of which have been subject to frequent burning events over the time period of this study (Chapter 2).

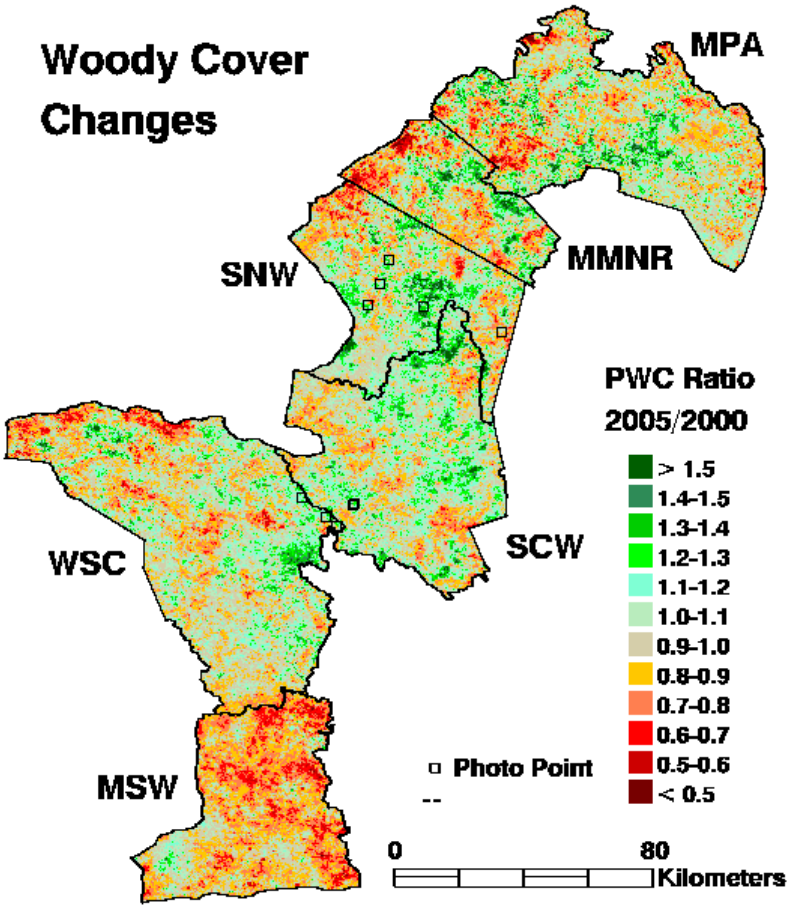

Figure 3-9: Ratio of PWC 2005 to 2000. Squares represent photo point locations for ground truthing.

On a regional level the results indicate that overall woody cover in the Serengeti woodlands (SNW, SCW) is increasing, while woody cover in MMNR, MPA, and WSC is decreasing, with MSW showing the strongest decrease (Figure 3-10). Regional averages provide a generalized picture of overall changes, however the frequency histograms (Figure 3-11) show that among the subregions regional differences are most distinct for MSW and otherwise largely overlap.

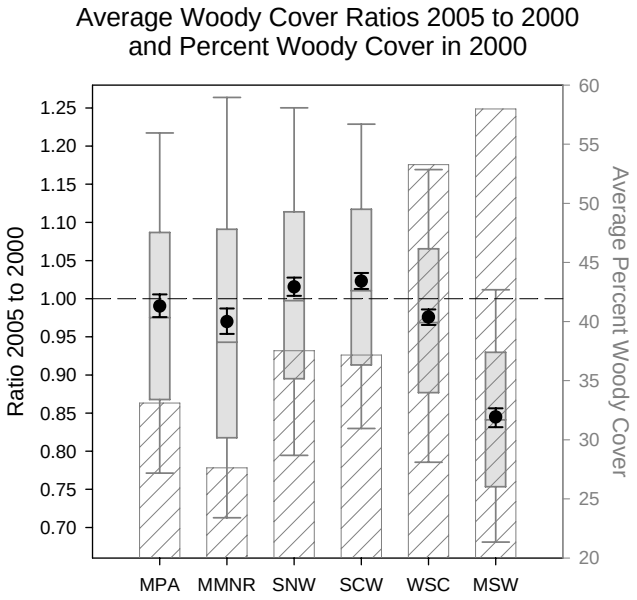

Figure 3-10: Average of woody cover ratios 2005 / 2000 per administrative region (black squares), ordered from north to south. Box plots (plain gray boxes and lines) show quartiles and extreme values within 1.5 interquartile ranges of the box top and bottom. Error ranges for the regional mean values were calculated from the standard error of the predicted PWC values. The upper and lower error limits are the corresponding regional means of the minimum and maximum ratios. PWC (line-pattern filled bars) was averaged for each region from the Landsat derived PWC product for the year 2000.

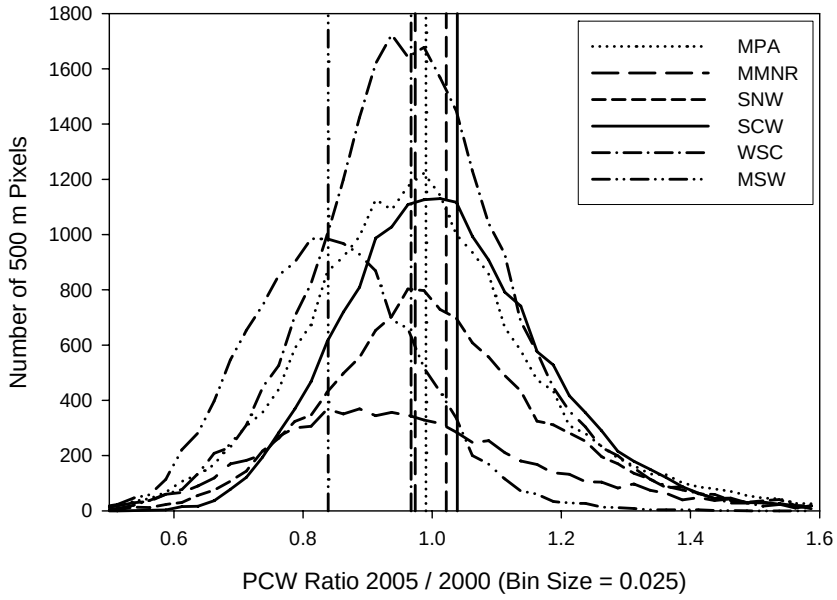

Figure 3-11: Frequency histograms of PWC ratios 2005 / 2000 per region.

Regional woody cover changes observed in our analysis generally agree with previous long-term trends reported in the literature. Lamprey (1984) found decreasing canopy coverage of trees and large shrubs in MPA between 1950 and 1983 by analyzing a time series of aerial photographs. Dublin (1991) documented declining woody cover in MMNR since the 1950s, continuing into the 1980s. Serneels and Lambin (2001a) reported pronounced loss of vegetative cover in MPA unlike other parts of the SMNR ecosystem, based on her analysis of a time series of Landsat data covering the period 1975-95. Walpole et al. (2004) found in 1999 MMNR largely dominated by grasslands and expects a continued decline of woody resources in the face of increasing browsing pressure. Sinclair and Arcese (1995) found increasing woody cover in the woodlands of SNP since the 1980s using a time series of ground based, oblique photographs at 22 permanent locations. We have found no references

in the literature to observations of woody cover trends in MSW. The habitats, plants and animal assemblages of MSW have received little attention by scientists in the past and are rarely known (Sinclair 1995). The results of this study underline the need to focus more attention on the Maswa area and investigate potential driving factors for woody cover changes which might be related to the fire regime and browsing pressure.

Important factors controlling woody cover in African savannas are thought to include climate, nutrient availability, fire and herbivory (Scholes and Archer 1997). Decreasing PWC in MPA and MMNR in comparison to increasing PWC in SNW and SCW has been linked to a combination of variations in fire regimes and elephant numbers (Dublin 1995). The fire regime and different levels of browsing pressure might be relevant factors explaining observed trends in MMNR, SNP and MSW.

3.6. Conclusion

The methodology described in this paper maps changes of woody cover in the SMNR savanna environment. The effectiveness of the algorithm can be explained on three grounds. Firstly the large number of observations obtained by MODIS reduces cloud problems by selecting pixels with minimum cloud coverage. Secondly the high temporal frequency of the MODIS time series exploits differences in phenological characteristics of woody and herbaceous plant cover. Woody plants stay green longer into the dry season while grasses and herbs become senescent earlier. Thirdly the exclusion of burned area related metrics minimizes unwanted contamination of the spectral reflectance of vegetation by char coal. Cloudiness, precipitation and other environmental conditions affecting vegetation and remote sensing observations

change between years. Our algorithm adjusts to changing conditions by being trained separately for each year.

While NIR reflectance during the dry season provided the single most important metric for the separation of woody cover from grasslands, the majority of the most important metrics were based on MIR reflectance. Our analysis showed MIR to provide superior separability of woody cover from grasslands throughout the year, except during the height of the wet season. The results of this study show the importance and benefit of selecting the best season for distinguishing woody and herbaceous cover and taking advantage of differences in phenology.

Limitations of the methodology result from the quality of the remote sensing data. Adjacent pixels in a MODIS 16-day composite might have different acquisition dates resulting in varying atmospheric conditions, sun illumination and view angles. These effects are mitigated, but not eliminated, by the MOD13 compositing algorithm (Huete et al. 1999). The heterogeneity of the MODIS data manifests itself in considerable variations between annual PWC estimates of subsequent years. For this reason estimation of year-to-year changes in woody cover has proven difficult. As a consequence we analyzed medium-term changes over a six-year time period using linear regression to arrive at a more reliable product. This approach assumes linear changes in woody cover between the first and last year of observation. It does not capture irregular patterns of woody cover change through time, resulting in a potential negative impact on the detectability of such changes by the type of time series analysis used in this study.

The results of this study provide the first spatially coherent data layer of woody cover changes over the entire Serengeti-Mara region. This study succeeds previous work focusing on smaller subregions, or using spatially limited samples representative for a larger area. The algorithm developed in this study works well for the study region and is likely to be superior to regional or global algorithms aiming to work well everywhere.

Further research will be undertaken using these data to investigate the importance of the fire regime and related factors on woody cover changes. Fire regime is characterized by fire frequency and intensity. Fire intensity is related to fuel load, which in turn is controlled by precipitation, grazing pressure and decomposition. Spatially explicit data layers of woody cover changes and controlling factors allow investigating their importance at different spatial scales.

The spatially explicit woody cover change product can be useful for analyzing changing habitat characteristics and potential impacts on wildlife distribution. Wildebeest prefer open grasslands. Lions and other predators use larger shrubs to stalk their prey and changes in woody cover might impact the number of kills. Woody cover also characterizes bird habitat.

Most savannas are dynamic systems and experience woody cover changes over time as part of natural cycles. The methodology described in this paper can be applied to other savanna areas to study such changes over longer time periods as the data archive of high resolution remote sensing imagery expands.

Chapter 4: Estimation of Fire Intensity in the Serengeti-Mara Region

4.1. Abstract

Fire plays an important role in the Serengeti-Mara ecosystem in East Africa. Fire intensity is a key factor of the fire regime and has a potential impact on vegetation structure. Fire intensity in the Serengeti-Mara region has not been estimated before over larger areas or extended time periods. In this study we use a model to estimate fire intensity between May 1, 2000 and April 30, 2006. This is done in a spatially coherent manner over the entire region. Fire intensity was estimated as a function of fuel load, fuel moisture, air relative humidity, wind speed, slope, and combustion completeness. Fuel load was calculated from grass production as a function of rainfall, while accounting for competitive effects from woody plants and herbivores. Fire events were derived using burned area maps from a previous analysis. Results indicate similar levels of fire intensity throughout the ecosystem despite significant differences in rainfall, mainly due to the leveling effect on fuel load levels by abundant large grazers.

4.2. Introduction

The Serengeti-Mara region in East Africa is subject frequent fires (Chapter 2). Fire is thought to control both the structure and composition of vegetation in the Serengeti National Park; particularly when considered in combination with grazing, browsing and climate (Norton-Griffiths 1979).

A key characteristic of the fire regime is fire intensity. It can have a significant impact on the level of fire damage to woody plants (Frost and Robertson 1987). Higgins et al. (2000) suggested that fire events and variations in fire intensity are driving factors for generating heterogeneity in woody plant distribution in savannas. The objective of this study is to estimate fire intensity in a spatially explicit manner in order to support subsequent analysis of fire impact on woody cover levels.

The most common index of fire intensity is fire line intensity, introduced by (Byram 1959). Fire line intensity is strongly related to damage of above-ground woody plant parts (Higgins et al. 2000). It is calculated as (Equation 1):

$$I = H \times W \times R \qquad (1)$$

where I is the rate of heat release per unit time and unit of spread of the fire front (kJ s^{-1} m^{-1}); H: heat yield per unit of fire fuel consumed (kJ kg^{-1}); W: fuel consumed (kg); R: rate of spread of the fire front (m s^{-1}).

Fire intensity within the study area has only been analyzed during single fire events at point locations and not over larger spatial extents or longer time periods. Field measurements of fire intensity are labor and resource intensive and not feasible over large regions. Stronach and McNaughton (1989) made point measurements of fire temperature and combustion completeness (CC) at several locations in Serengeti in June 1986. Both CC and fire temperature can be used as indicators of fire intensity, however, the measurements were not repeated or expanded over larger areas. The same authors also determined ash color-lightness and found that ash shades were correlated with CC and fire temperature. Gray-white ash indicated very-high-energy fires, while black ash indicated very-low-energy fires. McNaughton et al. (1998)

proposed to use these observations to derive fire intensity from albedo measurements by satellites. Sa et al. (2005) did so by relating ground based measurements of pre- and post fire spectral reflectance to CC. The data was collected during the SAFARI 2000 Third Intensive Field Campaign in the Western Province of Zambia. The relationship found between the change in spectral reflectance and CC was reversed from the findings of Stronach and McNaughton (1989). Darker surfaces indicated higher-intensity fires and were related to higher CC than lighter surfaces. The authors did not provide a calibrated method to use spaceborne remote sensing data to derive CC. The authors also expected post-fire spectral reflectance to be dependent on vegetation type. They suggest determining CC from spectral reflectance might not be feasible or severely limited for understory burns in woodland savannas. The non-constant relationship between ash color and fire intensity suggests a need to consider alternative approaches for estimating fire intensity over large areas.

Fire intensity or combustion rates might also be derived from fire radiative energy which can be measured by means of remote sensing (Kaufman et al. 1996; Wooster 2002). Spaceborne remote sensors however only provide near-instantaneous views of the fire front at the time of the satellite over pass. Such views are unlikely to provide reliable estimates of fire intensity across a fire's full spatial extent as they spread across the landscape. Airborne sensors could theoretically hover over a burning area and measure fire radiative energy on a more continuous basis. This approach is not practical though and has not been attempted in the study area.

This study estimates fire intensity in order to provide a basis for analyzing impacts on woody cover. The impact of fire on vegetation can also be estimated using

approaches that measure the qualitative variable of fire severity. Fire severity is often estimated using the normalized burn ratio (NBR) (van Wagtendonk et al. 2004; Epting et al. 2005, Cocke et al. 2005). NBR is a spectral index, computed from satellite or airborne remote sensing data as the difference between near-infrared (NIR) and middle-infrared (MIR) reflectance divided by their sum (Key and Benson 2006). NBR provides a relative measure of burn effects on vegetation by comparing pre- and postfire index values and needs to be calibrated using field data. It has been shown, however that the use of NBR in savanna using satellite data can be problematic. NBR is often insensitive to changes due to burning, as spectral change in NIR and MIR reflectance can often occur parallel to the NBR isolines (Roy et al. 2006). Therefore NBR does not seem an appropriate choice for the objectives of this paper.

Given the limitations of existing approaches, this study estimates fire intensity using an alternative approach based on a spatially explicit model. The model is applied over the entire Serengeti-Mara region between May 1, 2000 and April 30, 2006 and estimates fire intensity for areas burned twice or more. Fire intensity is derived using an empirical equation formulated by Higgins (2006) as a function of fire fuel load, fuel moisture, air humidity and wind speed. The empirical model is further adjusted for slope effects and combustion completeness. Fire fuel load is derived from grass biomass production as a function of rainfall, grazing and woody canopy effects.

4.2.1. Study Region

The study area encompasses the Serengeti National Park (SNP), the Maswa, Grumeti, and Ikorongo Game Reserves in Tanzania, as well as the northerly adjacent Maasai Mara National Reserve (MNR) in Kenya (Figure 4-1). The Serengeti short grass plains, as delineated by Gerresheim (1974) (Region 14), were excluded from the study area due to its extremely low fire frequency (Chapter 2). The study area has been subdivided into ecologically meaningful subregions after the Serengeti Landscape Classification by Gerresheim (1974). The classification delineates landscape units of uniform and distinct geomorphologic, hydrologic, soil, vegetation and microclimatic characteristics. Pennycuick (1975) combined these land regions into larger, ecologically meaningful units, corresponding to the seasonal occupancy by wildebeest. Gerresheim regions 17 and 19 were combined to the Maswa sub region (MSW); 9, 12, and 13 to the western Serengeti and Corridor sub region (WSC); 10 and 11 to Central Serengeti (CSG); and 3, 4, 7, and 8 to the Maasai Mara and Northern Serengeti sub region (MNS). MNS was further separated into northern Serengeti (NSG) and the Maasai Mara National Reserve (MNR). MNR is separated from SNP by the Kenyan-Tanzanian international border and is under different management. All subregions were restricted to the protected areas.

The dominant vegetation types are woodland and grassland savanna. Mean annual precipitation (MAP) in the study area increases along a southeast-northwest gradient from ca. 700 mm in the Southeast to 1100 mm in the Northwest (Sinclair 1979b). The dominant grazing animal in the ecosystem is the migrating wildebeest

(*Connochaetes taurinus*) with a total number of ca. 1.3 million (Campbell and Borner 1995).

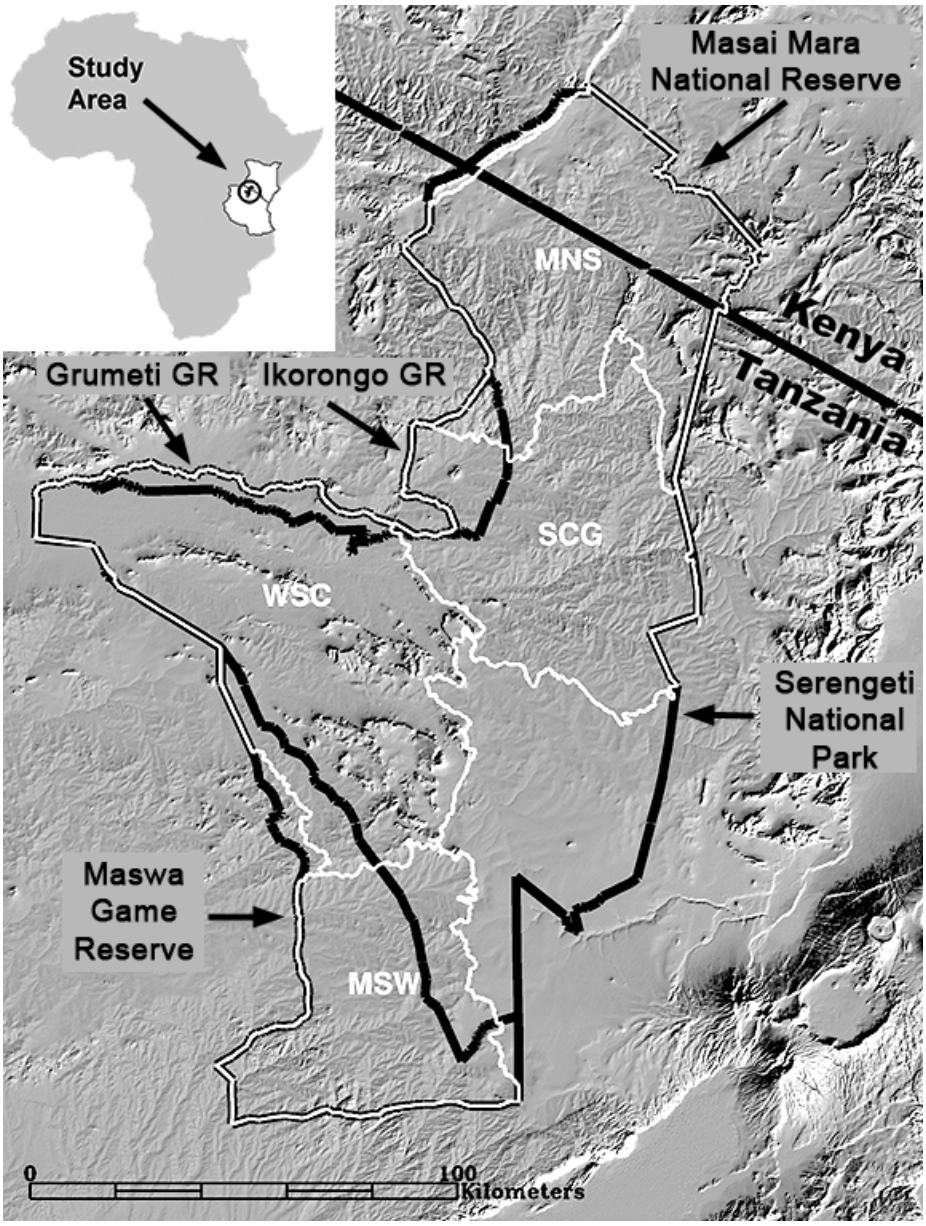

Figure 4-1: Shaded relief of the Serengeti-Mara region, lighted from the Southeast. Subregions: Maasai Mara and Northern Serengeti (MNS); Central Serengeti (CSG); Western Serengeti and Corridor (WSC); Maswa Game Reserve including southeastern most Serengeti (MSW). Source of digital elevation model: (CIAT 2004).

4.3. Methods

Fire intensity was calculated fore each 250 m x 250 m pixel using empirical relationships. The relationships were derived using multiple regression and data from 200 monitored fires in South African savannas by (Trollope 1998; Higgins 2006), ($P < 0.01$, d.f. = 196, $R^2 = 0.60$). The empirical fire intensity relationship was further refined in this study by including a slope factor A, and a combustion factor C (Equation 2; Figure 4-2).

$$I_{t(i,j)} = A_{(i,j)}(2939 + 08726C_{t(i,j)}G_{t(i,j)} - 7948\sqrt{M_{t(i,j)}} - 13.66H_{t(i,j)} + 200W_{t(i,j)}) \quad \textbf{(2)}$$

where I_t is fire intensity (kJ s^{-1} m^{-1}); t: time of fire occurrence; *(i,j)*: pixel coordinates of fire location; A: the average slope factor; C: combustion factor; G: grass biomass (kg ha^{-1}); M: fuel moisture (proportion of oven-dry grass weight); H: relative air humidity (%); W: wind speed (m s^{-1}). Data sources and all parameters in Equation (2) are described in sequence below. The fire intensity model was implemented in the ENVI/IDL version 4.2 software package.

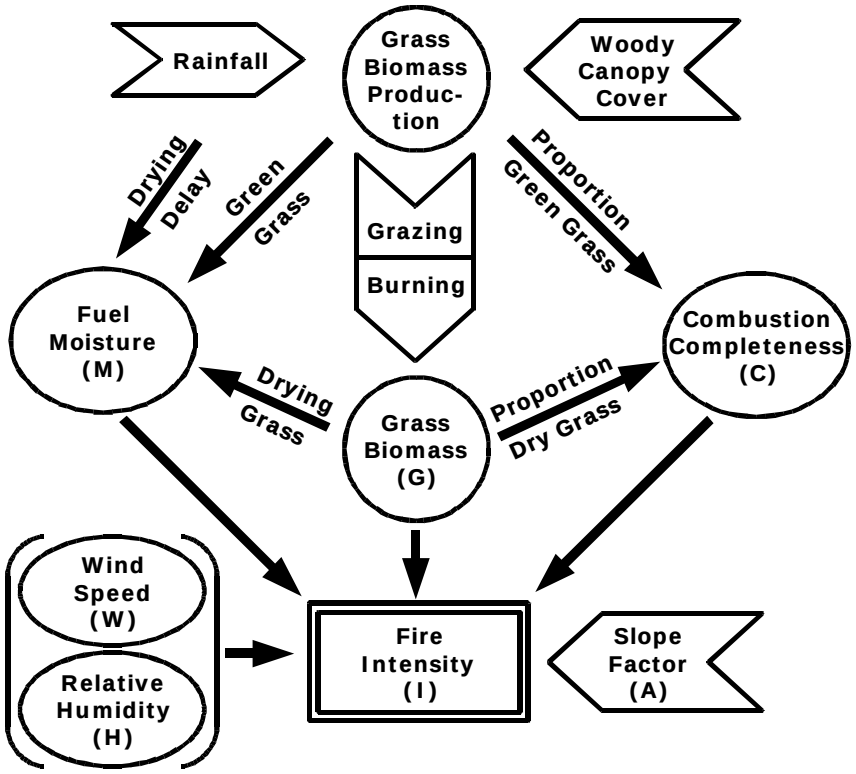

Figure 4-2: Flow chart of the fire intensity model used in this study. Block arrows represent input data sets; ovals contain derived data sets; letters in parenthesis correspond to Equation (2); tall parentheses embrace parameters for which constant values were used.

4.3.1. Data Sources

Spatially explicit data layers used to estimate fire intensity are listed in Table 4-1. Daily rainfall was derived from the Famine Early Warning System (FEWS) Dekadal Rainfall Estimates (RFE) version 2.0. RFE data are produced by an automated algorithm using observations from the Meteosat satellite in the infrared band, rain gauge reports, and microwave satellite observations (Xie and Arkin 1997). One dekad refers to a 10-day time period.

Slope was derived from the hole-filled version of the Shuttle Radar Topography Mission (SRTM) digital elevation model (Farr and Kobrick 2000; CIAT

2004). Slope values were aggregated from 90 m to 500 m horizontal resolution by calculating the mean slope value for each 500 m pixel.

Table 4-1: List of data sources.

Parameter	Spatial Resolution	Data Source
Rainfall (2000-2006)	0.1 deg (ca. 10 km)	Famine Early Warning System (FEWS) Rainfall Estimates (RFE 2.0) (Xie and Arkin 1997)
Woody Canopy Cover	30 m	Chapter 3
Burned Area	250 m	Chapter 2
Slope	90 m	Shuttle Radar Topography Mission (SRTM), (Farr and Kobrick 2000; CIAT 2004)

The following sections describe and justify the approaches used to develop each term in the fire intensity equation (equation 2) and figure 4.2.

4.3.2. Average Slope Factor A (Equation 2)

The average slope factor (A) is based on empirical relationships derived from experimental fires in Australian savannas, which are in close agreement with relationships developed elsewhere in the world (McArthur 1967; Luke and McArthur 1978; Cheney and Sullivan 1997). A fire burning up a 10° slope burns with twice the fire intensity than a fire on level ground, doubling again when burning up a 20° slope. A fire burning down a 20° slope will only burn with a quarter of the fire intensity on level ground. From these data and the associated diagram in Luke and McArthur (1978) three equations were derived (Table 4-2).

Table 4-2: Equations for calculating the slope factor. Equations were derived from empirical relationships and diagram in McArthur (1967).

Slope s (degrees)	Slope Factor a
$s < -10$	$a = -5/s$
$-10 < s < 10$	$a = \exp(0.0693s)$
$s < 10$	$a = 0.2s$

For the purpose of this study it was assumed 50% of the fires burn up and 50% down slope. The average slope factor A was calculated accordingly as the mean of these two effects (Table 4-3).

Table 4-3: Equations for calculating the average slope factor A as the average of up and down slope burning fires.

Slope s	Average Slope Factor A
$\|s\| > 10$	$A = 2.5/\|s\| + 0.1\|s\|$
$\|s\| < 10$	$A = 0.5 \times (e^{0.0693\|s\|} + e^{-0.0693\|s\|})$

4.3.3. Combustion Completeness C (Equation 2)

Based on experimental burning of tropical grasses in the laboratory combustion in tropical savannas is typically assumed to be almost complete, with fires consuming 90-95% of available fuel (Lobert et al. 1990; McNaughton et al. 1998). In contrast, fuel consumption in all of 18 experimental fires in Serengeti was considerably lower (Stronach and McNaughton 1989). However, these fire experiments were carried out in the early dry season, June 16-19, 1986. It has been shown, that fires later in the dry season generally do burn the fuel almost completely.

Shea et al. (1996) found mean grass consumption by fire generally exceeding 95% over a range of semi-arid to moist savannas in South Africa and Zambia (MAP 600-1170 mm). Hoffa et al. (1999) reported a CC of 98% at the end of the dry season in dambo grassland savannas in Zambia and Sa et al. (2005) measured a CC of 93% in the same savanna type in Zambia during the late dry season of 2000. In order to account for the effect of seasonally changing levels of CC, we used in this study an empirical equation described by Hoffa et al. (1999). The equation calculates the combustion factor C as a function of the proportion of green grass contained in the fire fuel load (Equation 3).

$$C = -2.1309 \times p + 1.3821 \qquad (3)$$

where C is the combustion factor, and p is the green grass dry matter fraction of total dry matter. In this study green grass is defined as the fraction of newly grown grass, before the start of the curing process.

4.3.4. Grass biomass G (Equation 2)

Fire fuel load was assumed to be equivalent to above ground grass biomass (G). G was estimated over three stages, namely: grass production, grass consumption by grazers, and burning events. G accumulates through time. Meaningful estimates of G require a starting point at which the baseline of G is known. Such a baseline is provided by burning events. After the first burning event (determined using the MODIS-based method described in Chapter 2), G was set to a baseline of zero, assuming a complete burn. In this study G and fire intensity was therefore only analyzed for pixels after the first burning event. G since the last burning event was calculated as (Equation 4):

$$G_{t(i,j)} = \sum_{t0}^{t} G_{p(i,j)} - \sum_{t0}^{t} G_{g(i,j)} \qquad (4)$$

where G_t is grass fuel load (kg ha^{-1}); t: time after the last burning event at time t_0; *(i,j)*: pixel coordinates; G_p: grass production (kg ha^{-1}); G_g: grass consumption by grazers (kg ha^{-1}). Grass production G_p and grass consumption G_g are discussed in the following two subsections.

Grass Production G_p (Equation 4)

Grass production G_p was estimated using an empirical linear relationship with rainfall, adjusted for competitive effects with woody plants and for the stimulating effect of grazing (Equation 5).

$$G_p = f \times l \times g \times R \qquad (5)$$

where G_p is the predicted above-ground grass production (kg ha^{-1}); f: woody canopy factor; l: grazing stimulating factor; g: growth coefficient (kg ha^{-1} mm^{-1}), and R rainfall (mm). The derivation of the terms for f, l and g are described in turn below.

a) The woody canopy factor (f) in Equation 5 was derived as a function of percent woody canopy cover. Woody plants can inhibit grass production as a result of light, nutrient and water competition. The effect of woody plants on grass production can be positive or negative. Belsky et al. (1989) compared grass productivity beneath and between canopies of Acacia tortilis and Adansonia digitata (Baobab) trees in semi-arid Tsavo National Park in Kenya (MAP 490 mm). Tree neighborhoods there had an increasing effect on grass production. Weltzin and Coughenour (1990) likewise found a positive impact of trees on herbaceous biomass production under tree canopies in the savanna environment in Turkana District, northwestern Kenya (MAP 395 mm). Grunow et al. (1980) on the other hand found a 38.6% reduction of

peak green grass biomass beneath tree canopies in the Nylsvley savanna in South Africa (MAP 610 mm). Mordelet and Menaut (1995) found in humid savanna in Côte d'Ivoire (MAP 1200 mm) a 26% lower grass production underneath tree canopies than between trees. Increased grassland productivity is most often associated with low-tree-density, drier savannas and decreased productivity with higher-tree-density, more humid savannas (Belsky et al. 1989). The Serengeti-Mara environment has an overall MAP of ca. 700 mm and corresponds to the higher-tree-density, more humid savanna type (Herlocker 1976; Chapter 3). We therefore assume an overall decreasing effect of woody cover on grass production in the study area.

A relationship was derived describing the effect of woody canopy cover on grass production. Grunow et al. (1980) reported peak live above-ground grass biomass for three levels of woody cover density in the Nylsvley savanna. These measurements were used to calculate the relative effect of tree canopy cover on peak above-ground grass biomass (Table 4-4).

Table 4-4: Relative effect (Factor) of percent tree canopy cover on peak live green grass biomass in the Nylsvley savanna in South Africa (Data source: Grunow et al. 1980).

Tree Canopy Cover (%)	Grass Bio-mass (g/m2)	Factor
0.0	88	1.000
27.5	78	0.886
100.0	54	0.614

Here we assume that the effect of woody canopy cover on peak green biomass is the same as the effect on grass production. Jameson (1967) presented a mathematical relationship to fit percent tree canopy cover and understory herbage production (Equation 6).

$$y = h - a(1 - e^{bX})^m \qquad (6)$$

where y is herbage production; x: percent tree canopy coverage; b: regulates curvature; m: inflection point, h: y-intercept; a: lower asymptote. Values for b and m were approximated iteratively using data from 14 locations in pinyon-juniper (*Pinus edulis, Juniperus* spp.) woodland in northern and central Arizona. We use the same approximated values for b and m, set h to 1, replace herbage production values with the factor values from Table 1 and solve for a using least squares fitting. Equation 7 and Figure 4-3 describe the fitted equation for calculating the relative effect of woody canopy cover on grass production.

$$f = 1 - 0.432(1 - e^{-0.036P})^{0.5} \qquad (7)$$

where f is the woody canopy factor and P percent woody cover.

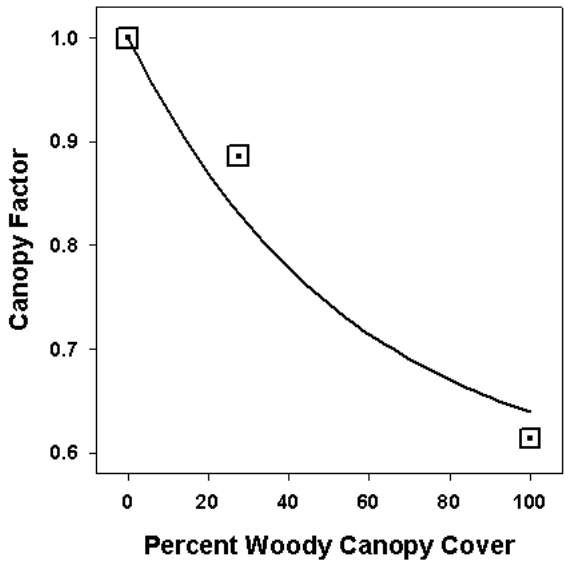

Figure 4-3: Function describing the relative effect of percent woody canopy cover on grass production (woody canopy factor f). Dotted squares represent measurements from the Nylsvley savanna (Grunow et al. 1980).

b) The grazing stimulation factor (l) in Equation 5 was derived from aboveground primary grass productivity (APP) data for SNP. McNaughton (1985) found substantially greater (APP) of forage in areas exposed to grazing compared to fenced control areas. Annual APP in fenced areas with no grazing was 357 g m^{-2} yr^{-1}, while APP in unfenced, grazed areas averaged 664 g m^{-2} yr^{-1}. The grazing stimulating factor *l* was calculated as the ratio between APP (grazed) over APP (fenced), l = 1.860.

c) The growth coefficient (g) in Equation 5 was estimated by Higgins et al. (2000) as g = 3.369 kg ha^{-1} mm^{-1} using data from southern African savannas ($P < 0.0001$, d.f. = 71).

Grass Consumption by Grazers Gg (Equation 4)

Grass consumption by grazers was estimated from animal numbers and their seasonal distribution. The main grazing animals in the Serengeti ecosystem are wildebeest (*Connochaetes taurinus*), zebra (*Equus burchelli*), buffalo (*Syncerus caffer*), Thomson's gazelle (*Gazella thomsonii*), topi (*Damaliscus korrigum*), and impala (*Aepyceros melampus*) (McNaughton 1985; Campbell and Borner 1995). The daily amount of grass consumed by grazers was calculated using animal census counts and daily food requirements (Sinclair 1975; FAO 1991; Bourn and Wint 1994) (Table 4-5).

Table 4-5: Census counts for main grazing animals per sub region. Grazing species in italic are migrating between subregions. Th. Gazelles: Thomson Gazelles; SNPR: Serengeti National Park Region, includes SNP, Grumeti Game Reserve, and Ikorongo Game Reserve; MSWG: Maswa Game Reserve. x: missing data. Census count for 1988, 1989, and 1990 were merged if no significant changes occurred. (*) Sum of census counts for SNP, and Ikorongo / Grumeti Game Reserves. The reported error is the larger of the individual census counts. (**) Animal census data for MNR were compiled from aerial censuses conducted by the Kenyan Department of Resource Surveys and Remote Sensing (DRSRS). Food Rq: daily food requirement per animal (kg grass dry matter per individual and day) (Sinclair 1975; FAO 1991; Bourn and Wint 1994).

Grazing Species	Sub-Region	Census Count	Standard Error	Census Year	Reference	Food Rq
Wildebeest	SNPR	1,300,000	x	2000	Thirgood et al. 2004)	4.23
Zebra	SNPR	191,028	11,550	1989/91	Campbell and Borner (1995)	4.78
Buffalo	SNPR	36,562	x	1992	Campbell and Borner (1995) (*)	8.41
Th. Gazelles	SNPR	355,493	21,576	1989/91	Campbell and Borner (1995)	0.72

Grazing Species	Sub-Region	Census Count	Standard Error	Census Year	Reference	Food Rq
Topi	SNPR	93,925	23,875	1991	Campbell and Borner (1995) (*)	2.85
Impala	SNPR	65,386	5,687	1988/89/91	Campbell and Borner (1995) (*)	1.69
Buffalo	MSWG	4,262	x	1988/89/91	Campbell and Borner (1995)	8.41
Impala	MSWG	3,204	42	1988/89/91	Campbell and Borner (1995)	1.69
Topi	MSWG	899	211	1988/89/91	Campbell and Borner (1995)	2.85
Buffalo	MNR	4,354	x	2000	DRSRS (**)	7.15
Th. Gazelles	MNR	11,623	x	2000	DRSRS (**)	0.72
Topi	MNR	2609	x	2000	DRSRS (**)	2.85
Impala	MNR	3580	x	2000	DRSRS (**)	1.69

Resident species were assumed to be ubiquitously distributed throughout their subregions. The migratory wildebeest and zebra follow similar circular migration routes every year. They typically occupy the Serengeti short grass plains from November to April, move northwest through WSC in May and June, pass through SCW in July, occupy MNS from August to October before returning to SGP (Pennycuick 1975; Campbell 1989; Mduma 1996; Thirgood et al. 2004). The northern, substantially smaller Mara-Narok migratory wildebeest and zebra herds mostly occupy areas north of MNR Serneels and Lambin (2001a) and were not included in the census counts. Table 4-6 shows the total amount of grass dry matter consumed per subregion in each season. Newly grown green grass is preferred by grazers and consumed first (McNaughton 1985). The model was adjusted to reproduce the same behavior. Any remaining food requirement is then satisfied by grazing a percentage of the remaining grass in the sub region.

Table 4-6: Total amount of grass dry matter (in t/day) consumed by the main resident and migratory herbivores in each subregion. Seasonal occupancy by migratory wildebeest and zebra changes between regions.

Region	Nov-Apr	May-June	July	Aug-Oct
SGP	6578	166	166	166
WSC	308	6720	308	308
SCW	221	221	6633	221
MNS	306	306	306	6718
MSW	44	44	44	44

4.3.5. Fuel Moisture M (Equation 2)

Fuel moisture is calculated by applying a drying factor. The drying factor is applied to newly grown grass starting after the first dekad with no rain. Once the drying process starts, subsequent rainfall has only a limited impact on curing (Cheney and Sullivan 1997). Fuel moisture of the curing grass is calculated using Equation 7 (Higgins et al. 2000).

$$M_c = M_{c,t-1} \times \exp(c \times t_{d,t}) \qquad (7)$$

where M_c is moisture content of curing grass (proportion of oven-dry weight); $M_{c,t-1}$: moisture content of curing grass in the previous time step; c: drying rate; $t_{d,t}$: number of drying days since the previous time step. Grass moisture content at the beginning of the curing process is around 200% of oven-dry weight. Perennial grasses, which are predominant in the study region, become fully cured after 9 weeks with a remaining moisture content of about 30% (Luke and McArthur 1978; Cheney and Sullivan 1997). A drying rate of c = -0.03 was chosen to reproduce these values.

Total fuel moisture Mt was calculated from the moisture content of green and curing grass as in Equation 8:

$$M_t = \frac{G_g + G_c}{G_G \times M_G + G_C \times M_C} \qquad (8)$$

where M_t is the moisture content (proportion of oven-dry weight); G_g: oven-dry weight of green grass; G_c: oven-dry weight of curing grass; M_g: grass moisture content at the start of curing; M_c: moisture content of curing grass.

4.3.6. Relative Humidity H and Wind Speed W (Equation 2)

Relative air humidity and wind speed were not available for the study area. Instead we applied the mean values found by (Trollope et al. 1991 in prep.) at the 200 fire locations used for the development of the fire intensity model. Average wind speed was W= 2.6 m s^{-1} and average relative humidity H = 36.6%.

4.3.7. Field Validation

Fire fuel load is the most important factor controlling fire intensity (Cheney and Sullivan 1997). Field validation was performed by the author for the grass biomass term G in Equation 2, representing fire fuel load. Grass biomass was measured in MNR during a field campaign in November 2003. Grass samples were collected at the center of seven relatively homogeneous grassland savanna areas extending at least 500 x 500 m. At each site grass biomass was clipped within 25 cm x 25 cm frames along a 100 m linear transect. Collection frames were placed along

the transect every 20 meters and in addition at locations where grass biomass visibly changed, i.e. at the start of each comparatively denser or less dense grass patch. The grass was clipped manually as close to the ground as possible, oven-dried at 120°C for 8 hours, and weighed. The average grass biomass of the sampled grassland area was interpolated from the grass weights in combination with their location along the transect. Table 4-7 shows the collection date, grass biomass collected in the field, and the model result of grass biomass. The correlation coefficient is r = 0.85.

Table 4-7: Date, latitude, longitude, grass biomass measured in the field (kg ha^{-1}), modeled grass biomass (kg ha^{-1}) and the difference between the two. Values are in increasing order of absolute deviation.

Date of Field Visit	Lat	Lon	Field Grass Biomass	Model Grass Biomass	Deviation
30 Nov 2003	-1.581	35.293	252	205	-47
30 Nov 2003	-1.577	35.303	113	191	77
30 Nov 2003	-1.571	35.292	408	225	-183
27 Nov 2003	-1.402	34.898	5,993	5,351	-642
26 Nov 2003	-1.579	35.170	876	2,468	1,592
22 Nov 2003	-1.459	35.097	649	2,499	1,850
21 Nov 2003	-1.579	35.170	467	2,468	2,001

The error range was estimated from the deviations between field data and model results (Equation 10).

$$e_G = \pm\sqrt{\frac{\sum (G_m - G_f)^2}{n-1}} \qquad (10)$$

where e_G is the error (g m^{-2}); G_m: the calculated grass biomass; G_f: field measurement of grass biomass, and n the number of observations. Using the values from Table 4 the error is then e_G = +/- 1,318 kg/ha. From e_G we can derive an approximate error

estimate for fire intensity by supplying e_G to Equation (2), assuming M, H, and W to be constant (Equation 11).

$$e_I = \bar{A}(0.8726 C_{\max} e_G) \qquad (11)$$

where $\bar{A}$ = 1.026651 is the mean average slope factor over the entire study area and C_{max} = 1.0 is the combustion completeness factor for complete combustion. The resulting error estimate for fire intensity is then e_I = +/- 1,180 kJ s^{-1} m^{-1}.

4.4. Results and Discussion

The results indicate similar levels of fire intensity in the subregions (Figure 4-4). At first this seems surprising: it could be expected that fire intensity would increase significantly in higher rainfall areas; particularly because higher rainfall increases grass biomass production, which in turn exerts most control on fire intensity. However, the lack of regional scale variations in fire intensity with precipitation can be explained by the dominance of large, migrating grazers. The main driver behind the migration of the ca. 1.3 million wildebeest and large numbers of zebras is availability of the food supply, controlled by rainfall (Pennycuick 1975; Boone et al. 2006). Grazing animals concentrate in areas of high rainfall and high grass production, exerting a leveling effect on grass biomass.

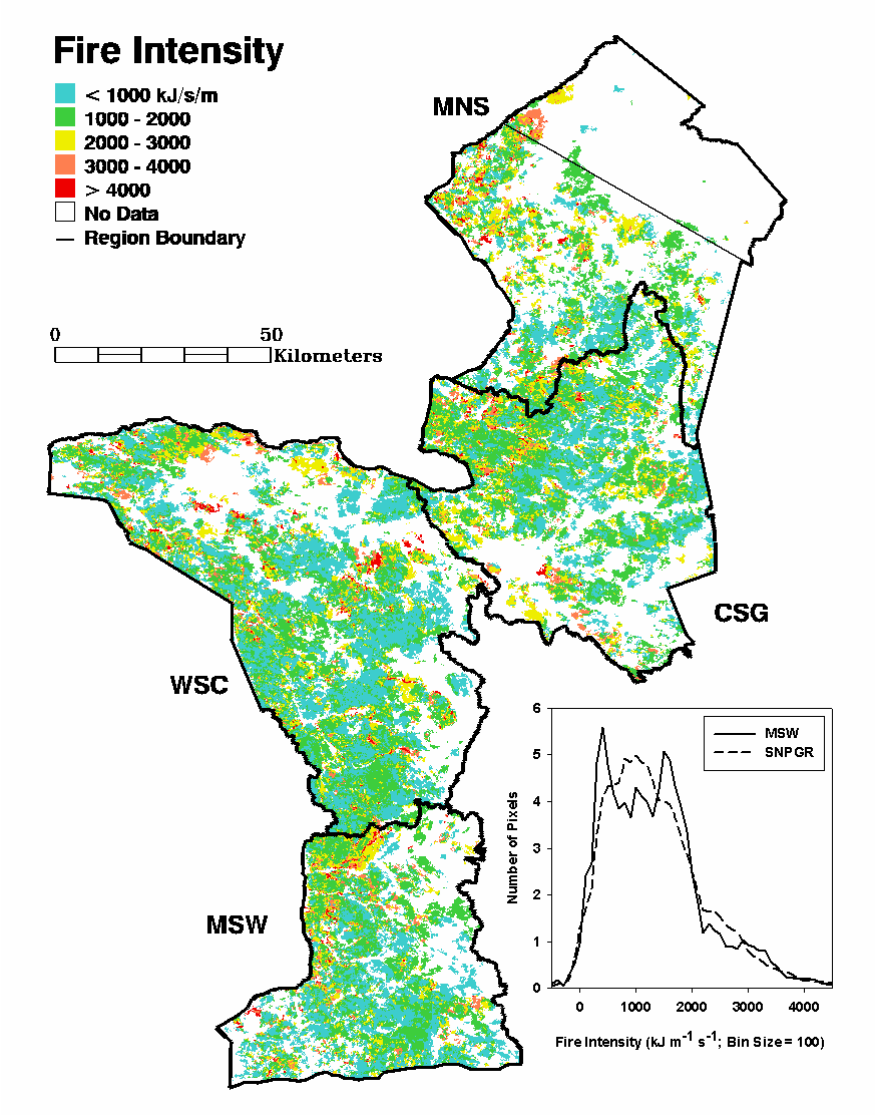

Figure 4-4 : Average fire intensity 2000-2005 estimated from rainfall, grazing and other factors. The frequency histograms show the number of 250 m pixels per fire intensity class (bin size 100 kJ s^{-1} m^{-1}) for each sub region.

While variation of fire intensity is limited on a regional scale, levels do vary over relatively small patches. In the model fire intensity varies mainly as a result of the patchiness of fire. It also varies due to spatial variations in the distribution of rainfall and herbivory, although to a lesser degree than fire effects because of the coarser spatial resolution of the data sets: rainfall has 10 km resolution and herbivory

in the model is regional, although the selective grazing of newly grown grass is replicated. The actual variation of grass biomass on the ground is reflected in the variability of the field data. This variability is likely due to the patchiness of rainfall, herbivory, and fire. Rainfall in this region often varies at scales of less than 10 km (Prins and Loth 1988) and might therefore not always be captured accurately by the FEWS rainfall dataset which has a resolution of 10 km. The movement patterns of herbivores, such as wildebeest also affect the variability of grass biomass. Wildebeest movements mainly depend on green grass availability, but are also affected by other factors which are not addressed in the fire intensity model, e.g. forage quality or the detectability and accessibility of distant patches of green grass to the herds. The fire intensity model is spatially explicit but might not replicate all spatial patterns adequately. Therefore higher confidence can be placed on regional averages of the model outcomes than on pixel-by-pixel results.

The distribution of fire intensity values shows a limited number of very low and even negative values (<1.5% negative). This indicates that the algorithm is underestimating fire intensity to some degree. A possible explanation could be that grass standing biomass is underestimated in areas with unrealistically low fire intensities. The combined effects of rainfall and grazing on grass production are also not well understood. This study uses an empirical relationship to derive grass production from rainfall. This relationship was derived using data from southern African savannas and is not adjusted to the local conditions in the study area. Soil type and nutrient availability affect both grass production and palatability to grazers. This affects the spatial distribution of grass biomass and grazing pressure and

consequently of grass biomass available as fire fuel load. This study also assumes the stimulating effect of grazing on grass production to be linear. The fire intensity model likely oversimplifies these relationships. Despite these shortcomings available field data still suggest a reasonable accuracy of the model results for grass biomass.

Since grazing is an important control on biomass and hence intensity, the model could be improved by developing a more sophisticated and spatially detailed model of animal migratory movements. In this study the large migrating wildebeest herds are assigned to subregions according to their historical occupancy of these areas at certain times of the year. It is likely that under changing rainfall conditions the migratory patterns change and the herds may occupy specific areas for variable lengths of time. Since grazing pressure has a major influence on grass biomass it will also affect fire intensity.

The model could further be improved by collecting additional field data of grass biomass through time to adjust the relationship between rainfall and grass production to local conditions. Additional research is needed on the opposing effects of grazing on fire intensity. Grazing reduces grass biomass and at the same time stimulates grass production. Additional field data are also needed for verifying the results in different areas of the ecosystem and at different times.

4.4.1. Conclusion

Fire intensity was estimated using an empirical model with validation performed for the biomass term. The results of this study are consistent with the dominant effect of the key species wildebeest on shaping the ecosystem. Findings

suggest that by controlling grass biomass grazers also affect fire intensity with potential implications for the distribution of woody plants.

Estimating fire intensity using satellite derived and spatially coherent data layers in combination with field data is a useful approach to help characterize the fire regime. Modeling fire intensity is a viable approach in the face of limited possibilities of measuring it over larger spatial areas and longer time periods. The results of this study are an important contribution to investigations of the fire regime and provide a basis for analyzing the effects of fire on the Serengeti-Mara ecosystem.

Chapter 5: The influence of fire and precipitation on woody cover changes in the Serengeti-Mara ecosystem 2000-2005

5.1. Abstract

This study analyzes the impact of precipitation and the fire regime on changes in woody cover between 2000 and 2005 in the Serengeti-Mara region in East Africa. We integrate three data layers provided by previous analyses (burned area, fire intensity, woody cover change) and precipitation. The datasets are used to assess the dynamics of woody cover changes and underlying causes. Virtually all of Serengeti National Park (SNP) and the Maswa Game Reserve (MSW) and one third of the Maasai Mara National Reserve (MNR) burned at least once during the study period. Burned woodland savanna of less than 600 mm mean annual precipitation showed significantly larger decreases in woody cover than any other part of the ecosystem despite similar fire frequency and lower levels of fire intensity. Woody cover within woodland savanna was more sensitive to variations in precipitation and fire intensity than within grassland savanna. Burned areas in MNR were subject to significantly larger woody cover decreases than comparable areas in SNP. Results suggest that significant losses of woody cover occur a) in areas burned during low rainfall conditions of less than 600 mm annual precipitation and after six weeks or more without rainfall and b) in areas burned infrequently with a fire return interval of 6 years or more.

5.2. Introduction

Fire is a common disturbance in African savannas. It plays an important role for the structure of savanna vegetation (Walter and Breckle 2002). Fire can reduce the density of woody plants in savannas (Bond and van Wilgen 1996). Fire has been recognized as an important ecosystem driver for generating spatial and temporal heterogeneity of savanna vegetation (Scholes and Archer 1997; van Wilgen et al. 2003; Parr and Andersen in print), and others.

Other important factors for regulating woody cover are thought to include climate, soil, and browsing effects. Walter (1971) linked the distribution of woodland and grassland savannas and woody cover density to rainfall levels and the water budget of the soil. Stony soils with low water-holding capacity which allow water to percolate to deeper soil horizons favor woody plants, while herbaceous plants have a competitive advantage on finely textured soil which store and absorb all the water received from precipitation. Browsing by elephants has been identified as an important factor for the distribution of woodlands by Bourliere and Hadley (1983), Leuthold (1977), Dublin et al. (1990), and others.

Woody plants and grasses are antagonistic plant types, one usually excluding the other (Scholes and Archer 1997). Higgins et al. (2000) suggested that the coexistence of trees and grasses is controlled by fire, whereby woody plant seedlings escape the flame zone within the grass layer during periods of low disturbance.

Fire is a very dominant factor in the Serengeti-Mara ecosystem (Chapter 2). It was described as a major driver for changes of woody cover in this region (Norton-Griffiths 1979). Fire is in combination with elephant browsing thought to be

responsible for major losses of woody cover in the northernmost part of the ecosystem (Dublin et al. 1990). Woody cover in the Serengeti-Mara region has changed markedly over the last 100 years. During several cycles open grassland savannas have been replaced by dense woodland savannas and vice versa (Dublin 1991).

Norton-Griffiths (1979) found that the average portion of area burned annually in the Serengeti National Park (SNP), excluding the short grass plains, between 1962 and 1972 was in the range of 50 to 75%. Over the same time period SNP experienced a decline in woody cover. The relative decrease of woody cover density during the same time period ranged from 10% in the South to 50% in the North. The paper concluded with the anticipation that woodlands were going to stabilize at low cover density due to an observed decrease in fire frequency, mainly as a result of increased grazing pressure by wildebeest, and stable elephant numbers.

The decline of woodlands in SNP however, did not continue into the 1970s and 1980s. Sinclair and Arcese (1995) reported a marked increase in tree regeneration at the end of the 1970s, remaining high throughout the 1980s. Suggested reasons were a combination of decreased fuel load due to increasing wildebeest numbers, reduced burning due to unfavorable climatic conditions and reduced browsing due to the removal of up to 80% of the elephant population in SNP by poachers.

By contrast in the northerly adjacent Maasai Mara National Reserve (MNR) there was little if any regeneration of woody vegetation during the same time period. Dublin et al. (1990) attributed the maintenance of open woodland and grassland savanna in MNR to the combined impact of fire and elephant browsing.

Salvatori et al. (2001) suggested high fire intensities as the primary cause for low or decreasing levels of woody cover in MNR. A total of 96 vegetation plots were investigated between 22 May and 13 June 1997, distributed at random, stratified over grass and woody dominated vegetation types. In 32% of the 42 burned plots, shrubs in the height class 1-4 m had been burned and were dead, as a result of fire.

Precipitation is positively related to fire fuel load and thus potentially limits the establishment of woody plants through increased fire intensity. At the same time increased amounts of precipitation has a positive effect on the development of woody plants through increased water supply.

There has been no spatially coherent analysis of woody cover changes over the entire Serengeti-Mara ecosystem in relation to precipitation, extent of burned areas, fire frequency, and fire intensity. Previous studies were limited spatially to subregions of the ecosystem and based on localized measurements and spatial and temporal sub samples. This study investigates the relative effects of precipitation, fire frequency (Chapter 2) and fire intensity (Chapter 4) on woody cover changes (Chapter 3).

The specific objectives of this study are to a) determine the relative importance of fire frequency, seasonality, intensity and precipitation for woody cover changes in the study area, and b) investigate possible explanations for regional differences in woody cover changes. This study provides a novel analysis over the whole ecosystem using spatially continuous data layers of woody cover changes and fire characteristics at near-daily resolution. This type of analysis has only become possible in recent years with the advent of high return frequency and high resolution

satellite systems and distribution of the data at affordable prices or at no cost. The results of this study provide an improved understanding of the drivers of woody cover changes in the study area between 2000 and 2005 and allow suggestions for future developments.

5.3. Methods

5.3.1. Study Area

The Serengeti-Mara region is located on the high interior plateau of East Africa (Sinclair 1995), straddling Kenyan-Tanzanian border (Figure 5-1). The study area encompasses the combined areas of Serengeti National Park and Grumeti and Ikoma Game Reserves (SNPGR), the wider Maswa Game Reserve area (MSW), and the Maasai Mara National Reserve (MNR). The study area was restricted to the same spatial extent as the fire intensity product (Chapter 4), covering regions 3, 4, 7, 8-13, 17, and 19 of the Serengeti Landscape Classification (Gerresheim 1974). For purposes of this analysis MSW was defined as the extent of Gerresheim regions 17 and 19, which combine the Maswa Game Reserve and the southwestern-most part of Serengeti National Park (SNP). The Serengeti Short Grass Plains area (Gerresheim region 14) was excluded in accordance with the woody cover change product used in this analysis (Chapter 3).

Wildebeest are the key species in the Serengeti-Mara region. Large numbers migrate annually in a circular pattern between the North and South of the ecosystem and have an important impact on grass biomass through grazing. The vegetation in

the study area is characterized by woodland and grassland savanna (Herlocker 1976; Reed et al. 2004).

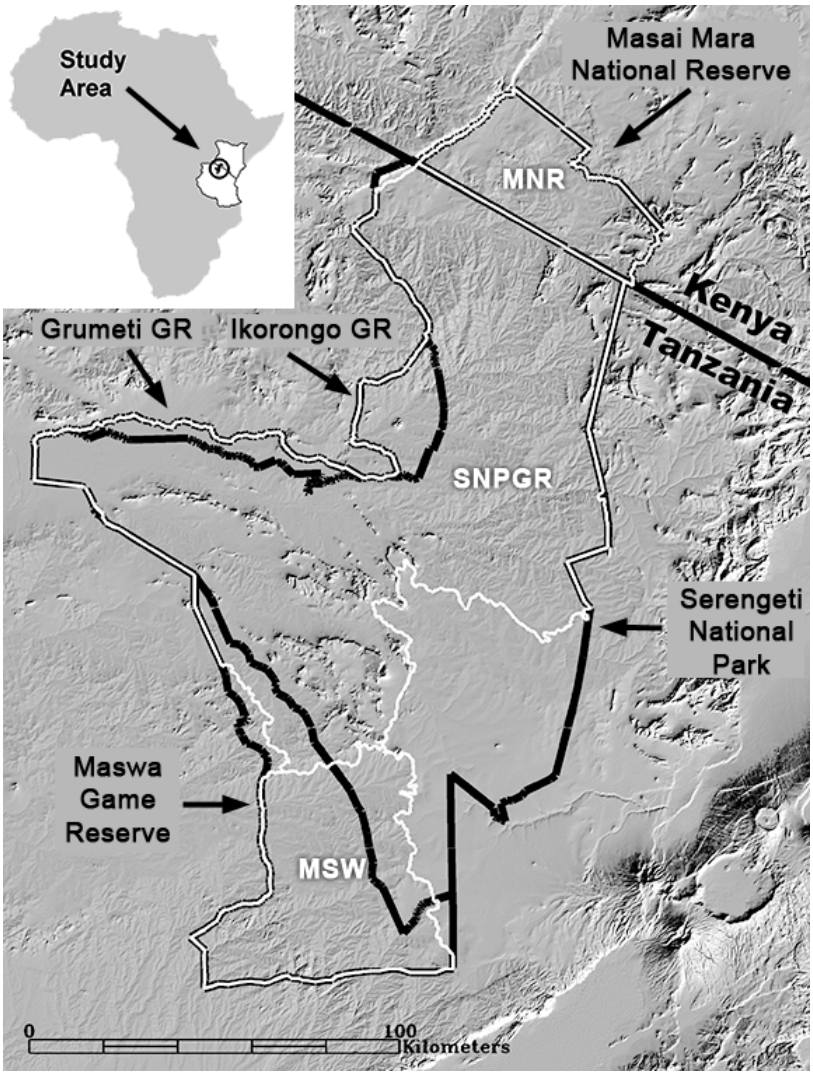

Figure 5-1: Shaded relief of the study area in the Serengeti-Mara region in East Africa. MNR: Maasai Mara National Reserve; SNPGR: Serengeti National Park including Grumeti and Ikorongo Game Reserves; MSW: wider Maswa Game Reserve area. Source of digital elevation model: CIAT (2004).

5.3.2. Data Sets

The datasets for describing woody cover changes, the fire regime, precipitation, and vegetation type are described in the following subsections.

Data and Methods Used to Estimate Woody Cover Changes

Woody cover changes for the Serengeti-Mara region between 2000 and 2005 were derived in Chapter 3 from a time series of MODerate-resolution Imaging Spectroradiometer (MODIS) at 500 m resolution and field data (Figure 3-9). The definition of woody cover includes trees, shrubs, and dwarf shrubs. Percent woody cover estimates were derived for each year 2000 to 2005. Percent woody cover refers to the proportion of the area covered by woody plant canopies when projected vertically to the ground. For each 500 m pixel a regression line was fitted and used to predict a percent woody cover value for the first and the last year of the time series. Change of woody canopy cover is expressed as the ratio of the predicted percent woody cover value of the last year over the first year (woody ratio). Therefore a ratio of less than 1.0 indicates decreasing and greater than 1.0 increasing woody cover.

Data and Methods Used to Characterize the Fire Regime

The fire regime is characterized by fire frequency, seasonality, and intensity. Fire frequency and seasonality was derived from near-daily burned area maps (Chapter 2). The burned area product was generated using an automated algorithm to process daily MODIS imagery at 250 m resolution. Fire frequency was expressed as the ratio of years burned over all years. Fire intensity was estimated in Chapter 4 using a fire intensity model, mainly based on fire fuel load, fuel moisture, slope, and combustion completeness. In the model fire fuel load was estimated from grass

production as a function of rainfall, while accounting for competitive effects from woody plants and grazing pressure.

Data and Methods Used to Estimate Rainfall

Rainfall data was required both for the 2000-2005 periods of the MODIS data and for a longer time period to obtain long-term averages. Rainfall between May 1, 2000 and April 30, 2006 was derived from the Famine Early Warning System (FEWS) Dekadal Rainfall Estimates (RFE) version 2.0 dataset at 0.1 degrees resolution, approximately 10 km (Xie and Arkin 1997). One dekad refers to a time period of 10 days. Longer term precipitation from May 1996 to April 2000 was derived from the FEWS RFE version 1.0 time series at 0.1 degrees resolution. Rainfall estimates for the time period after 2000 were generated by an improved version of the FEWS RFE algorithm. Therefore absolute rainfall values might not be directly comparable but could still be useful to approximate general regional trends.

Monthly precipitation data since 1979 at much coarser spatial resolution was provided by NOAA/OAR/ESRL PSD, Boulder, Colorado, USA, from their Web site at http://www.cdc.noaa.gov/. The NOAA CPC Merged Analysis of Precipitation Enhanced dataset (CMAP) has a spatial resolution of 2.5 degrees (ca. 280 km) and the study area is covered by subsections of three grid cells. Although the CMAP grid cells extend far beyond the boundary of the study area, the data can provide an approximation of longer-term trends over the larger region.

Data and Methods to Determine Vegetation Types

Two vegetation types, woodland and grassland savanna, were derived from the Serengeti-Mara 2000 vegetation map by (Reed et al. 2004). Grassland savannas

include treed and shrubbed grasslands, with tree and shrub canopy cover up to 20%, and grasslands mixed with emerging woody plants and dwarf shrubs. Woodland savannas represent vegetation with tall shrub and/or tree cover exceeding 20% canopy coverage (Figure 5-2).

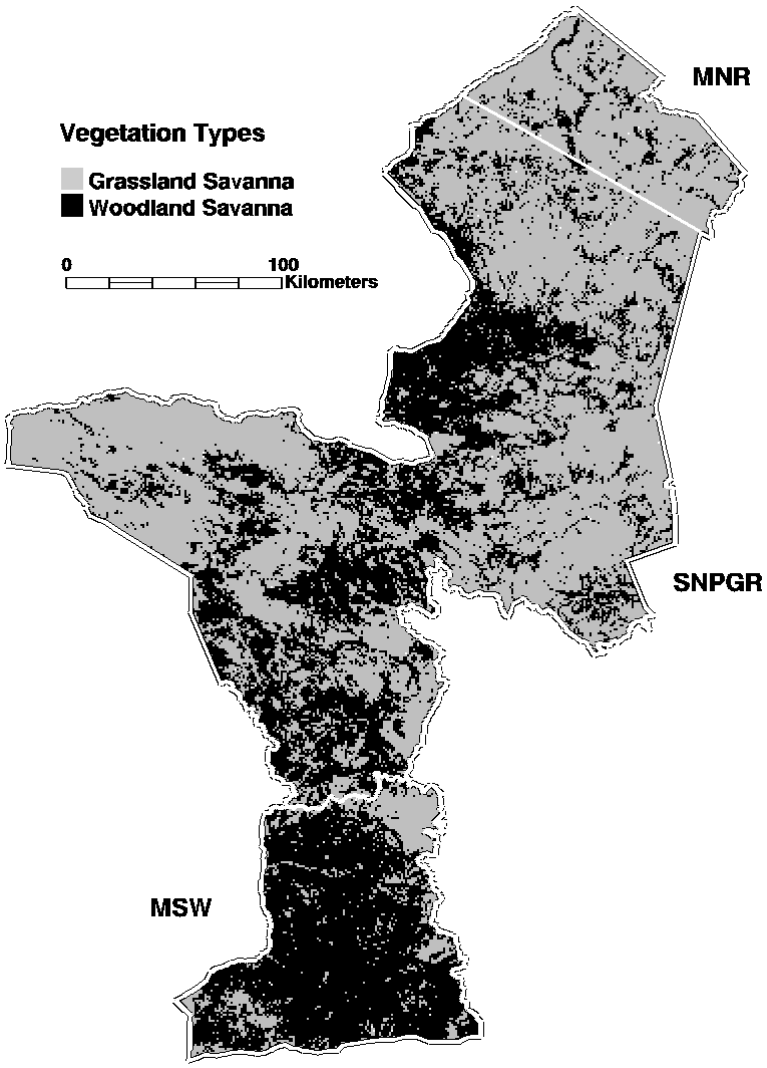

Figure 5-2: Distribution of woodland and grassland savannas in the Serengeti/Mara ecosystem. Data source: Reed et al. (2004).

5.3.3. Methods Used in the Statistical Analysis of the Relationships Between Woody Cover Changes, the Fire Regime and Rainfall

This section describes the four main parts of the statistical analysis which are: a) addressing spatial autocorrelation, b) multiple regression analysis (MLR), c) splitting the data into subsets using regression tree analysis, and d) testing whether subsets of the data are different in terms of the relationship between fire parameters and precipitation. The latter statistical analysis was performed using the t-test and the Wilcoxon-Mann-Whitney test. Data processing was carried out in the R 2.2.1 statistical software package.

a) Addressing spatial autocorrelation: Linear regression analysis requires low or no correlation between data samples in order to produce reliable results. Counter to this ideal requirement spatial autocorrelation between samples is a common problem in spatially continuous data layers. In gridded data sets spatial autocorrelation can be alleviated by resampling to the spatial resolution corresponding to the range of the semivariogram (Curran 1988). Figure 5-3 shows the empirical semivariogram and the fitted exponential variogram model for the woody ratio product. The semivariogram was calculated using the "gstat" extension package in R.

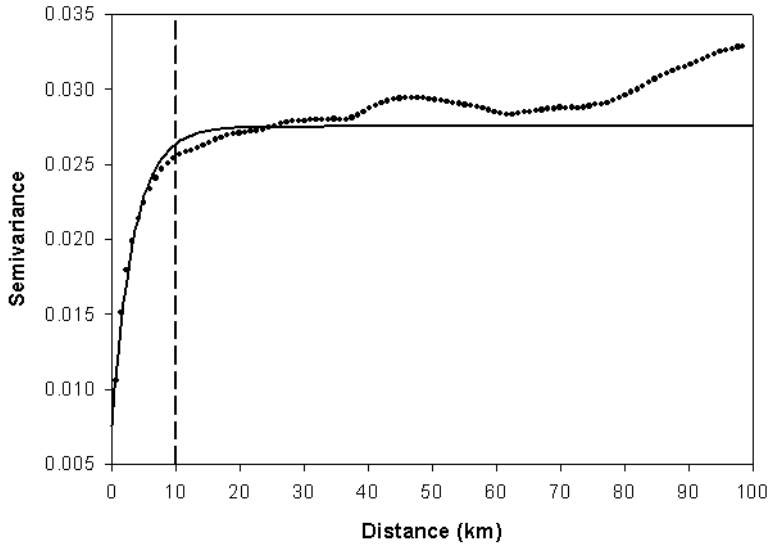

Figure 5-3: Empirical semivariogram and fitted exponential variogram model for the woody ratio product. The dashed line indicates the distance at which variogram range occurs.

The estimated range of the variogram model was 10 km. All data layers were aggregated to 10 km resolution. Data values were selected for aggregation within each 10 km pixel according to the majority occurrence of both the fire frequency class and vegetation type. This method of aggregation allowed to maintain precise fire frequency values and accurate woody cover change and precipitation values for the represented vegetation type.

Fire frequency varied from 0 to 6 fire occurrences over the six year time period of this study. However fire intensity estimates were only available for areas burned twice or more. The MLR analysis was therefore restricted to areas with 2 or more fire occurrences. Within each 10 km pixel all 500 m pixels of the most frequent fire occurrence class were selected. Within those the pixels of the most frequent vegetation class, woodland or grassland savanna, were selected. The mean value of

the selected pixels for each variable was assigned to the aggregated pixel. No value was assigned if the selected 500 m pixels combined covered less than 5% of the area of the 10 km pixel. The total number of aggregated pixels was 118.

b) Multiple Linear Regression analysis (MLR): The purpose of the MLR was to determine the relative importance of fire variables and rainfall on changes in woody cover. To perform this analysis woody cover change was expressed as the ratio of percent woody canopy cover in 2005 over 2000 (woody ratio). Areas with a woody ratio of less than 1.0 were decreasing, and greater than 1.0 increasing in woody canopy cover. Independent variables in the MLR were mean annual precipitation (MAP), fire frequency expressed as the ratio of the number of years burned over all years, and mean fire intensity. Correlations between all independent variables were low ($r^2 < 0.137$). All variables were log transformed for the MLR analysis. Log transformation is a standard technique in regression and makes coefficients comparable for variables measured in different units.

c) Splitting of the data into subsets using regression tree analysis: The explanatory power of MLR can be improved by splitting the data into meaningful subgroups. Low multiple r squared values and regression coefficients can be a result of subgroups in the dataset within which the relationship between independent and dependent variables is different or opposing. MLR analysis over the whole dataset would thus incorporate these different or opposing effects and weaken the explanatory power of the result. Separate analysis of subgroups of the data can also help to improve the understanding of underlying dynamics.

The data were divided into more homogeneous subgroups using regression trees. Regression trees were considered an appropriate basis for partitioning because they are less sensitive to spatial autocorrelation than linear regression methods and are able to effectively model correlative relationships despite autocorrelation in the data (Cablk et al. 2002). Regression trees divide data sets into more homogeneous subgroups. Regression trees are binary structured classifiers, also known as recursive partitioning regression. The data are repeatedly split into more homogeneous subgroups, minimizing the residual sum of squares of the dependent variable (Breiman et al. 1984). For the regression tree analysis the pixel data was used at the full resolution of 500 m in order to provide the maximum range of values and detail. The regression tree was calculated using the "tree" extension package in R. The tree was grown until the within-node deviance in the end nodes was 0.01 times or less of the deviance of the root node. The tree was otherwise not pruned, due to our interest in the first, most important splits.

d) Testing whether the data subsets are different: Data subsets were tested for statistically significant differences by testing the null hypothesis that the means were equal. The tests were performed using the two-sided t-test and Wilcoxon-Mann-Whitney test. The t-test was used for log-transformed datasets, normally distributed with homogeneous variances and continuous variables. Normal distribution was tested using the Kolmogorov-Smirnov test. Homogeneity of variances was tested using the F-test. The Wilcoxon-Mann-Whitney (WMW) test was used in cases where parameters did not meet the requirements of the t-test, i.e. the variances were not homogenous or the variable not continuous. P-values for the WMW test were

calculated using the Streitberg and Röhmel Shift-Algorithm for both tied and untied samples. Unlike the t-test the non-parametric WMW test does not require homogeneity of variances and converts the data into ranks before the test is carried out. It is therefore also appropriate for fire frequency, which is not continuous, and for parameters with non-homogeneous variances between subgroups. The WMW test statistics were calculated using the "exactRankTests" extension package in R.

e) Deriving the relative importance of potential woody cover change drivers: The relative importance of each potential driver for woody cover change was investigated using the random forest statistical technique. Unlike regression analysis random forests can produce meaningful results even if the variables are highly correlated. Random forests are based on regression trees but at each node instead of evaluating all possible splits a random subset of the training data and splitting variables is generated. A large number of trees are calculated, in this study 10^5, and the final results determined as the average of all tree outcomes Breiman (2001). The random forest technique allows to calculate the overall importance of each variable as the mean increase in node purity from the parent to the child nodes. The importance is measured as the residual sum of squares and calculated as the average increase over all parent nodes of all trees split by the specific variable. A relatively large value of mean increase in node purity indicates a relatively high importance and vice versa. It is this measure which is used here to determine the relative importance of the variables as potential drivers of woody cover change. Random forests statistics were calculated using the "randomForest" extension package in R.

5.4. Results and Discussion

5.4.1. Fire Regime

Fire frequency, seasonality, and fire intensity characterize the fire regime. This section describes findings for each of these three parameters for the study area.

a) Fire frequency was high throughout central and southern SNPGR, lower in northern SNPGR and very low, in comparison, in MNR. Figure 5-4 shows the number of burn events within the study period and percent area burned. The overall area left unburned during the study period within SNPGR and MSW combined was 14.6%, in MNR 65.6%. Areas mapped as unburned in SNPGR and MSW are mostly small and spatially disparate patches, many of which might have burned just the year before the beginning of the study period. Furthermore the algorithm is expected to under, rather than overestimate the extent of burned areas (Chapter 2) and individual burned pixels might have been misclassified as unburned. As a consequence the total area within SNPGR and MSW without significant short-term influence of fire might be even lower.

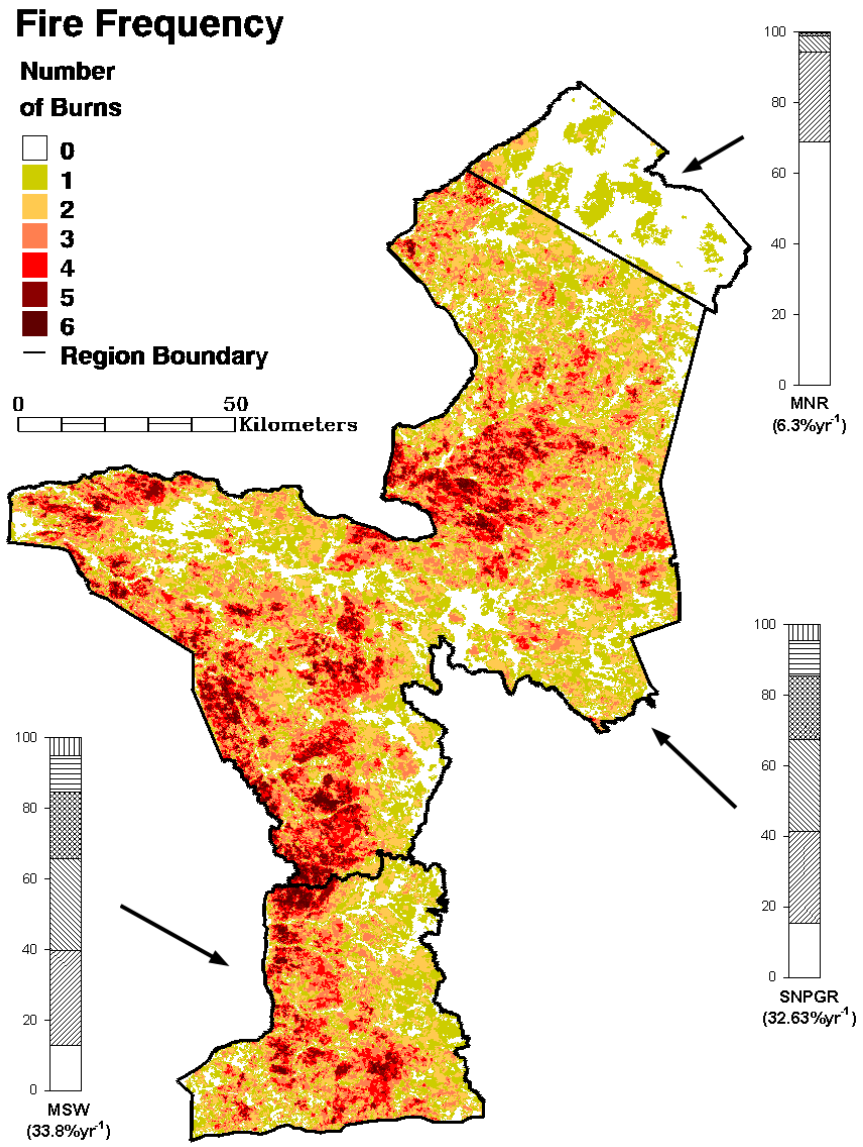

Figure 5-4: Number of burns between May 1, 2000 and April 30, 2006. Bar charts show percent area burned at each frequency per sub region. Average percent area burned per year is given in parenthesis. Data source: Chapter 2.

b) The Seasonality of fires is here described as the number of days after the last rainfall event before the fire. Figure 5-5 shows histograms of the seasonal distribution of fire and rainfall for each sub region and a map of the average days since the last rainfall (no-rain days) before the fire. This representation of seasonality

shows the distribution of fire events in relation to rainfall distribution and seems to be more meaningful than absolute dates in areas where the local and seasonal distribution of rainfall can vary significantly. The number of no-rain days shows a similar southeast-northwest gradient as precipitation. Spatial patterns of no-rain days show a striking resemblance with woody cover changes in MSW (Chapter 3). MSW had the longest average time period of no-rain days (41.8) and the lowest MAP (580 mm) during the study period.

In the study area burning was largely restricted to the dry season June to August, peaking in June. Most fires in SNPGR are initiated by the park management, preferentially in the early dry season (Trollope et al. 2005). Fires also originate from poachers often near the western borders where poaching is more frequent (Campbell and Hofer 1995).

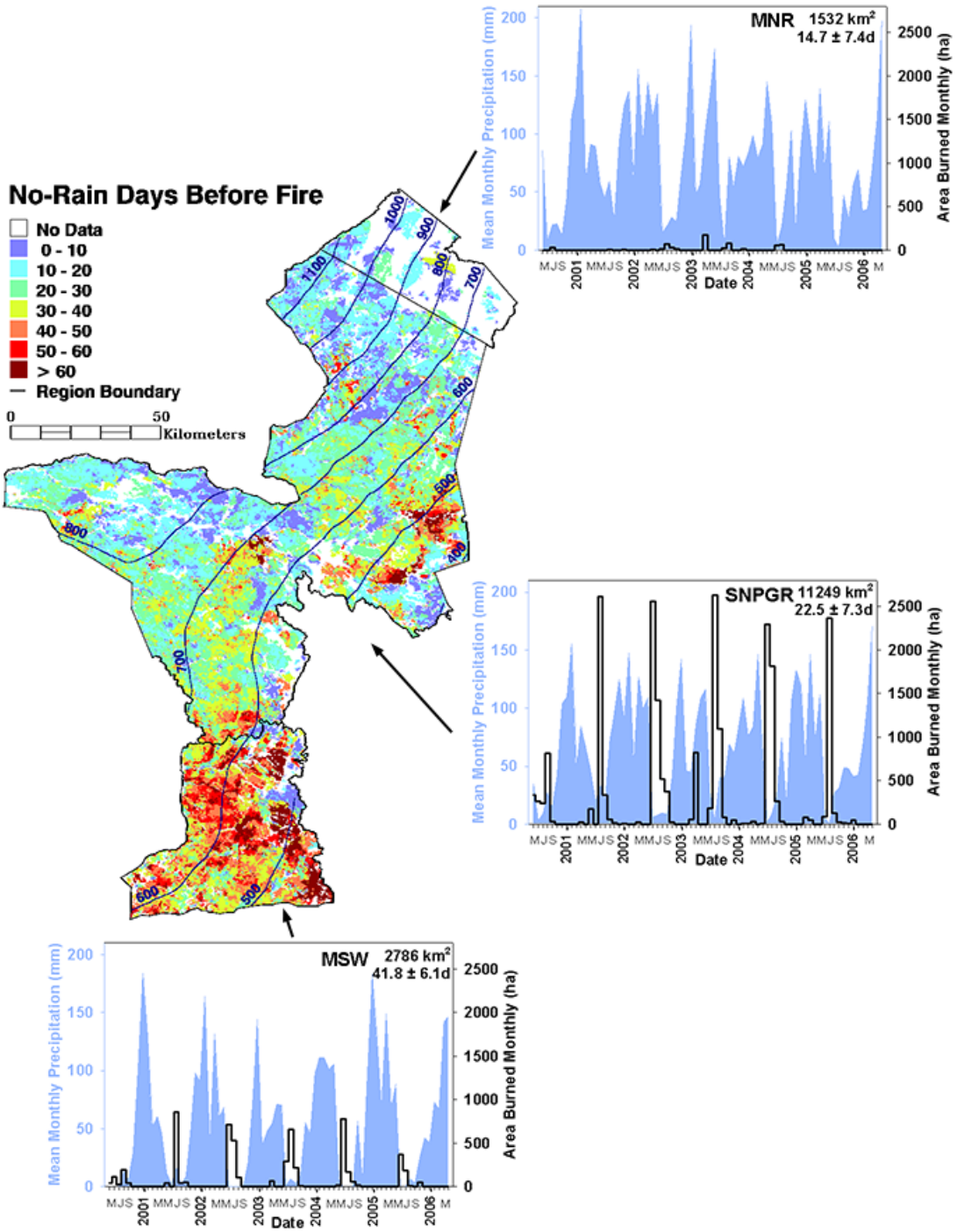

Figure 5-5: Seasonality of fires. The map shows the average number of days since the last rainfall before the fire (no-rain days). Contour lines represent MAP for 2000-2005. Histograms for each sub region show the time of burning and precipitation levels, total area and the average number of pre-fire no-rain days ± the standard error.

c) Fire intensity levels were similar within each sub region (see Chapter 4, Figure 4-4). Note that fire intensity was only estimated for areas burned two times or more, due to requirements of the model algorithm. Almost all burned areas in MNR burned only once within the study period and fire intensity estimates were not available for these areas. Fire intensity results might therefore not be representative for fires in MNR.

5.4.2. Statistical Analysis Results

MLR Using the Complete Dataset

MLR was used to test for significant relationships between changes in woody cover, the fire regime and rainfall. MLR was carried out using woody ratio as the dependent variable. Independent variables were mean annual precipitation (MAP), fire frequency, fire intensity, and vegetation type. Pre-fire no-rain days was highly correlated with MAP (correlation coefficient = -0.696) and was for this reason excluded from the MLR. Dominant vegetation types in the study area were woodland and grassland savanna (Figure 5-2). In the MLR vegetation type was represented by a dummy variable, assuming 1 for woodland and 0 for grassland savanna. The use of dummy variables is a common technique in MLR to incorporate categorical variables. The MLR model explained 11.9% of the variation. Vegetation type and fire intensity were significant (Table 5-1).

Table 5-1: MLR results for woody cover changes in the study area. MAP (mm); ffreq: fire frequency (ratio); fint: fire intensity (kJ s^{-1} m^{-1}). All variable were log transformed.

Variables	Coefficient	t-Value	Signif.
(Intercept)	0.7496	2.333	*
MAP	-0.0458	-1.005	
Ffreq	-0.0153	-0.364	
Fint	-0.0736	-2.159	*
VEG	0.0534	2.352	*

Significance codes: 0 '***' 0.001 '**' 0.01 '*' 0.05 '.' 0.1 ' ' 1
Multiple R-Squared: 0.119, p-value: 0.0059

Splitting the Data into Subsets Using Regression Tree Analysis

Thresholds for dividing the dataset into meaningful subgroups were derived by a regression tree using the full 500 m resolution dataset (Figure 5-6). The tree first split off a small subgroup, 2.4 % of the total, which has very high precipitation and very low woody ratio values. This small number of pixels all appear along the northwestern fringe of northern SNPGR and MNR and were considered outliers and not representative for the study region in general. The first major split occurs at the second node, separating the data into groups of high and low precipitation, MAP threshold of 598.4 mm. The low precipitation group splits further into woodland and grassland savanna. Woodland savanna shows a much lower woody ratio than grassland savanna.

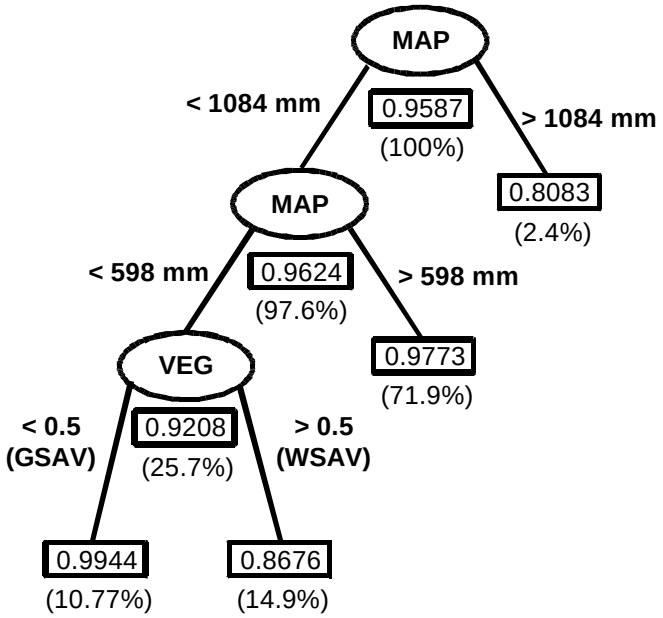

Figure 5-6: Regression tree using woody ratio as the dependent variable. The data set is split at the nodes (ovals) by applying thresholds of the specified variable. MAP: mean annual precipitation; VEG: vegetation type (0=grassland savanna (GSAV); 1=woodland savanna (WSAV)). Values along the lines are splitting criteria. Numbers in boxes are average woody ratios of the pixels in each node. In parentheses is the percentage of the total number of pixels in each node.

The aggregated 10 km dataset was split into four subgroups using the precipitation threshold of 598.4 mm determined by the regression tree. The four groups were low precipitation woodland (LP-WSAV) and grassland savanna (LP-GSAV), and higher precipitation woodland (HP-WSAV) and grassland savanna (HP-GSAV). MLR was carried out separately for each group.

Testing Whether MLR of the Dataset Subgroups are Different

Multiple r squared was highest for LP-WSAV, explaining 79.7% of the variation. Both precipitation and fire intensity coefficients were negative and significant (Table 5-2). HP-WSAV showed similar, but weaker relationships,

explaining 24.1% of the variation (d.f. = 29, p = 0.0436). The fire intensity coefficient was negative and very significant (b = -0.1800, p = 0.0075). MLR for LP-GSAV did not yield significant relationships for any of the variables (multiple $r^2 = 0.111$, d.f. = 16, p = 0.5866), nor did MLR for HP-GSAV (multiple $r^2 = 0.101$, d.f. = 47, p = 0.1698).

Table 5-2: MLR results for dry woodland savannas, MAP < 598.4 mm. The independent variable was woody ratio. MAP (mm); ffreq: fire frequency (ratio); fint: fire intensity (kJ s^{-1} m^{-1}).

Variables	Coefficient	t-Value	Signif.
(Intercept)	3.32361	3.883	**
MAP	-0.36665	-3.219	*
Ffreq	0.18383	1.452	
Fint	-0.15098	-2.203	.

Significance codes: 0 '***' 0.001 '**' 0.01 '*' 0.05 '.' 0.1 ' ' 1
Multiple R-Squared: 0.797, p-value: 0.0168

Interpretation of the MLR Results

The MLR results need to be interpreted in light of the overall rainfall conditions in the Serengeti-Mara region during the study period. Records indicate that MAP from 2000 to 2005 was lower than the long-term average of the preceding 20 years. Precipitation in the southwestern CMAP grid cell indicates considerably lower levels than the long-term average 1979-1999 (Figure 5-7). The driest year on record since 1979 was 1999, the year immediately preceding the time period of this study. The northwestern and northeastern CMAP grid cells similarly indicate below average rainfall conditions after 1998, but to a lesser extent. However, these northern CMAP grid cells might be less representative for the study areas because the northwestern

cell is largely dominated by Lake Victoria and the northeastern grid cell is divided by the Great Rift Valley.

The higher resolution precipitation time series provided by FEWS shows a similar trend as CMAP. Averages were calculated for 12-month time periods starting May 1, 1996. Note that the FEWS algorithm was improved in 2000 and the absolute precipitation values before and after this year might not be directly comparable.

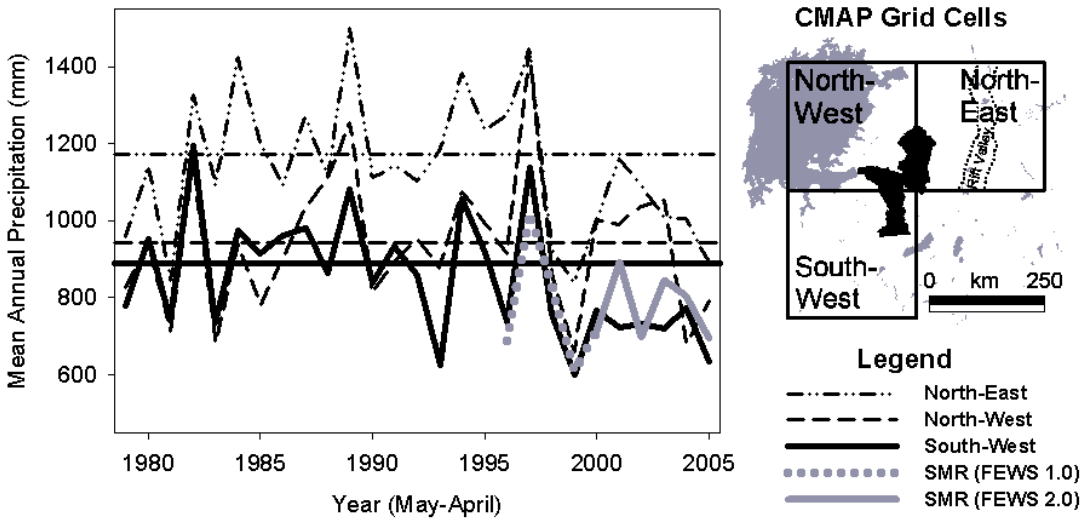

Figure 5-7: MAP for the three 280 km CMAP grid cells covering the study area. The map shows the study area in black, Lake Victoria and water surfaces in gray and the Rift Valley as dotted lines. Years start on May 1 and end on April 30 the following year. Horizontal lines are mean values 1979 to 1999. Gray lines represent MAP for the Serengeti-Mara region (SMR) provided by the FEWS RFE version 1.0 algorithm from 1996-1999 and RFE version 2.0 from 2000-2005.

Precipitation can have opposing effects on woody plants. Higher rainfall levels increase the available water supply in the soil and favor the development of woody plants over grasses. At the same time higher precipitation also increases grass biomass and thus fire fuel load and fire intensity. MLR results for both LP-WSAV

and HP-WSAV show negative and significant precipitation coefficients. This indicates that during the study period higher precipitation levels had a negative effect on woody cover through increased fuel loads. This is supported by the fact that fire intensity coefficients were also negative and significant for both LP-WSAV and HP-WSAV. Variations in rainfall may not have been sufficient to replenish the water supply in deeper soil layers to promote increased woody plant growth. Available rain water may have mostly been taken up by grasses in the top soil layer, fostering grass production and increasing the fire fuel load. This negative effect could be reversed under higher rainfall conditions.

Low precipitation levels might also be responsible for the lack of significant relationships in burned grassland savanna areas between woody cover changes and both fire parameters and precipitation. Low rainfall conditions lasting one or several years have the potential to weaken or kill low shrubs and emerging woody plants. Any fire event under such conditions might have a maximum effect on low shrubs and dwarf shrubs beyond which any additional variations in the fire regime or precipitation are not relevant. In woodland savannas on the other hand woody plants are taller and their roots reach deeper into the soil. Low rainfall conditions will have a lower immediate impact and single fire events, especially at low fire intensity, are less likely to kill established trees and shrubs than high fire intensity events. This could explain why variations in fire intensity and precipitation levels are significant within burned areas of woodland savannas but not so within grassland savannas.

Relative Importance of Potential Drivers of Woody Cover Change

The relative importance of each fire regime variable as potential driver for woody cover change was investigated for the entire study area and separately for woodland and grassland savanna regions. Only areas burned twice or more within the study period are considered here due to restrictions of the fire intensity modeling algorithm. Importance was assessed using the mean increase in node purity of 10^5 random forest trees respectively for each area (Table 5-3). The relative importance of the variables for each region is discussed in turn below.

Table 5-3: Variable importance for driving woody cover change calculated as the mean increase in random forest node purity. The highest importance values are shown in italic. All: entire study area; GSAV: grassland savanna areas; WSAV: woodland savanna areas; ffreq: fire frequency; fint: fire intensity; no-rain: number of days without rainfall before the fire.

Variable	**All**	**GSAV**	**WSAV**
ffreq	0.4089	0.2257	0.1720
fint	0.4014	*0.2405*	0.1501
norain	*0.5448*	0.2306	*0.2671*

The most important fire regime variable when considering the entire study area is the number of days without rainfall before the fire, representing fire seasonality. The same is true when considering only woodland savanna areas. This indicates late-season burning to have the highest effect for causing woody cover changes in woodland savanna areas.

For woody cover change in burned grassland savanna areas fire intensity is more important than fire frequency or fire seasonality (no-rain days). Fire intensity is mainly controlled by fuel load which is highly affected by grazing pressure. This is

consistent with the notion that the large wildebeest herds exert an importance influence on the balance between woodland and grassland savannas through their grazing impact. Grazing levels cause heterogeneity of aboveground grass biomass or fire fuel load and thus affect fire intensity which in turn is important for woody cover changes in grassland savannas.

5.4.3. Woody Cover Changes in Maswa Game Reserve Region

The largest decrease in woody cover was observed in MSW. In the following we test whether these observations can be explained by the fire regime or precipitation. Virtually all of MSW burned at least once during the study period. All aggregated pixels of the LP-WSAV group fall within MSW. We can test the difference of mean parameter values of the LP-WSAV against the HP-WSAV group for statistical significance. The pre-fire no-rain days variable is highly correlated with precipitation and for this reason was excluded from the MLR analysis. For the comparison of means each variable is treated independently and the no-rain days variable was included here because of the striking similarity of spatial patterns in MSW between woody cover decreases and no-rain days. Statistical significance can be tested using a t-test, if the data has homogeneous variance, is normally distributed and continuous. These requirements were not fulfilled by all parameters. Fire frequency is not continuous and for MAP and pre-fire no-rain days the variance was not homogeneous when testing values for LP-WSAV and HP-WSAV (MAP: $F=5.5$, d.f. = 107, $p = 0.0086$; No-rain days: $F=6.3$, d.f. = 107, $p < 0.00053$). Therefore the WMW test was used.

The results show no-rain days in LP-WSAV significantly higher and MAP, woody ratio, and fire intensity significantly lower than in HP-WSAV (Table 5-4). Fire frequency was slightly higher in LP-WSAV, but both mean values were close to 0.5 indicating the same average fire return interval of 2 years, and the difference was only slightly significant.

Table 5-4: t-test results for differences between low precipitation woodland savannas (LP-WSAV, MAP < 598.4 mm) and higher precipitation woodland savannas (HP-WSAV, MAP > 598.4 mm). W: Wilcoxon-Mann-Whitney statistic; no-rain: number of pre-fire no-rain days (days); MAP (mm); wratio: woody ratio; fint: fire intensity (kJ s^{-1} m^{-1}); ffreq: fire frequency (ratio). Variables are sorted in decreasing significance (increasing p-value).

	no-rain	**MAP**	**wratio**	**fint**	**ffreq**
LP-WSAV	42.1	541	0.8483	1141	0.517
HP-WSAV	24.0	723	0.9754	1571	0.457
W	67	965	950	869	360
p	4.865e-06	4.013e-05	7.440e-05	0.0015	0.0574
Signif.	***	***	***	**	.

Significance codes: 0 '***' 0.001 '**' 0.01 '*' 0.05 '.' 0.1 ' ' 1

The data describes a less aggressive fire regime in LP-WSAV in comparison to HP-WSAV. This should have a promoting effect on woody cover in LP-WSAV, however the data show significantly lower woody ratio in LP-WSAV than in HP-WSAV. This leaves the low precipitation levels or long period of rainless pre-fire days as a more reasonable explanation for woody cover decreases in MSW, rather than differences in the fire regime. MAP and no-rain days are highly correlated. Both had very low p-values and were highly significant for the separation of LP-WSAV and HP-WSAV, but no-rain days even more so. The distribution of rainless days in

LP-WSAV, which corresponds to almost exactly to MSW, shows a very similar spatial pattern as woody cover decreases, particularly along its northern border with WSC (Chapter 3, Figure 5-5). These results indicate that for woody cover decreases both the annual sum of rainfall and its distribution throughout the year in relation to fire are important. Fire seems to have the strongest decreasing effect on woody cover in years of less than approximately 600 mm rainfall and after a dry spell of ca. six weeks (42 days) or more.

Another potential factor causing woody cover decreases is browsing by elephants. Elephant numbers in SNPGR and MSW however have been low since at least the mid 1980s. They are only recovering very gradually (Campbell and Borner 1995) and we are not aware of any information suggesting significantly increasing or high elephant numbers in MSW.

5.4.4. Woody Cover Changes in the Maasai Mara National Reserve

The results show that burned areas in the Maasai Mara National Reserve show a similarly large decrease in woody cover as in MSW, yet precipitation levels were much higher. Therefore low rainfall conditions might not explain woody cover decrease in MNR the same way as they do in MSW. This leads to the question whether differences in the fire regime could provide a better explanation.

The vast majority of burned areas in MNR only burned once and for this reason the following analysis is focused on single-burned areas. We can compare woody ratio and precipitation of single burned areas in MNR with corresponding areas in SNPGR of the same grassland savanna vegetation type and the same minimum precipitation level of 687 mm. The data was log-transformed and

subgroups tested for normality using the Kolmogorov-Smirnov test. None of the subgroups deviated significantly from the normal distribution ($D < 0.181$; $p > 0.176$). Homogeneity of variances was tested using an F-test. All subgroups showed homogeneous variances ($p > 0.05$). Therefore the t-test is applicable for testing the subgroups for statistically significant differences (Table 5-5, Figure 5-8).

Table 5-5: t-test results for comparing single burned and unburned areas in the MNR and SNPGR. B: burned; UB: unburned; wratio: woody ratio; MAP (mm).

	wratio	**MAP**	**Region**	**wratio**	**MAP**	**Region**	**wratio**	**MAP**
MNR B	0.894	927.1	MNR B	0.894	927.1	SNPGR B	0.979	851.9
SNPGR B	0.979	851.9	MNR UB	1.017	895.2	SNPGR UB	0.987	841.9
t	-3.318	1.696	t	-3.422	0.608	t	-0.300	0.340
d.f.	25.1	12.4	d.f.	21.2	19.98	d.f.	47.3	56.2
p	.0043	.0115	p	.0025	.55	p	.7653	.7354
sig.	**		sig.	**		sig.		

Significance codes: 0 '***' 0.001 '**' 0.01 '*' 0.05 '.' 0.1 ' ' 1								

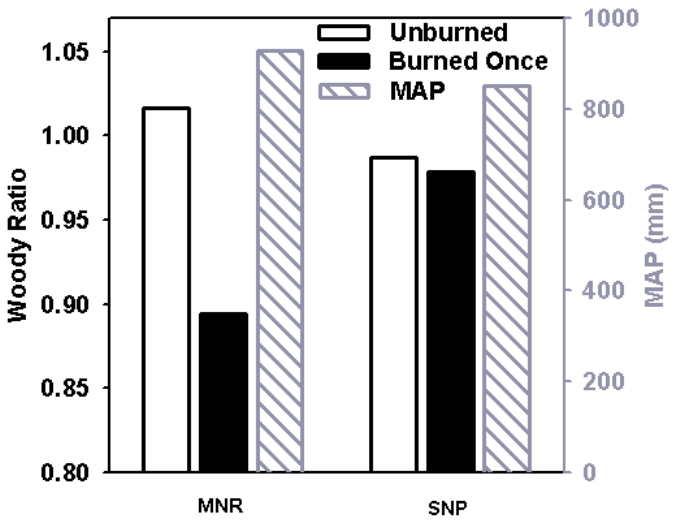

Figure 5-8: Woody ratio and MAP in MNR and SNPGR for unburned areas and areas burned once. MAP corresponds to areas burned once.

The difference in woody cover decrease between single-burned areas in MNR and corresponding areas in SNPGR is large and significant. Differences in precipitation are small and not significant. Unburned areas in MNR show a significantly higher woody ratio than single-burned areas in MNR. In SNPGR there is no significant difference in woody ratio between unburned and single-burned areas. Fire intensity estimates were not available, because the vast majority of burned areas in MNR only burned once during the study period.

There are two possible explanations for these observations. Fire intensity could be higher in MNR during the early burning season before the arrival of the great wildebeest herds, which consume large amounts of grass biomass. Another explanation could be that due to much lower fire frequency in MNR woody plants are less adapted to fire events, in contrast to SNPGR, which has a much higher fire frequency and could be close to a fire climax state. Infrequent fire events, separated by 5 or more years, could therefore have a much larger impact on emerging fire-prone woody plants. This would only be true if the medium-term fire regime was fairly constant. Burning practices and policies have not changed significantly during the past 10 years or longer in either SNPGR or MNR (Trollope et al. 2005; Heath 2003).

5.5. Conclusion

The results of this study show that almost the entire area of SNPGR and MSW is affected by fire on average every 2-3 years. Within these areas woody cover is affected by fire differently depending on vegetation types and precipitation levels. The strongest effects occurred in woodland savannas under low rainfall conditions of 600 mm mean annual precipitation or less and burned six weeks or more after the last

rainfall event. In higher rainfall areas fire seems to have a larger decreasing effect on woody cover with a fire return interval of six years or more.

The analysis of fire regime variables as potential drivers of woody cover change has shown that fire frequency is less important than fire intensity and fire seasonality. The results indicate that for controlling woody cover using fire it is important to burn at the right time, i.e. late in the dry season and when fuel load accumulation is high, rather than burning indiscriminately at high frequency. However, the data available for this study only allowed the analysis of areas burned twice or more within the 6-year study period. For analyzing the long-term influence of fire frequency a much longer time series, e.g. 15 to 20 years, is necessary.

This study provides an improved understanding of the dynamic relationship between the fire regime, precipitation and woody cover changes in the Serengeti-Mara region. The results indicate that woody cover decreases between 2000 and 2005 in the Maswa Game Reserve region occurred during dry years with less than 600 mm precipitation, in combination with fire after six or more weeks without rainfall. Changing precipitation patterns in the face of global climate change and extended droughts in the future could well spell similar consequences for African woodland savannas. Global climate could cause increased climate variability and more El Niño-like conditions (Houghton et al. 2001), which are often associated with rainfall surpluses in Eastern Africa (Camberlin et al. 2001). The observed decrease of woody cover in the southern parts of the study area might therefore be temporary if the rainfall levels increase again. Woody cover could be promoted by frequent burning during high rainfall years and strict fire control during drought periods and vice versa.

On the other hand findings suggest infrequent burning at a fire return interval of five years or more might also lead to increased susceptibility of woody vegetation to fire and a consequently larger decrease of woody cover. It is not conclusive however whether the observed significant woody cover decrease within single burned areas in MNR are due to decreased fire tolerance of woody plants in MNR's low fire frequency environment or are due to possibly higher levels of fire intensity in the early dry season. This question needs further investigation and field studies.

This study considers only a comparatively brief time span of six years from 2000 to 2005. A continuation of the analysis over a longer time period would be desirable to determine medium and long-term trends. The study provides a useful framework for the design of complementary field campaigns to investigate woody cover changes on the ground under different precipitation and fire conditions. The use of remote sensing tools in combination with field data is a powerful approach for continued regional analysis and monitoring over the long-term.

Chapter 6: Conclusion

6.1. Summary of Research

Review of Research Objectives

This dissertation identified patterns of woody cover change in the Serengeti-Mara savanna ecosystem from 2000 to 2005 and determined the role of fire regime parameters and precipitation for driving these changes on a regional basis. This was done by developing applied remote sensing and modeling tools in combination with field data. The research objectives listed in Chapter 1, Section 1.2 are divided into a set of three science objectives and three methodological objectives. The latter were a prerequisite to address the former and are reviewed here first.

Chapter 2 addressed objective (3): production of a series of burned area maps at high spatial and temporal resolution. A new algorithm was developed to provide the first automatically derived maps of burned areas in the study region; furthermore this was achieved at relatively high spatial resolution of 250 m. The results provide near-daily time and location of individual fires. The burned area time series provides the foundation for the characterization of the fire regime and subsequent analysis of impacts on woody cover changes. The burned area product is also of potential value to other research groups.

Objective (4) was to detect changes of woody canopy cover density as they are typical for savanna environments. In Chapter 3 woody cover changes were derived from remote sensing and field data. The methodology adapted and advanced the concept of vegetation continuous fields. It did so by employing a random forest

technique and made the process applicable to prolonged woody cover changes in the Serengeti-Mara savanna environment by combining data over a six year time period. The methodology provided results at 250 m resolution whereas corresponding continental or global products are at much coarser resolution of 500 m to 8 km. The results agreed well with field data and anecdotal observations.

Chapter 4 estimated fire intensity in the study region, addressing objective (5). Fire intensity is the third essential component for characterization of the fire regime (the other two, fire frequency and seasonality were derived in Chapter 2). The methodology to derive fire intensity used the results of Chapters 2 and 3 to a limited extent, but is largely based on the amount and spatial distribution of fire fuel load, which was modeled from precipitation and grazing pressure by the large wildebeest herds and other dominating herbivores. The approximation of fire intensity in this study by means of modeling is a workable alternative to impractical or unfeasible field measurements over large areas. The parameters used in the model itself however would benefit from additional field data both for fine tuning and validation. Field measurements of the individual parameters in the fire intensity equation would also allow determining the error range of each parameter and how these contribute to the overall accuracy of the fire intensity estimate.

Chapter 5 brought together the results of Chapters 2 to 4, addressing the science objectives: (1) characterization of spatial patterns of woody cover change; (2) analyzing the role of the fire regime and precipitation for woody cover changes. The chapter focused on areas which showed the relatively largest woody cover changes overall and in response to fire. Woody cover decrease was most severe a) in burned

areas with mean annual precipitation (MAP) below 600 mm and b) in areas above 600 mm MAP burned infrequently after an average of six years or more.

Woody Cover Changes

This study provided for the first time a spatially comprehensive and conjoint view of both woody cover changes and the fire regime over the entire Serengeti-Mara region. Results indicated that the Serengeti-Mara region has been subject to continuing changes of woody cover between 2000 and 2005 partly in response to fire and climate conditions. Overall woody cover levels in central and northern SNP continued to increase, a trend which has been active since the early 1990s (Sinclair and Arcese 1995). At that time wildebeest numbers were stable at approximately 1.3 million animals, up from less than 200,000 in the late 1950s (Mduma et al. 1999). A decrease in fire intensity due to the removal of grass biomass by increased numbers of grazers is thought to have initiated this trend. This dissertation confirmed both comparatively low levels of fire intensity and a continuing overall increase of woody cover in central and northern SNP.

The woody cover change product revealed markedly larger woody cover decreases in the wider Maswa Game Reserve area than in any other similar-sized area within the study region. The MSW region has been much less studied or surveyed than Serengeti National Park (SNP) or the Maasai Mara National Reserve (MNR). These new observations might draw increased attention to this buffer zone of SNP.

Late Burning Under Dry Conditions

Results from Chapter 5 need to be interpreted in recognition that the time period of this study was discriminated by lower than normal levels of MAP compared

to long-term averages. This allowed the effects of fire to be observed only under relatively dry conditions. The driest sub region, i.e. the wider Maswa Game Reserve area is that in which woody cover decreases in burned areas were largest, despite significantly lower average levels of fire intensity. This and the considerably larger number of pre-fire days without rainfall underline the importance of fire seasonality, offsetting differences in fire intensity during the time period of this study. Woody cover decreases could be amplified by browsing elephants which are not considered in this study. Elephant levels in SNP and MSW have remained low since the 1980s but could recover in the future.

Infrequent Burning

The results of this research suggest that woody plant communities were more severely affected by fire in regions which burned comparatively infrequently with a fire return interval of six years or more. This effect was observed in the Masai Mara Game Reserve (MNR). MNR was the only region for which low fire frequency during an extended time period starting at least five to ten years before 2000 can be assumed. MNR has historically been subject to high grazing and browsing pressure and remained locked in a grassland state since the 1980s. The observed sensitivity of woody vegetation to infrequent fires could be explained in different ways: 1) higher fire intensity through accumulated fuel loads; 2) adaptations of vegetation to different fire regimes; 3) browsing effects. Each factor is discussed below.

Fire intensity is mainly controlled by fire fuel load. Fuel load accumulation was limited in both MNR and SNP through the leveling effect of abundant grazers, mainly migrating wildebeest, which selectively concentrate in areas of high grass

biomass production. Therefore, sensitivity of woody vegetation to infrequent fire events might not have been due to higher fire intensities in MNR. However, fire intensity estimates for MNR were largely unavailable because the vast majority of burned areas in MNR only burned once and estimates could not be derived for single-burned areas. A conclusive answer to the actual level of fire intensities in MNR can only be provided by analyzing a longer time series and by use of additional field data than was available here.

Woody vegetation could also have adapted differently to low and high fire frequencies over the medium to long term. Adaptation could be reflected in either changing species composition or in physiognomic adaptations of woody plants, e.g. changes in bark thickness. Such adaptations would make woody plant communities and individuals respectively more or less sensitive to fire. To answer the question whether different levels of adaptation to fire exist in the study area more detailed field studies on the ground would be necessary. The results of this dissertation hold the potential to serve as a precursor for such field studies.

Browsing effects by elephants play an important role in MNR due to high elephant numbers. Interactions between browsing and burning have been described by Dublin (1995) who found that elephants and other browsers showed a distinct preference for seedlings in burned areas. As a consequence browsing effects on seedlings were significantly higher in burned areas than in unburned areas.

Findings from Chapter 5 are also valuable when we consider that the impact of historic fire frequency on the sensitivity of woody cover to fire has received little attention in the Serengeti-Mara research literature; indeed, it was rarely investigated

as part of a larger regional comparison. Such a large scale approach was possible in this study through the generation of spatially comprehensive, remote sensing based data layers.

Future woody cover changes in MNR mainly depend on four factors: fire frequency and seasonality, browsing pressure, climate and fire intensity, as discussed in order below. Fire frequency and seasonality will likely remain the same presuming no major change in fire management takes place. This would maintain the possible decreasing effects of infrequent fires on woody cover. Browsing pressure by elephants and other browsers is expected to remain high or increase in the coming years (Dublin 1995; Walpole et al. 2004). This would maintain or increase the negative effect of browsing on woody plant seedlings in burned areas.

Future climate might show overall higher MAP but could become more variable and increase the occurrence of severe drought years. Severe drought years can increase the vulnerability of woody plants to fire especially when burned late in the dry season. Years with exceptionally low rainfall can also cause significant drops in wildebeest numbers (Mduma et al. 1999). As a consequence grazing pressure would be reduced until the herds have recovered and fire fuel loads and fire intensity temporarily increased. All of these effects would have detrimental consequences for woody cover and it might be expected that MNR remains dominated by grassland savanna in the foreseeable future.

Fire Regime Parameters as Potential Drivers of Woody Cover Change

The data for the six-year time period of this study showed that fire seasonality is the most important fire regime parameter for controlling woody cover changes in

woodland savanna areas. In grassland savanna areas fire intensity was most important. Fire intensity is significantly affected by grazing pressure from the large migrating wildebeest herds.

Fire seasonality or the seasonal timing of fire is dependent on management decisions since the majority of fires are of anthropogenic origin (Trollope 2005). The results of this study indicate that the timing of fire is more important than fire frequency, i.e. reduction of woody cover in woodland savanna areas might be achieved by late season burning rather than high frequency burning.

A spatially and temporally detailed analysis of the long-term effects of fire regime parameters on woody cover will become feasible in the future as the archive of high resolution remote sensing data expands. The reliable identification of single drivers of woody cover change under varying conditions demands a significantly longer time series and ideally improved datasets for fuel load and fire intensity by inclusion of ground truthing data, as well as the incorporation of additional important factors not considered in the study. Further important factors are the distribution of soil nutrients, woody plant species distribution and grazing pressure by elephants. The latter has rarely been investigated in the MSW area and previous studies have often focused on the Kenyan part of the ecosystem due to generally low elephant numbers in Serengeti since the 1980s (Dublin 1995).

Global Climate Change and Woody Cover Changes

During the late 19th century significant environmental change occurred in the Serengeti-Mara region. A rinderpest epidemic wiped out over 95% of wildebeest and Maasai cattle (Sinclair 1979a). Grazing pressure and fire frequency was dramatically

reduced and over the following decades grassland savannas which had been dominating the region were converted to a denser woodland savanna type (Dublin 1995). The rinderpest epidemic in the 1890s coincided with an extended period of severe drought with the rains failing completely in 1897 and 1898. Gillson (2006) identified this devastating time period as a large infrequent disturbance (LID) of the regional climate and ecosystem, capable to cause lasting effects on the environment. Similar extreme climate events are predicted to be a possible feature of global climate change.

Global average surface temperature increased in the 20th century by 0.6 ± 0.2 ºC and it is very likely that the warming trend will continue or accelerate during the 21st century as predicted under all Intergovernmental Panel on Climate Change (IPCC) scenarios. Much more uncertain are projections of the future distribution of precipitation. In general the IPCC global multi-model ensemble of annual mean change of precipitation predicts increasing rainfall for East Africa (Houghton et al. 2001).

However Hulme et al. (2001) pointed out that future changes of rainfall in East Africa are not well defined and only little work has been published on climate change scenarios specifically for Africa. One of the more important controlling factors for interannual rainfall variability in Africa is the El Niño/Southern Oscillation (ENSO) with East Africa showing one of the most dominant levels of ENSO influences. It is not clear how ENSO events will develop under future climate, mainly because most climate models have not accounted for ENSO appropriately. Camberlin (2004) suggested that the teleconnections between ENSO in the Pacific

and climate in East Africa might weaken in the future due to rising global temperature and changing sea surface temperatures. Warm ENSO episodes have become more frequent, persistent and intense since the mid 1970s, however strong decadal-scale modulations in the ENSO teleconnections indicate that past observations of the magnitude of influence of ENSO on East Africa might not apply the same way in the coming decades.

McHugh (2005) used coupled ocean-atmosphere general circulation models to analyze future rainfall in East Africa. Four out of nineteen models performed well when evaluated against observed rainfall in East Africa. Using these models projections of rainfall into the future under a scenario of CO_2 increase of 1% per year indicate enhanced levels of annual and seasonal rainfall extending from the most significantly affected coastal areas to the East African plateau encompassing the Serengeti-Mara region.

Despite the shortcomings and uncertainties of the model predictions for future precipitation in the wider region of the study area it increasing rainfall receipt is indicated by most studies as a likely scenario in the coming decades. This scenario would have two main implications: Firstly, it makes another LID event caused by a devastating lack of rainfall over several years less likely. Such an LID could cause a significant short term loss of woody cover as was indicated by the observations in MSW during the dry conditions of the study period. Increased rainfall would rather promote the recovery of woody plants in MSW due to reduced drought stress and improved water availability to trees and shrubs in the dry season. Secondly, increased rainfall would enhance grass production and potentially also aboveground grass

biomass accumulation of fire fuel load. However, increased grass biomass would in turn lead to an increased number of wildebeest and other herbivores. Greater numbers of herbivores exert higher grazing pressure thus largely offsetting the potentially higher accumulation of grass biomass and fire fuel load. Therefore fire intensity might remain comparatively stable and not become a limiting factor for woody plant establishment.

6.2. Implications and Future Directions

The burned area, fire intensity and woody cover change data layers produced in this dissertation and their analysis in combination with precipitation have advanced our knowledge about the fire regime and its links to changes in vegetation types of the Serengeti-Mara region. The developed methodologies and results have implications reaching beyond the immediate goals of this study. High resolution burned area maps have a large number of potential applications for research questions around fire, including animal movements in response to fire, changes in the composition of vegetation communities, and fire emissions in dependence of amount of fuel load burned and fire seasonality. The developed approach has the potential to be applied to other savanna areas of similar ecological characteristics, but in the described form is expected to work well only in areas with similar persistence of char after burning. The method might be extended to areas without a temporally persistent char layer by incorporating training data from these areas and adjusting the choice of indices in the algorithm. The algorithm also has the potential to be advanced to operational status and become a useful tool for management authorities.

The woody cover change product has been used in this study to investigate woody cover changes in burned areas under different rainfall and fire conditions. However, woody cover changes are also potentially affected by other important factors which might be more apparent in areas of low fire frequency. Such areas exist in the northern part of the study area in MNR and particularly outside of the protected areas in the northerly adjacent Narok region. The Narok region is inhabited by Maasai pastoralists. Human population density has increased substantially over the last decades together with the number of bomas (Maasai huts or households) (Lamprey and Reid 2004), increasing the pressure on natural resources and possibly affecting woody cover levels. The number of elephants is also substantially higher in the northern part of the ecosystem and it has been shown that elephant browsing in combination with fire can cause significant woody cover decreases (Dublin et al. 1990). Soil type and nutrient availability can also impact maximum sustainable levels of woody cover density (Sankaran et al. 2005). The results of this dissertation provide a basis to evaluate the importance of these additional factors in relation to fire effects.

It is important for continued monitoring of the fire regime and woody cover changes that future versions of the data products are validated in more depth. This is particularly true for the fire intensity and woody cover change products. Fire intensity is mainly dominated by fire fuel load or grass biomass. Frequent collection of grass biomass before burning on a continued basis would allow validating fire fuel load estimates in different parts of the ecosystem.

The research presented in this thesis demonstrates that remote sensing data and methods in combination with field data can provide viable tools to investigate

questions about fire regimes and vegetation dynamics over longer time periods and at regional scales. This study provides the first spatially comprehensive regional view of these factors extending over both the Tanzanian and Kenyan part of the ecosystem. The results highlight the prevalence of fire in most of the ecosystem, particularly large woody cover decreases in the South in areas burned under drought conditions, and different sensitivity of woody cover to fire in the low fire frequency areas in the North compared to other areas. The algorithms developed in this study have the potential to be applied to other savanna areas and provide a basis for future research, monitoring and management.

References

Asner, G.P., Elmore, A.J., Olander, L.P., Martin, R.E., & Harris, A.T. (2004). Grazing systems, ecosystem responses, and global change. *Annual Review of Environment and Resources, 29*, 261-299

Asner, G.P., Wessman, C.A., Schimel, D.S., & Archer, S. (1998). Variability in leaf and litter optical properties: Implications for BRDF model inversions using AVHRR, MODIS, and MISR. *Remote Sensing of Environment, 63*, 243-257

Barbosa, P.M., Gregoire, J.M., & Pereira, J.M.C. (1999). An algorithm for extracting burned areas from time series of AVHRR GAC data applied at a continental scale. *Remote Sensing of Environment, 69*, 253-263

Belsky, A.J., Amundson, R.G., Duxbury, J.M., Riha, S.J., Ali, A.R., & Mwonga, S.M. (1989). The Effects of Trees on Their Physical, Chemical, and Biological Environments in a Semi-Arid Savanna in Kenya. *Journal of Applied Ecology, 26*, 1005-1024

Bond, W.J. (1997). Fire. In R.M. Cowling, D.M. Richardson & S.M. Pierce (Eds.), *Vegetation of southern Africa* (pp. 421-446). Cambridge, UK: Cambridge University Press

Bond, W.J., & van Wilgen, B.W. (1996). *Fire and Plants*. London, U.K.: Chapman and Hall

Boone, R.B., Thirgood, S.J., & Hopcraft, J.G.C. (2006). Serengeti wildebeest migratory patterns modeled from rainfall and new vegetation growth. *Ecology, 87*, 1987-1994

Bourliere, F., & Hadley, M. (1983). Present day savannas: an overview. In F. Borliere (Ed.), *Tropical Savannas* (pp. 1-17). Amsterdam: Elsevier

Bourn, D., & Wint, W. (1994). Livestock, land use and agricultural intensification in sub-saharan Africa. In, *ODI Network Paper 37a* (p. 22). London: Overseas Development Institute

Breiman, L. (1996). Bagging predictors. *Machine Learning, 24*, 123-140

Breiman, L. (2001). Random Forests. *Machine Learning, 45*, 5-32

Breiman, L., Friedman, J., Olshen, R., & Stone, C. (1984). *Classification and Regression Trees*. Monterey, California: Wadsworth International Group

Byram, G.M. (1959). Combustion of forest fuels. In K.P. Davis (Ed.), *Forest fire: control and use* (pp. 61-89). New York: McGraw-Hill

Cablk, M., White, D., & Kiester, A.R. (2002). Assessment of spatial autocorrelation in empirical models in ecology. In J.M. Scott, P.J. Heglund, M.L. Morrison, J.B. Haufler, M.G. Raphael, W.A. Wall & F.B. Samson (Eds.), *Predicting Species Occurrences—Issues of Accuracy and Scale* (pp. 429-440). Washington: Island Press

Camberlin, P., Janicot, S., & Poccard, I. (2001). Seasonality and atmospheric dynamics of the teleconnection between African rainfall and tropical sea-

surface temperature: Atlantic vs. ENSO. *International Journal of Climatology, 21*, 973-1005

Camberlin, P., Chauvin, F., Douville, H., & Zhao, Y. (2004). Simulated ENSO-tropical rainfall teleconnections in present-day and under enhanced greenhouse gases conditions. *Climate Dynamics, 23*, 641-657

Campbell, K., & Borner, M. (1995). Population trends and distribution of Serengeti herbivores: implications for management. In A.R.E. Sinclair & P. Arcese (Eds.), *Serengeti II. Dynamics, management and conservation of an ecosystem* (pp. 117-145). Chicago: University of Chicago Press

Campbell, K., & Hofer, H. (1995). People and wildlife: spatial dynamics and zones of interaction. In A.R.E. Sinclair & P. Arcese (Eds.), *Serengeti II. Dynamics, management and zones of interaction* (pp. 534-570). Chicago: University of Chicago Press

Campbell, K.L.I. (1989). Programme report. In. Arusha, Tanzania: Serengeti Ecological Monitoring Programme

Cheney, P., & Sullivan, A. (1997). *Grassfires: fuel, weather, and fire behaviour*. Canberra, Australia: CSCIRO Publishing

Chuvieco, E., Martin, M.P., & Palacios, A. (2002). Assessment of different spectral indices in the red-near-infrared spectral domain for burned land discrimination. *International Journal of Remote Sensing, 23*, 5103-5110

Chuvieco, E., Ventura, G., Martin, M.P., & Gomez, I. (2005). Assessment of multitemporal compositing techniques of MODIS and AVHRR images for burned land mapping. *Remote Sensing of Environment, 94*, 450-462

CIAT (2004). Hole-filled seamless SRTM data, available from http://gisweb.ciat.cgiar.org/sig/90m_data_tropics.htm. In: International Centre for Tropical Agriculture (CIAT)

Cocke, A.E., Fule, P.Z., & Crouse, J.E. (2005). Comparison of burn severity assessments using Differenced Normalized Burn Ratio and ground data. *International Journal of Wildland Fire, 14*, 189-198

Congalton, R.G. (1991). A Review of Assessing the Accuracy of Classifications of Remotely Sensed Data. *Remote Sensing of Environment, 37*, 35-46

Curran, P.J. (1988). The Semivariogram in Remote-Sensing - an Introduction. *Remote Sensing of Environment, 24*, 493-507

Darling, F.F. (1960). *An ecological reconnaissance of the Mara plains in Kenya Colony*. Washington, D.C.: The Wildlife Society

DeFries, R.S., Hansen, M., Townshend, J.R.G., & Sohlberg, R. (1998). Global land cover classifications at 8 km spatial resolution: the use of training data derived from Landsat imagery in decision tree classifiers. *International Journal of Remote Sensing, 19*, 3141-3168

DeFries, R.S., Hansen, M.C., & Townshend, J.R.G. (2000a). Global continuous fields of vegetation characteristics: A linear mixture model applied to multi-year 8 km AVHRR data. *International Journal of Remote Sensing, 21*, 1389-1414

DeFries, R.S., Houghton, R.A., Hansen, M.C., Field, C.B., Skole, D., & Townshend, J. (2002). Carbon emissions from tropical deforestation and regrowth based on satellite observations for the 1980s and 1990s. *Proceedings of the National Academy of Sciences of the United States of America, 99*, 14256-14261

DeFries, R.S., Lovelands, T.R., Hansen, M.C., Townshend, J.R.G., & Janetos, A.C. (2000b). A new global 1-km dataset of percentage tree cover derived from remote sensing. *Global Change Biology, 6*, 247-254

DeFries, R.S., Townshend, J.R.G., & Hansen, M.C. (1999). Continuous fields of vegetation characteristics at the global scale at 1-km resolution. *Journal of Geophysical Research D: Atmospheres, 104*, 16,911-916,923

Dublin, H.T. (1986). Decline of the Mara woodlands: the role of fire and elephants. In, *Department of Zoology* (p. 228). Vancouver, Canada: University of British Columbia

Dublin, H.T. (1991). Dynamics of the Serengeti-Mara woodlands. *Forest and Conservation History, 35*, 169-178

Dublin, H.T. (1995). Vegetation dynamics in the Serengeti-Mara ecosystem: the role of elephants, fire, and other factors. In A.R.E. Sinclair & P. Arcese (Eds.), *Serengeti II. Dynamics, management and conservation of an ecosystem* (pp. 71-90). Chicago: University of Chicago Press

Dublin, H.T., Sinclair, A.R.E., & McGlade, J. (1990). Elephants and fire as causes of multiple stable states in the Serengeti-Mara woodlands. *Journal of Animal Ecology, 59*, 1147-1164

Emerton, L., & Mfunda, I. (1999). Making Wildlife Economically Viable for Communities Living around the Western Serengeti, Tanzania. In, *Evaluating Eden Series Discussion Paper, No. 1* (p. 34). London: International Institute for Environment and Development

Epting, J., Verbyla, D., & Sorbel, B. (2005). Evaluation of remotely sensed indices for assessing burn severity in interior Alaska using Landsat TM and ETM+. *Remote Sensing of Environment, 96*, 328-339

FAO (1991). *Guidelines: land evaluation for extensive grazing*. Rome: Food and Agricultural Organization

Farr, T.G., & Kobrick, M. (2000). Shuttle Radar Topography Mission produces a wealth of data. *American Geophysical Union Eos Trans. AGU, 81*, 583-585

Folse, L.J. (1982). An Analysis of Avifauna-Resource Relationships on the Serengeti Plains. *Ecological Monographs, 52*, 111-127

Friedl, M.A., & Brodley, C.E. (1997). Decision tree classification of land cover from remotely sensed data. *Remote Sensing of Environment, 61*, 399-409

Frost, P.G.H., & Robertson, F. (1987). The ecological effects of fire in savannas. In B.H. Walker (Ed.), *Determinants of Tropical Savannas* (pp. 93-140). Harare, Zimbabwe: IRL Press

Gillson, L. (2006). A 'large infrequent disturbance' in an East African savanna. *African Journal of Ecology, 44*, 458-467

Gerresheim, K. (1974). The Serengeti Landscape Classification-Map and Manuscript. In. Nairobi, Kenya: Afr. Wildl. Leadership Fdn.

Grunow, J.O., Groeneveld, H.T., & Dutoit, S.H.C. (1980). Above-Ground Dry-Matter Dynamics of the Grass Layer of a South-African Tree Savanna. *Journal of Ecology, 68*, 877-889

Ham, J., Chen, Y.C., Crawford, M.M., & Ghosh, J. (2005). Investigation of the random forest framework for classification of hyperspectral data. *IEEE Transactions on Geoscience and Remote Sensing, 43*, 492-501

Hansen, M. (2003). Global percent tree cover at a spatial resolution of 500 meters: first results of the MODIS vegetation continuous fields algorithm. *Earth Interactions, 7*, 1-15

Hansen, M.C., DeFries, R.S., Townshend, J.R.G., & Sohlberg, R. (2000). Global land cover classification at 1 km spatial resolution using a classification tree approach. *International Journal of Remote Sensing, 21*, 1331-1364

Hansen, M.C., DeFries, R.S., Townshend, J.R.G., Sohlberg, R., Dimiceli, C., & Carroll, M. (2002). Towards an operational MODIS continuous field of percent tree cover algorithm: examples using AVHRR and MODIS data. *Remote Sensing of Environment, 83*, 303-319

Hansen, M.C., Dubayah, R., & Defries, R. (1996). Classification trees: an alternative to traditional land cover classifiers. *International Journal of Remote Sensing, 17*, 1075-1081

Heath, B. (2003). Personal Communication. In. Mara Conservancy, P.O. Box 63457, Muthaiga 00619, Nairobi, Kenya, e-mail: <mara@triad.co.ke>

Herlocker, D. (1976). *Woody vegetation of the Serengeti National Park*. College Station: Texas A&M University

Higgins, S.I. (2006). Personal Communication. In. Technical University of Munich, 85350 Freising-Weihenstephan, Germany, Email: <Higgins@wzw.tum.de>

Higgins, S.I., Bond, W.J., & Trollope, W.S.W. (2000). Fire, resprouting and variability: a recipe for grass-tree coexistence in savanna. *Journal of Ecology, 13*, 295-299

Hoffa, E.A., Ward, D.E., Hao, W.M., Susott, R.A., & Wakimoto, R.H. (1999). Seasonality of carbon emissions from biomass burning in a Zambian savanna. *Journal of Geophysical Research-Atmospheres, 104*, 13841-13853

Houghton, J.T., Ding, Y., Griggs, D.J., Noguer, M., van der Linden, P.J., & Dai, X. (2001). *Climate Change 2001: The Scientific Basis*. Cambridge, U.K.: Cambridge University Press

Huete, A.R., Justice, C.O., & VanLeeuwen, W. (1999). Modis Vegetation Index (MOD13) Algorithm Theoretical Basis Document. In (p. 142). Greenbelt, Maryland: University of Maryland/ NASA - GSFC

Huete, A.R., & Tucker, C.J. (1991). Investigation of Soil Influences in AVHRR Red and near-Infrared Vegetation Index Imagery. *International Journal of Remote Sensing, 12*, 1223-1242

Hulme, M., Doherty, R., Ngara, T., New, M., & Lister, D. (2001). African climate change: 1900-2100. *Climate Research, 17*, 145-168

Jameson, D.A. (1967). Relationship of Tree Overstory and Herbaceous Understory Vegetation. *Journal of Range Management, 20*, 247-249

Jensen, J.R. (2005). *Introductory digital image processing : a remote sensing perspective*. Upper Saddle River, N.J.: Prentice Hall

Kasischke, E.S., & French, N.H.F. (1995). Locating and Estimating the Areal Extent of Wildfires in Alaskan Boreal Forests Using Multiple-Season Avhrr Ndvi Composite Data. *Remote Sensing of Environment, 51*, 263-275

Kaufman, Y.J., Remer, L.A., Ottmar, R.D., Ward, D.E., Li, R.R., Kleidman, R., Fraser, R.S., Flynn, L., McDougal, D., & Shelton, G. (1996). Relationship between remotely sensed fire intensity and rate of emission of smoke: SCAR-C experiment. In J.S. Levine (Ed.), *Biomass Burning and Global Change* (pp. 685– 696). Cambridge, MA: MIT Press

Key, C.H., & Benson, N.C. (2006). Landscape assessment (LA); Remote sensing measure of severity: the normalized burn ratio. In D.C. Lutes, R.E. Keane, J.F. Caratti, C.H. Key, N.C. Benson, S. Sutherland & L.J. Gangi (Eds.), *FIREMON: Fire effects monitoring and inventory system; Gen. Tech. Rep. RMRS-GTR-164-CD* (pp. LA25-LA41). Fort Collins, CO: U.S. Department of Agriculture, Forest Service, Rocky Mountain Research Station

Lamprey, R.H. (1984). Maasai impact on Kenya savannah vegetation: a remote sensing approach. *Ph. D. Thesis, University of Aston, Birmingham, U.K.*

Lamprey, R.H., & Reid, R.S. (2004). Expansion of human settlement in Kenya's Maasai Mara: what future for pastoralism and wildlife? *Journal of Biogeography, 31*, 997-1032

Lawrence, R.L., & Wright, A. (2001). Rule-based classification systems using classification and regression tree (CART) analysis. *Photogrammetric Engineering and Remote Sensing, 67*, 1137-1142

Leuthold, W. (1977). Changes in tree populations of Tsave East National Park, Kenya. *East African Wildlife Journal, 15*, 61-69

Lobert, J.M., Scharffe, D.H., Hao, W.M., & Crutzen, P.J. (1990). Importance of Biomass Burning in the Atmospheric Budgets of Nitrogen-Containing Gases. *Nature, 346*, 552-554

Luke, R.H., & McArthur, A.G. (1978). *Bushfires in Australia*. Canberra, Australia: Australian Government Publication Service

Mayaux, P., Bartholome, E., Fritz, S., & Belward, A. (2004). A new land-cover map of Africa for the year 2000. *Journal of Biogeography, 31*, 861-877

McArthur, A.G. (1967). *Fire behaviour in eucalypt forests*: Commonwealth of Australia, Department of National Development, Forestry and Timber Bureau

McHugh, M.J. (2005). Multi-model trends in East African rainfall associated with increased CO2. *Geophysical Research Letters, 32*

McNaughton, S.J. (1985). Ecology of a grazing ecosystem: the Serengeti. *Ecological Monographs, 55*, 259-294

McNaughton, S.J., Stronach, N.R.H., & Georgiadis, N.J. (1998). Combustion in natural fires and global emissions budgets. *Ecological Applications, 8*, 464-468

Mduma, S.A.R. (1996). Serengeti wildebeest population dynamics: regulation, limitation and implications for harvesting. In, *Department of Zoology* (p. 192). Vancouver: University of British Columbia, Canada

Mduma, S.A.R., Sinclair, A.R.E., & Hilborn, R. (1999). Food regulates the Serengeti wildebeest: a 40-year record. *Journal of Animal Ecology, 68*, 1101-1122

Moisen, G.G., & Frescino, T.S. (2002). Comparing five modelling techniques for predicting forest characteristics. *Ecological Modelling, 157*, 209-225

Mordelet, P., & Menaut, J.C. (1995). Influence of Trees on Aboveground Production Dynamics of Grasses in a Humid Savanna. *Journal of Vegetation Science, 6*, 223-228

Morgan, J.N., & Sonquist, J.A. (1963). Problems in the analysis of survey data and a proposal. *Journal of the American Statistical Association, 58*, 415-434

Norton-Griffiths, M. (1979). The influence of grazing, browsing and fire on the vegetation dynamics of the Serengeti. In A.R.E. Sinclair & M. Norton-Griffiths (Eds.), *Serengeti - Dynamics of an Ecosystem* (pp. 310-352). Chicago: University of Chicago Press

Oesterheld, M., Loreti, J., Semmartin, M., & Paruelo, J.M. (1999). Grazing, fire, and climate effects on primary productivity of grasslands and savannas. In L.R.

Walker (Ed.), *Ecosystems of disturbed ground* (pp. 287-305). Amsterdam: Elsevier

Pacala, S.W., Hurtt, G.C., Baker, D., Peylin, P., Houghton, R.A., Birdsey, R.A., Heath, L., Sundquist, E.T., Stallard, R.F., Ciais, P., Moorcroft, P., Caspersen, J.P., Shevliakova, E., Moore, B., Kohlmaier, G., Holland, E., Gloor, M., Harmon, M.E., Fan, S.M., Sarmiento, J.L., Goodale, C.L., Schimel, D., & Field, C.B. (2001). Consistent land- and atmosphere-based US carbon sink estimates. *Science, 292*, 2316-2320

Parr, C.L., & Andersen, A.N. (in print). Patch Mosaic Burning for Biodiversity Conservation: a Critique of the Pyrodiversity Paradigm. *Conservation Biology*

Pellew, R.A. (1983). The Giraffe and Its Food Resource in the Serengeti .1. Composition, Biomass and Production of Available Browse. *African Journal of Ecology, 21*, 241-267

Pennycuick, L. (1975). Movements of migratory wildebeest population in the Serengeti area between 1960 and 1973. *East African Wildlife Journal, 13*, 65-87

Pinty, B., & Verstraete, M.M. (1992). GEMI: a non-linear index to monitor global vegetation from satellites. *Vegetatio, 101*, 15-20

Prins, H.H.T., & Loth, P.E. (1988). Rainfall Patterns as Background to Plant Phenology in Northern Tanzania. *Journal of Biogeography, 15*, 451-463

Qi, J., Kerr, Y.H., & Chehbouni, A. (1994). External Factor Consideration in Vegetation Index Development. In, *Physical Measurements and Signatures in*

Remote Sensing, Sixth Symposium of International Society of Photogrammetric and Remote Sensing (pp. 723-730). Val d'Isere, France: ISPRS

Reed, D., Anderson, M., Dempewolf, J., Metzger, K., & Serneels, S. (2004). Land cover and physiognomic vegetation mapping of the Serengeti - Masai Mara ecosystem. In, *89th Annual Meeting of the Ecological Society of America*. Portland, Oregon

Roberts, D.A., Smith, M.O., & Adams, J.B. (1993). Green Vegetation, Nonphotosynthetic Vegetation, and Soils in Aviris Data. *Remote Sensing of Environment, 44*, 255-269

Roy, D.P., Boschetti, L., & Trigg, S.N. (2006). Remote sensing of fire severity: Assessing the performance of the Normalized Burn Ratio. *Ieee Geoscience and Remote Sensing Letters, 3*, 112-116

Roy, D.P., Jin, Y., Lewis, P.E., & Justice, C.O. (2005). Prototyping a global algorithm for systematic fire-affected area mapping using MODIS time series data. *Remote Sensing of Environment, 97*, 137-162

Sa, A.C.L., Pereira, J.M.C., & Silva, J.M.N. (2005). Estimation of combustion completeness based on fire-induced spectral reflectance changes in a dambo grassland (Western Province, Zambia). *International Journal of Remote Sensing, 26*, 4185-4195

Salvatori, V., Van Gils, H.A.M., Egunyu, F., Skidmore, A.K., & De Leeuw, J. (2001). The effects of fire and grazing pressure on vegetation cover and small

mammal populations in the Maasai Mara National Reserve. *African Journal of Ecology, 39*, 200-204

Sankaran, M., Hanan, N.P., Scholes, R.J., Ratnam, J., Augustine, D.J., Cade, B.S., Gignoux, J., Higgins, S.I., Le Roux, X., Ludwig, F., Ardo, J., Banyikwa, F., Bronn, A., Bucini, G., Caylor, K.K., Coughenour, M.B., Diouf, A., Ekaya, W., Feral, C.J., February, E.C., Frost, P.G.H., Hiernaux, P., Hrabar, H., Metzger, K.L., Prins, H.H.T., Ringrose, S., Sea, W., Tews, J., Worden, J., & Zambatis, N. (2005). Determinants of woody cover in African savannas. *Nature, 438*, 846-849

Schaller, B.G. (1972). *The Serengeti lion: A study of predator-prey relations*. Chicago: University of Chicago Press

Scholes, R.J. (1997). Savanna. In R.M. Cowling, D.M. Richardson & S.M. Pierce (Eds.), *Vegetation of southern Africa* (pp. 258-277). Cambridge, UK: Cambridge University Press

Scholes, R.J., & Archer, S.R. (1997). Tree-Grass Interactions in Savannas. *Annual Review of Ecology and Systematics, 28*, 517-544

Scholes, R.J., & Hall, D.O. (1996). The carbon budget of tropical savannas, woodlands and grasslands. In A. Breymeyer, D.O. Hall, J.M. Melillo & G.I. Agren (Eds.), *Global Change: Effects on Coniferous Forests and Grasslands* (pp. 69-100). Chichester: John Wiley

Scholes, R.J., & Walker, B.H. (1993). *Synthesis of the Nylsvley Study*. Cambridge, UK: Cambridge University Press

Serneels, S., & Lambin, E.F. (2001a). Impact of land-use changes on the wildebeest migration in the northern part of the Serengeti-Mara ecosystem. *Journal of Biogeography, 28*, 391-407

Serneels, S., & Lambin, E.F. (2001b). Proximate causes of land-use change in Narok district, Kenya: A spatial statistical model. *Agriculture, Ecosystems and Environment, 85*, 65-81

Shea, R.W., Shea, B.W., Kauffman, J.B., Ward, D.E., Haskins, C.I., & Scholes, M.C. (1996). Fuel biomass and combustion factors associated with fires in savanna ecosystems of South Africa and Zambia. *Journal of Geophysical Research, 101*, 23551-23568

Simon, M., Plummer, S., Fierens, F., Hoelzemann, J.J., & Arino, O. (2004). Burnt area detection at global scale using ATSR-2: The GLOBSCAR products and their qualification. *Journal of Geophysical Research-Atmospheres, 109*

Sinclair, A.R.E. (1975). The Resource Limitation of Trophic Levels in Tropical Grassland Ecosystems. *Journal of Animal Ecology, 44*, 497-520

Sinclair, A.R.E. (1979a). Dynamics of the Serengeti ecosystem: process and pattern. In A.R.E. Sinclair & M. Norton-Griffiths (Eds.), *Serengeti: dynamics of an ecosystem* (pp. 1-30). Chicago: University of Chicago Press

Sinclair, A.R.E. (1979b). The Serengeti environment. In A.R.E. Sinclair & M. Norton-Griffiths (Eds.), *Serengeti: dynamics of an ecosystem* (pp. 31-45). Chicago: University of Chicago Press

Sinclair, A.R.E. (1995). Serengeti past and present. In A.R.E. Sinclair & P. Arcese (Eds.), *Serengeti II. Dynamics, management and conservation of an ecosystem* (pp. 3-30). Chicago: University of Chicago Press

Sinclair, A.R.E., & Arcese, P. (1995). Equilibria in plant-herbivore interactions. In A.R.E. Sinclair & P. Arcese (Eds.), *Serengeti II. Dynamics, management and conservation of an ecosystem* (pp. 91-113). Chicago: University of Chicago Press

Stelfox, J.G., Peden, D.G., Epp, H., Hudson, R.J., Mbugua, S.W., Agatsiva, J.L., & Amuyunzu, C.L. (1986). Herbivore dynamics in southern Narok, Kenya. *Journal of Wildlife Management, 50*, 339-347

Stronach, N.R.H., & McNaughton, S.J. (1989). Grassland fire dynamics in the Serengeti ecosystem, and a potential method of reprospectively estimating fire energy. *Journal of Applied Ecology, 26*, 1025-1033

Stroppiana, D., Gregoire, J.M., & Pereira, J.M.C. (2003a). The use of SPOT VEGETATION data in a classification tree approach for burnt area mapping in Australian savanna. *International Journal of Remote Sensing, 24*, 2131-2151

Stroppiana, D., Pinnock, S., Pereira, J.M.C., & Gregoire, J.M. (2002). Radiometric analysis of SPOT-VEGETATION images for burnt area detection in Northern Australia. *Remote Sensing of Environment, 82*, 21-37

Stroppiana, D., Tansey, K., Gregoire, J.M., & Pereira, J.M.C. (2003b). An algorithm for mapping burnt areas in Australia using SPOT-VEGETATION data. *IEEE Transactions on Geoscience and Remote Sensing, 41*, 907 - 909

Talbot, L.M., & Talbot, M.H. (1963). *The wildebeest in western Masailand, East Africa*. Washington, D.C.: The Wildlife Society

Tansey, K., Gregoire, J.M., Binaghi, E., Boschetti, L., Brivio, P.A., Ershov, D., Flasse, S., Fraser, R., Graetz, D., Maggi, M., Peduzzi, P., Pereira, J., Silva, J., Sousa, A., & Stroppiana, D. (2004). A global inventory of burned areas at 1km resolution for the year 2000 derived from SPOT VEGETATION data. *Climatic Change, 67*, 345-377

Thirgood, S.J., Mosser, A., Tham, S., Hopcraft, J.G.C., Mwangomo, E., Mlengeya, T., Kilewo, M., Fryxell, J., Sinclair, A.R.E., & Borner, M. (2004). Can parks protect migratory ungulates? The case of the Serengeti-Mara wildebeest. *Animal Conservation, 7*, 113-120

Thomlinson, J.R., Bolstad, P.V., & Cohen, W.B. (1999). Coordinating methodologies for scaling landcover classifications from site-specific to global: Steps toward validating global map products. *Remote Sensing of Environment, 70*, 16-28

Townshend, J.R.G., Justice, C.O., & Kalb, V.T. (1987). Characterization and classification of South American land cover types using satellite data. *International Journal of Remote Sensing, 8*, 1189–1207

Trigg, S.N., Roy, D.P., & Flasse, S.P. (2005). An in situ study of the effects of surface anisotropy on the remote sensing of burned savannah. *International Journal of Remote Sensing, 26*, 4869-4876

Trollope, W.S.W. (1984). Fire in savanna. In P.V. Booysen & N.M. Tainton (Eds.), *Ecological Effects of Fire in South African Ecosystems*. Berlin: Springer-Verlag

Trollope, W.S.W. (1998). Effect and Use of Fire in the Savanna Areas of Southern Africa. In: Department of Livestock and Pasture Science, Faculty of Agriculture, University of Fort Hare, Alice, South Africa

Trollope, W.S.W., Everson, C.S.E., & Tainton, N.M. (1991 in prep.). Effect and use of fire in the grassland and savanna areas of southern Africa. *Veld and pasture management in South Africa*

Trollope, W.S.W., Trollope, L.A., & Austin, C.B. (2005). Recommendations on fire management in the Serengeti National Park, Tanzania. In (p. 50). Alice, South Africa: Department Livestock & Pasture Science, University Fort Hare

Tucker, C.J., Townshend, J.R.G., & Goff, T.E. (1985). African land-cover classification using satellite data. *Science, 227*, 369–375

UNEP (2003). Serengeti National Park, Tanzania. In (pp. http://sea-bov.unep-wcmc.org/sites/wh/serenget.html). Cambridge, U.K.: Protected Areas Programme, UNEP World Conservation Monitoring Centre

van Wagtendonk, J.W., Root, R.R., & Key, C.H. (2004). Comparison of AVIRIS and Landsat ETM+ detection capabilities for burn severity. *Remote Sensing of Environment, 92*, 397-408

van Wilgen, B.W., Trollope, W.S.W., Biggs, H.C., Potgieter, A.L.F., & Brockett, B.H. (2003). Fire as a driver of ecosystem variability. In J.T. du Toit, K.H. Rogers & H.C. Biggs (Eds.), *The Kruger experience* (pp. 149-170). Washington: Island Press

Vermote, E.F., & Vermeulen, A. (1999). Atmospheric correction algorithm: spectral reflectances (MOD09). In (p. 107). College Park, United States: University of Maryland, Dept. of Geography

Waller, R.D. (1990). Tsetse fly in western Narok, Kenya. *Journal of African History, 31*, 81-101

Walpole, M.J., Nabaala, M., & Matankory, C. (2004). Status of the Mara woodlands in Kenya. *African Journal of Ecology, 42*, 180-188

Walter, H. (1971). *Ecology of tropical and subtropical vegetation*. Edinburgh: Oliver & Boyd

Walter, H., & Breckle, S.W. (2002). *Walter's Vegetation of the earth : the ecological systems of the geo-biosphere*. New York: Springer

Weltzin, J.F., & Coughenour, M.B. (1990). Savanna Tree Influence on Understory Vegetation and Soil Nutrients in Northwestern Kenya. *Journal of Vegetation Science, 1*, 325-334

Wooster, M.J. (2002). Small-scale experimental testing of fire radiative energy for quantifying mass combusted in natural vegetation fires. *Geophysical Research Letters, 29*

Xie, P., & Arkin, A. (1997). A 17-year monthly analysis based on gauge observations, satellite estimates, and numerical model outputs. *Bulletin of the American Meteorological Society, 78*, 2539–2558